Politecnico di Milano

Department of Civil, Environmental & Land Management Engineering

Master Thesis

Analysis and design of R/C flat-slab structures subjected to gravity and lateral loads

---

Luis Felipe Mohedano Millan

ID: 937900

Advisor:

Prof. Luca Martinelli

Milano - A.Y. 2020-2021

Acknowledgements

Throughout the writing of this thesis, I have received a great deal of support and assistance. First and foremost, I would like to express my deepest thanks to my thesis supervisor, Prof. Luca Martinelli for his invaluable advice, guidance and continuous support during the writing of this dissertation. Your knowledge, expertise and patience helped culminate this thesis.

I would also like to thank The National Council of Science and Technology (Consejo Nacional de Ciencia y Tecnología CONACYT) for the funding and economic support offered to me during my master's degree program.

In addition, I would also like to extend my gratitude to my family for the unconditional love and support during this adventure far away from home. Finally, many thanks to all my friends that I have made during my stay in Milan, who have been there for me during all this time.

Luis Felipe Mohedano Millan

Milan, June of 2022

Abstract

The use of flat-slabs as building floor solution is quite common all around the world. In recent years, the increase of use of flat slab floor systems in moderate to high seismic zones in Europe has aroused the concern of many researchers because the behavior of such structures under seismic actions is not completely understood. Although this type of floor system has certain advantages over other floor systems, flat slab structure are susceptible to suffer a punching shear failure when a correct design is not performed.

The aim of this dissertation is to study the punching shear behavior of reinforce concrete flat slab structures without punching shear reinforcement under vertical and lateral loads. A total of three different structures with lateral-force resisting systems (shear walls) are analyzed and designed to evaluate the impact of punching shear in the structural design. These structures are intended to represent a typical residential building. The three structures proposed are analyzed using the Finite Element Method (FEM) through the software Midas Gen 2020 (v2.3). The design of the structures is carried out considering the provisions given by Eurocode 2 and Eurocode 8. Flat-slabs and columns are designed as secondary seismic elements.

An experimental study is considered to calibrate the FEM models. The aforementioned experimental study was carried out by Coronelli et al. at ELSA laboratory of the European Commission's Joint Research Centre. The specimen studied was a full-scale two-story flat-slab structure subjected to vertical and lateral loads.

The models proposed to analyze the structures showed a good correspondence between the numerical and the experimental global structural behavior. Experimental results of the performance of the slab-column connections are compered with the numerical results obtained for the different structures presented.

The results obtained showed the importance of the correct modelling of flat-slab structures under lateral loading. A stiffness reduction factor for bending of 0.25 is suggested for slabs when a flat-slab structure is linearly analyzed inside FEM software. Additionally, when designing this type of structures, a Gravity Shear Ratio (GSR) between 0.3 an 0.4 is suggested. The use of large spans is not recommended when the structure is subjected to lateral loads and lateral-force resisting systems should be present.

Sommario

L'uso di piastre in calcestruzzo armato senza travi come soluzione dei solai degli edifici è abbastanza comune in tutto il mondo. Negli ultimi anni, l'aumento dell'uso di questo sistema di solai in zone di intensità simica da moderata ad alta in Europa ha suscitato preoccupazione in molti ricercatori perché il comportamento di tali strutture durante le azioni sismiche non è completamente compreso. Sebbene questo tipo di sistema a piastra presenti alcuni vantaggi rispetto ad altri sistemi, è suscettibile di subire punzonamento quando non viene eseguita una progettazione strutturale corretta.

Lo scopo di questa tesi è di studiare il comportamento a punzonamento a taglio di strutture a piastra senza travi in calcestruzzo armato senza armatura trasversale sotto carichi verticali e laterali. Un totale di tre diverse strutture con sistemi di resistenza alle forze laterali (pareti di taglio) vengono analizzate e progettate per valutare l'impatto del punzonamento nella progettazione strutturale. Queste strutture intendono rappresentare un tipico edificio residenziale. Le tre strutture proposte vengono analizzate utilizzando il Metodo degli Elementi Finiti (FEM) tramite il software Midas Gen 2020 (v2.3). La progettazione delle strutture viene effettuata tenendo conto delle disposizioni dell'Eurocode 2 e dell'Eurocode 8. Il sistema a piastra e le colonne sono progettati come elementi sismici secondari.

Uno studio sperimentale è considerato per calibrare i modelli FEM. Il suddetto studio sperimentale è stato condotto da Coronelli et al. presso il laboratorio ELSA del European Commission's Joint Research Centre. L'esemplare studiato era una struttura full-scale con sistema a piastra senza travi a due piani soggetta a carichi verticali e laterali.

I modelli proposti per l'analisi delle strutture hanno mostrato una buona corrispondenza tra il comportamento strutturale globale del modello numerico e

quello sperimentale. I risultati sperimentali delle prestazioni di connessioni piastra colonna sono confrontati con i risultati numerici ottenuti per le diverse strutture presentate.

I risultati ottenuti hanno mostrato l'importanza della corretta modellazione delle strutture a soletta piana sotto carico laterale. Un fattore di riduzione della rigidità per flessione di 0. 25 è suggerito per le piastra quando la struttura viene analizzata linearmente all'interno del software FEM. Inoltre, quando si progetta questo tipo di strutture, si suggerisce un rapporto di taglio gravitazionale (GSR) compreso tra 0.3 e 0.4. L'uso di grandi luci non è raccomandato quando la struttura è soggetta a carichi laterali e sempre all'interno della struttura devono essere presenti sistemi resistenti alle forze laterali.

Contents

List of Figures

List of Tables

Chapter 1

Introduction

Flat slabs are commonly used in office buildings, hospitals, hotels, schools, malls and among others type of buildings. Although their behavior under lateral loading is not well understood, the use of reinforced concrete flat-slab floor systems has increased significantly in recent years becoming one of the most common solutions for building floors.

A reinforced concrete slab is a structural element intended to bear loads acting orthogonally to its mean plane. It is a flat element having a small thickness compared to its other two dimensions. Generally, slabs may be divided into two main categories:

- Beam-less slabs (Fig. 1.1).
- Slabs supported on beams (Fig. 1.2).

Beam-less slabs, better known as flat-slabs, are simple plate elements of uniform thickness supported directly by columns. The basic form of a flat slab is illustrated in Fig. 1.1a. Additionally, another common sub-type of beam-less slabs is the flat slab with drop panels Fig. 1.1b. The use of a flat slab with drop panels is matter of the magnitude of the design loading and the length of spans. Generally, the strength of flat slab is limited by the punching shear strength at sections near the columns. Therefore, the use of drop panels and column capitals is governed by the necessity of increasing the punching shear resistance of the slab-column connection because these additional elements, provide an increase of the shear strength around the column.

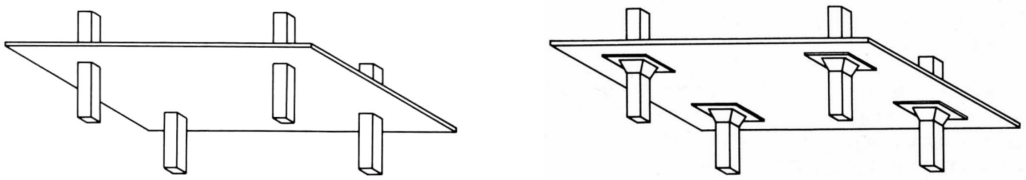

(a) Flat slab (b) Flat slab with drop panels

Figure 1.1: Beamless slabs

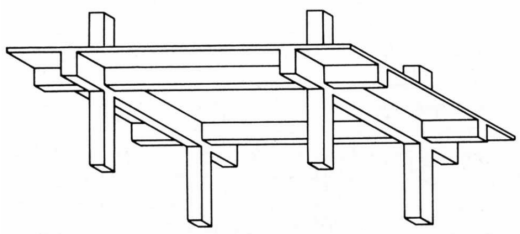

Figure 1.2: Slab supported by beams

Flat-slabs systems exhibit some advantages over the use of conventional floor systems. Construction time is shorter, and they required an easier formwork to be built. From the architectural point of view, this type of floor system better uses the vertical space of construction, resulting in lower story heights.

Nevertheless, flat slab systems present some serious issues:

- Presence of potentially large transversal displacements.
- They are susceptible to significant stiffness reduction after cracking of the elements under gravitational and lateral loads.
- Susceptible to brittle shear failure at slab-column connections (punching shear failure).

Punching shear failure can be briefly described as a localized failure in the slab-column connection. This failure occurs when a highly complex state of stress develops around the column due to a high concentrated force acting in the column. Consequently, the slab collapses around a conical surface above the column (Fig. 1.3) leading to the penetration of the slab into the column. Because of the

brittle nature of this type of failure and also because it can lead to a catastrophic progressive collapse of the whole structure, it must be completely avoided.

Figure 1.3: Punching shear failure mechanism

Another important problem associated with the use of flat-slabs systems, is the lack of practical information for the design of those structures when they are subjected to seismic action. Although, sufficient information exists for the design of flat-slabs structures under gravity loads, their behavior under lateral lads is still not well understood. When a flat-slab structure is subjected to an earthquake action, development of high shear stress due to unbalanced moments occurs at slab-column connections generating an even more complex phenomenon to be analyzed. Some mechanical models have been developed but the complexity of them, makes impossible to be used in practical design.

In Europe, current efforts are focused in getting experimental data which can be included in codes in a more practical way. In fact, one of the objectives of this dissertation is to design a flat-slab building under seismic action, using the most recent knowledge and experimental data available in literature.

1.1 Objectives

The topic of this dissertation is the analysis and the design of a reinforced concrete flat-slab structures subjected to gravity and lateral loads according to the current European regulations. A recent work conducted by Coronelli et al. [1], is used as a guide for the initial dimensioning of the elements of the structures analyzed here, and later, to compare the results numerical results obtained with the experimental ones.

The main aim of this work is to analyze the influence of the punching shear in the design of flat-slab buildings without punching shear reinforcement. To achieve

this, three different structures with different structural layout configurations are proposed. In all the cases, a resisting lateral system is present in the structures as a primary seismic element to resist the lateral loading under seismic actions. Punching shear will be analyzed by placing grater focus on:

- Dimensions of the primary seismic structural elements.
- In plane dimension of the whole structure.
- Use of different slab spans.
- Different concentrations of hogging steel reinforcement near slab-column connections.

Defining a correct procedure for modeling flat-slab structures under lateral loads in commercial software for structural analysis, is another goal of this thesis. Based on experimental results, some recommendations will be given to model in a better and more reliable way flat-slab structures. Finally, a comparison between the current provisions and the newest criteria available in literature to get the resistance values of punching shear at slab-column connection under gravity an lateral loads, will be performed.

1.2 Structure of the Thesis

This thesis has been structured into seven chapters

- Chapter 1: This chapter introduces the main topic and offers an overall overview of the work done in this dissertation. Here, the reasons and objectives for developing this thesis are also presented.
- Chapter 2: The available literature is addressed here in order to identify the past work that researchers have done on the behavior about flat-slab structures under lateral loading.
- Chapter 3. The available methods capable of modeling flat-slab structures under lateral loads are presented.

- Chapter 4. The punching shear phenomenon is described here, and several different models developed throughout the years are reviewed. Current provisions included in codes to compute the shear resistance of a slab-column connections are also given here.

- Chapter 5. A detailed description of the three structures analyzed is given here. The experimental research, this work has been base on, is also described in this chapter.

- Chapter 6. The results obtained are processed, presented, and discussed. Some recommendations are given based on the results obtained.

- Chapter 7. Here, the final conclusions are highlighted. It is also stated here, if the objectives have been achieved given all the analysis and results obtained.

Chapter 2

State of the art

The increasing use of flat-slab systems in seismic European regions has resulted in a rise of interest on the part of many researchers because the behavior of this type of structure under seismic actions is not yet perfectly understood. In recent years, significant number of experiments have been conducted to evaluate the behavior of this type of structures under cyclic lateral loading in order to provide a solid base experimental knowledge to be included in construction codes.

The current version of Eurocode 8 [2] does not provide specific rules for the design of flat-slabs for seismic actions. Only Eurocode 2 [3] provides specific provision for the design of flat-slabs and punching verification under the action of gravitational loads. To overcome this situation, experimental works on slab-column connections under cyclic loading, along with the development of suitable model for design, have been carried out.

At the time of writing this dissertation, many experiments conducted are mainly based on small-scale test with isolated internal slab-column connections [4]. Generally, all the experiments that have been carried out over time, can be classified into three main categories: isolated slab-column connections, single complete floors, and complete frames consisting of at least two stories [5].

2.1 European experimental research

In 1993, Farhey et al. [6] conducted one of the first tests in Europe on isolated flat slab-column connections subjected to horizontal loading (Fig. 2.1). The main objectives of this work were to study the resistance and final shear failure mechanism of the specimens, the influence of the cross-section dimension of the column and the contribution of the vertical gravity load on shear resistance of the slab-column connection.

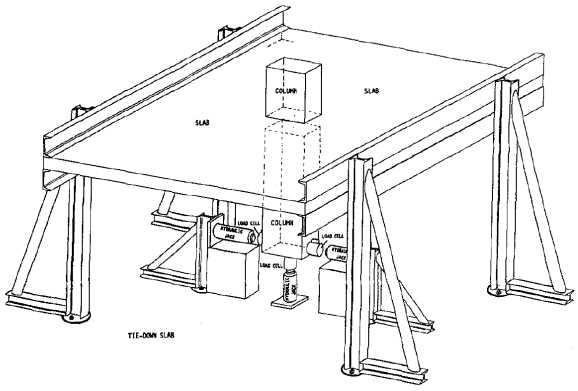

Figure 2.1: Test setup. Farhey et al. [6]

Later in Portugal, several tests on flat slab-column connection were carried out. Five specimens were tested under combined vertical and horizontal loading by Almeida et al. [7]. They showed that horizontal cyclic loading is very harmful to slab-column connections, producing a high detrimental effect on the stiffness of the connection and, consequently, high horizontal inter-story drifts ratios. Additional test were carried out considering specimens with punching shear reinforcement, such as stirrups [8], headed studs [9] [10] and post installed bolts [11].

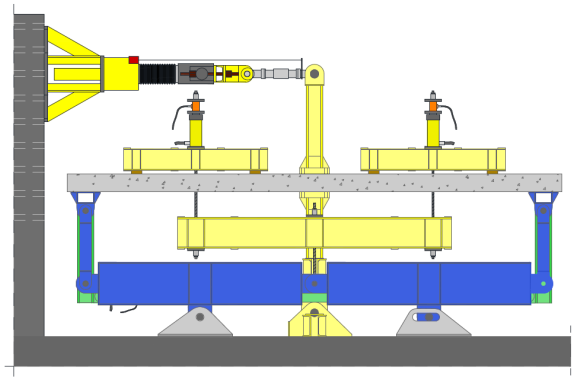

Figure 2.2: Test setup. Almeida et al. [7]

Testing a full scale internal connection specimens without transversal reinforcement, Drakatos et al. [12] evaluated the influence of different lateral load history (monotonic vs reversed cyclic) for different gravity loads and reinforcement ratios. They demonstrated that cyclic loading produces a reduction of the deformation capacity, specially for slabs with low reinforcement ratios. Additionally, they confirmed that the increasing of gravity loads reduces the stiffness and the moment capacity of slab-columns connections.

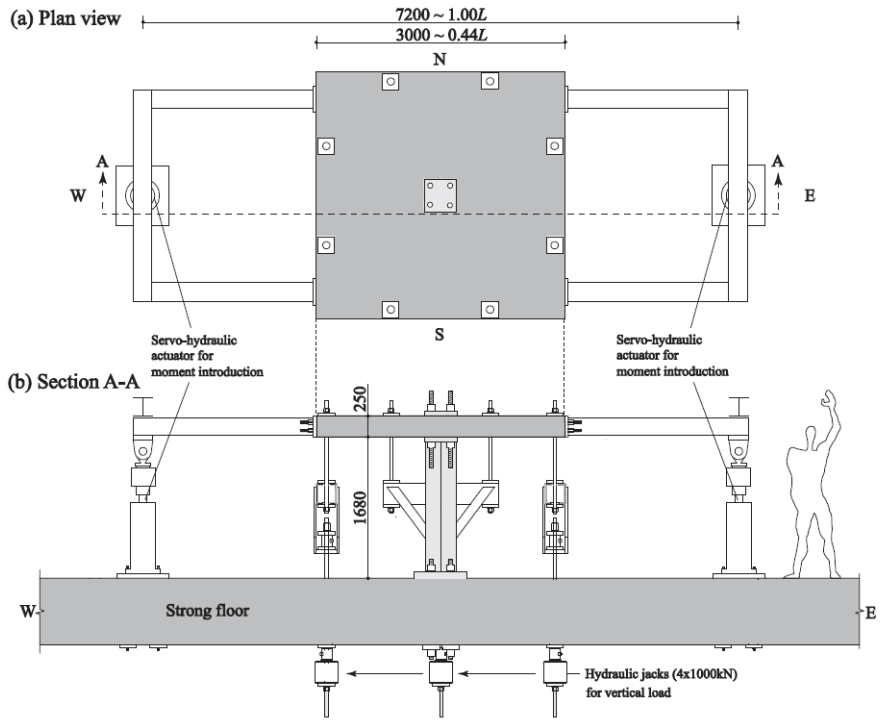

Figure 2.3: Test setup. Drakatos et al. [12]

In literature, experimental research in Europe on real scale multi-story flat-slab buildings is really limited. With the aim of assessing the seismic response of a flat slab structure, Coelho et al. [13] carried out a pseudo-dynamic tests on full-scale three story Reinforced concrete flat-slab building. The specimen (Fig. 2.4), with only one bay on each direction was set up in order to study the behavior of the different types of slab-column connection (internal, edge and corner column connection). Results showed a serious damage in edge columns due to the accumulation of torsion and flexural effects. It was also confirmed the small slab participation against lateral loads and the higher flexibility of the system compared to traditional frame structures. For this reason, the authors suggested the use of lateral resisting structural elements to limit deformation under earthquake excitation.

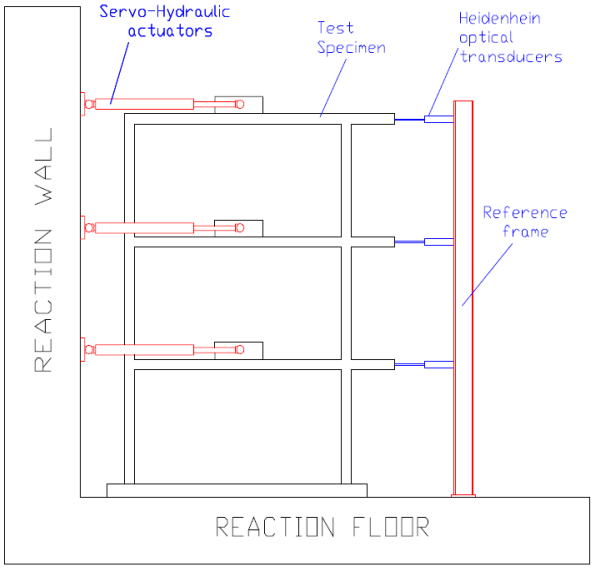

Figure 2.4: Test setup. Coelho et al. [13]

One of the most recent work at the moment this dissertation was written, was carried out by Coronelli et al. [1]. They tested a full-scale two-story flat slab structure with three by two bays, allowing the evaluation of the performance of interior, edge, and corner slab-column connections under gravitational and lateral loads. The principal objectives of this research program were to verify the seismic performance of flat slab frames in structures with earthquake resistant walls and to study the performance of the system beyond the design displacements [14].

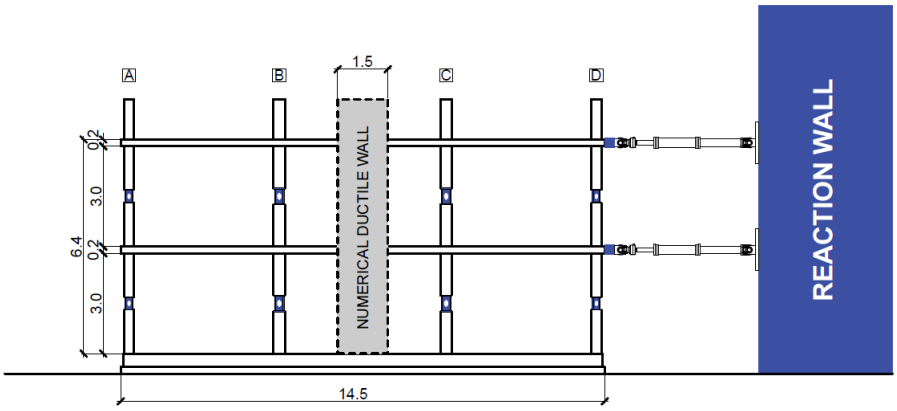

Figure 2.5: Test setup. Coronelli et al. [14]

The results of the tests carried out by Coronelli et al. [1] indicate that flat slab structures combined with shear walls have a nearly elastic response, with a maximum inter-story drift ratio of 0.4% under lateral loading at Ultimate Limit

State. It was also observed that for a flat slab structure without lateral resisting elements, a global ultimate drift ratio higher than 2.5% is reached, confirming the existing knowledge in the literature.

2.2 North American experimental research

North American research has produced a larger database of tests. Extensive studies have been carried out since 1970s leading to the implementation in code specifications. Most of the old experimental data was summarize by Pan and Moehle [15], the database consisted of small-scale tests on isolated internal slab-column connections without shear reinforcement under vertical and lateral loads.

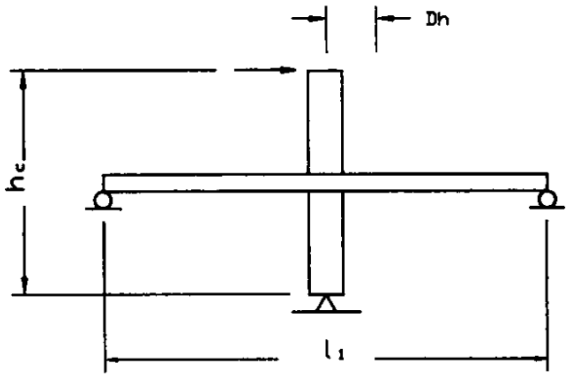

Figure 2.6: Schematic setup for tests from database. Pan and Moehle [15]

They stated that the level of gravity load applied to slab is crucial for the lateral ductility of the specimens establishing a relationship between the drift of the structure and the Gravity Shear Ratio (GSR).

In 1984, Moehle and Diebold [16] carried out tests on a two-story reinforced concrete flat-slab structure on a shaking table. The structure was built at 0.3 full-scale of a typical residential building. The structure was tasted using 11 base motions of increasing intensity up to 0.83g lateral acceleration. The specimen behaved elastically until it reached 1.5% of drift ratio. A maximum drift ratio of 5% was registered without reaching collapse of the structure.

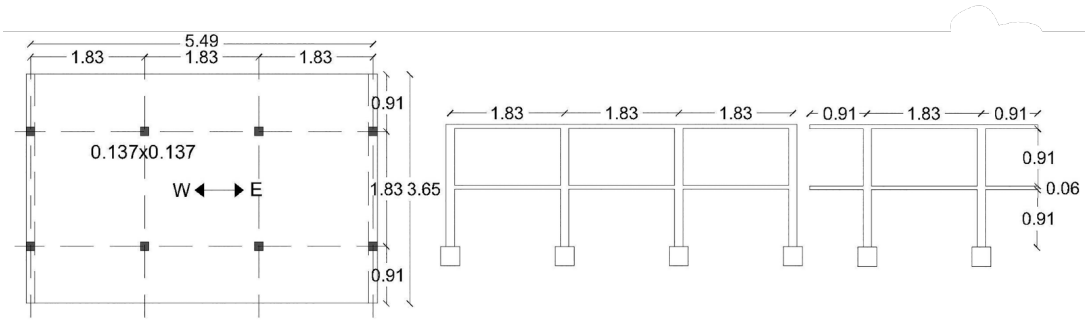

Figure 2.7: Specimen geometry. Moehle and Diebold [17]

Later, Hwang and Moehle [18] tested a reinforce flat-slab structure constructed at 0.4 full-scale. The slab was composed of nine panels and without shear reinforcement. Different column geometries and reinforcement layout in the slab-column connection were used. The specimen was tested under vertical and biaxial lateral loads, in fact, this is the only studied that considered biaxial lateral loading. The structure showed an elastic response up to 1% of drift and a maximum drift capacity of 4%. Punching of several connections were observed at drift between 3.1% and 3.7%. The GSR was equal to 0.3.

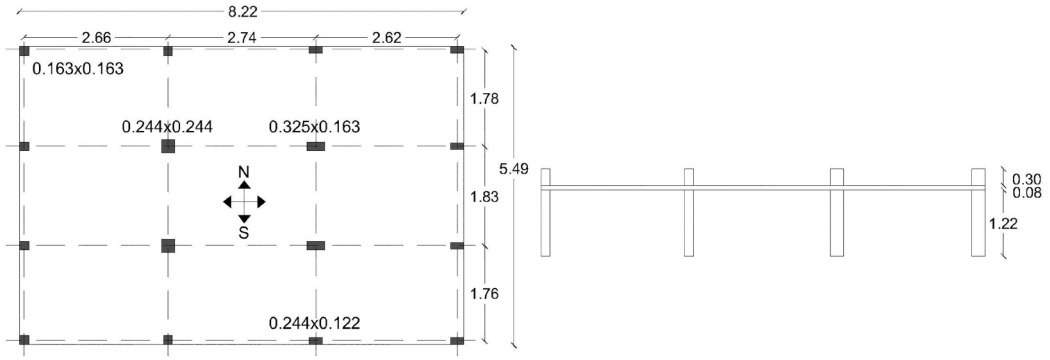

Figure 2.8: Specimen geometry. Hwang and Moehle [17]

Kang and Wallace [19] performed shake table tests on an approximately 1/3 scale two reinforced concrete two-story slab column frames in 2004. One of the specimens consisted of post-tensioned slab and both had punching shear reinforcement consisted of stud rails. They obtained through the experimental testing, lateral drift ratios of around 3% and 4% before punching failure for the reinforced concrete and the post tension frame, respectively. For the reinforce concrete structure, a peak value of 3.4% was registered with a clear strength deterioration after a drift ratio of 2.5%.

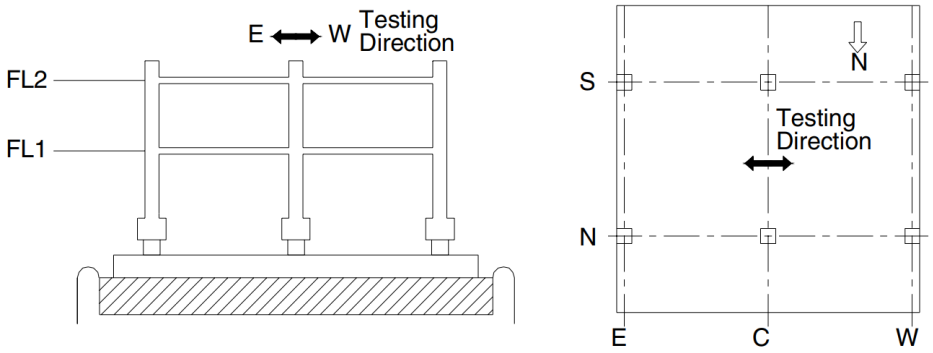

Figure 2.9: Test Specimen. Kang and Wallace [19]

Additional experimental studies were carried out by Rha et al. [20]. They tested five half-scale reinforced concrete slab-column frame specimens under gravity and lateral loads. The specimens were intended to represent a complete story of two-by-two bays. Different slab reinforcement ratios were used along with different loading histories (monotonic versus reversed cyclic). Maximum drift ratios between 4 and 6% were registered. It is worth noticing that the internal joins punched at 1.5% for cyclic loading whereas the same connection failed at 5.5% drift for monotonic loading.

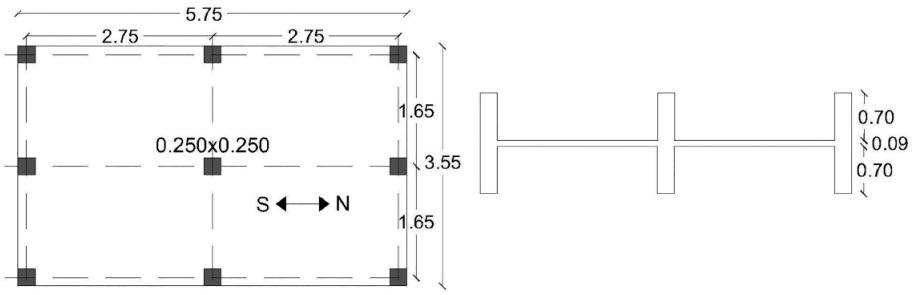

Figure 2.10: Specimens geometry. Rha et al. [17]

Most recent work has been developed by Fick et al. [21]. They studied a full-scale three-story reinforced concrete flat slab frame (Fig. 2.11). The structured was tasted under cycles of increasing quasi-static lateral displacement imposed at the top floor. The structures reached a roof drift ratio of 1.5% without any important structural damage. When the roof ratio reached the value of 2.9%, punching failure was observed in the internal slab-column connection with an inter-story drift ratio of 3.3%.

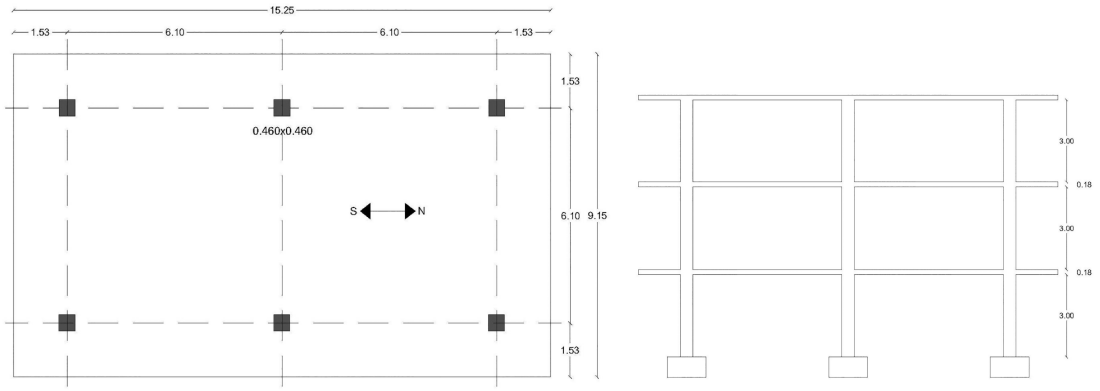

Figure 2.11: Specimen geometry. Fick et al. [17]

Summarizing all the data from North American and European literature which was previously described, it can be observed that slab-column connections reach ultimate drift ratios with values between 2.5% an 6% for gravity shear ratios corresponding to typical design situations (between 0.2 and 0.4) [17].

The lack of tests and analysis on full-scale structures due to laboratory dimensions and economical limitation, seems to be one of the biggest problems to acquire an accurate representation of the phenomenon. It is also evident that there is a need for developing a deeper knowledge of the behavior of slab-column connection as a part of the whole structure (real scale buildings) and to adequate practical provisions and recommendations inside codes for the design of flat slab elements under seismic actions.

Chapter 3

Existing methods for modelling flat-slab structures

The study of the behavior of a flat-slab structure in seismic zones, is becoming more and more important since its use has been increasing in recent years. Although many uncertainties exist derived from the lack of knowledge and understanding about the performance of slab-column connection under lateral loading, different methods to analyze and design flat-slab structures has been developed over the years. Nowadays, the most used methods of analysis for determining the actions acting on this type of structures are the Finite Element Method, along with another practical method described in American regulations (ACI Building Code), the Equivalent Frame Method.

3.1 Equivalent Frame Method

The Equivalent Frame Method (EFM) is a simple approximate method for the analysis of two-way slabs systems under gravity and lateral loads [22]. This method is capable of representing a tri-dimensional structure by a series of two-dimensional frames running into the two directions of the building (Fig. 3.1). Each equivalent frame, in which the structure is divided, consists of a row of columns and a wide continuous beam oriented along the column centerlines. This wide beam is bounded laterally by panel centerlines on either side of the columns.

Basically, the equivalent frame is divided into three main parts (Fig. 3.2):

- The horizontal slab strip, including any beams that are present.
- The vertical support elements.
- Any existing additional element providing moment transfer between horizontal and vertical elements (e.g. drop panels).

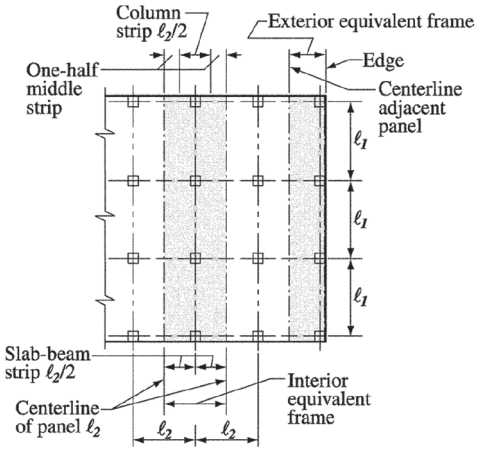

Figure 3.1: In plan subdivision of equivalent frames [22]

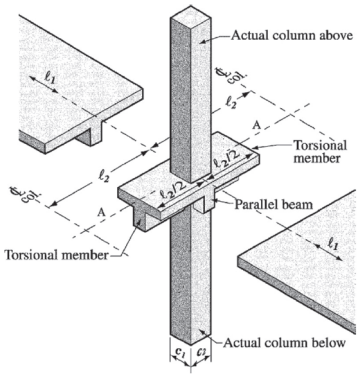

Figure 3.2: Equivalent frame [22]

When only gravity loads are acting in the structure, EFM allows each floor to be considered as a separately frame with far ends of columns fixed. Under lateral loads, the entire frame must be considered for the analysis. Therefore, the complete analysis of a slab system for a building, consists of analyzing a

series of equivalent frames spanning longitudinally and transversely through all the building.

The horizontal members in the equivalents frame are referred to as slab-beams elements. These elements consist of either only a portion of the slab with or without drop panels, or the slab and beams running parallel to the equivalent frame. The stiffness of the slab-beams elements may be based on the gross area of the uncracked cross section of the concrete. The increased stiffness of members within the column slab joins when drop panels are present, is accounted for. Additionally, any variation in the cross section at points outside of joints must be also considered.

It is also important to highlight that the moment of inertia of slab-beams elements framing into the column, from the center column to the face of the column, is stiffer than the clear span portion of the element. Here, the moment of inertia is assumed to be equal to the moment of inertia of the slab-beam at the face of the column divided by the quantity [1 - c_2/l_2]^2.

$$I_{gc} = \frac{I_g}{\left[1 - (c_2/l_2)\right]^2} \tag{3.1}$$

Where:

I_{gc}	is the uncracked moment of inertia inside the column;
I_g	is the uncracked moment of inertia just outside the column;
c_2	is the column side dimension in transversal direction;
l_2	is the slab beam width of the equivalent frame

Regarding to columns members, the moment of inertia of columns at any section outside of the joints may be based on the gross area of the concrete, allowing any variations in the moment of inertia due to changes in the column cross section along the length of the element. Within the depth of the slab-beam at a joint, moment of inertia must be assumed to be infinite. Although the stiffness in this part is infinite, slab-beams elements are able to rotate which allows moment redistribution between adjacent panels.

Column stiffness is based on a column length from the middle depth of the

slab above to the middle depth of the slab below. The equivalent stiffness of the column takes into consideration the flexural stiffness and the contribution of the torsional stiffness of the slab-beams member framing into the column. The stiffness of the equivalent columns can be found as:

$$\frac{1}{K_{ec}} = \frac{1}{\sum K_c} + \frac{1}{K_t} \tag{3.2}$$

Where:

$\sum K_c$	is the sum of flexural stiffness of the columns above and below the slab which frame into the join being considered;
K_t	is the torsional stiffness of slab-beams framing into the column

According to ACI 421.3R-15 [22] ,several simplified assumptions are required in order to compute the torsional stiffness. An approximate expression for the torsional stiffness of the slab-beams elements framing into the column is shown below:

$$K_t = \sum \frac{9E_{cs}C}{l_2\left(1 - \frac{c_2}{l_2}\right)^3} \tag{3.3}$$

Where:

E_{cc}	is the Young's modulus of concrete;
C	is the torsional constant

The torsional constant is defined by the following expression:

$$C = \sum \left(1 - 0.63\frac{x}{y}\right)\frac{x^3 y}{3} \tag{3.4}$$

Where:

x	is the shorter dimension of the rectangular area considered of the torsional element;
y	is the longer dimension of the same area

Finally, the value k_{ec} obtained, based on the flexibility of the column and the torsional member, is the equivalent stiffness used in the analysis to compute the internal action acting in the frame.

Despite the fact this method offers a simple way to analyze a flat slab structure and it also provides good results for simple structures, in some cases it can result cumbersome depending on the complexity of the structure. In addition to this, many considerations and simplification are done under the fact that only gravitational loads are acting (e.g. simplification for computation of torsional stiffness). This could lead to a serious potential errors when designing a flat-slab structures under lateral loads.

3.2 Finite Element Method

The Finite Element Method (FEM) is a powerful computational tool for analyzing flat-slabs and in general, every structural element. In this method, the slab member is divided into a mesh of elements having a finite size. These finite elements are usually triangular or quadrilateral elements connected at nodes. It is an approximate numerical method and its accuracy depends primarily, on the size of the finite element.

Generally, FEM is used when the geometry of the slab is very complex, there are openings or when unusual loads are present. Although many FEM software are available and they are relatively simple to use, the designer must understand how the software is working and what is the best way to model a structure because, depending on the size of the mesh, the geometry of the finite element, the material properties and the boundary conditions; the accuracy of the results can significantly be affected. Additionally to this, the engineer is responsible of the validation of the results before using them for designing. The most simple and basic verification is the validation of equilibrium in the vertical and horizontal direction.

The principal disadvantages of using FE analysis for modelling a flat-slab structure are listed below:

- Setting up the model can take a relative high time, especially for complex

geometries.

- Coupled with the high time consuming of setting up the model, human errors can also be present and difficult to be identified during checking of the model.
- It requires a high level of expertise and engineering judgment by the user.
- When the structure being modeled is large and very complex, a significant computational power and time is necessary. Sometime the complete modeling of a structure is unviable leading to carry out an analysis floor by floor.

Some FEM software can perform both, linear and non-linear analysis. Generally, linear analysis is enough to carry out the design at ultimate limit states. To perform a linear analysis some assumptions are considered, one of the is the assumption that reinforced concrete is as an isotropic and homogeneous material, which in reality it is not. When a more sophisticate analysis is needed, non-linear analysis is used. This analysis is especially useful when the cracked behavior of the concrete, or the yielding of the steel needs to be modeled.

A description of how the modeling of a flat-slab member should be carried out using linear analysis, is described below.

First of all, the initial dimensioning of the structural elements should be performed by and initial hand calculation for ultimate limit state conditions. Once the initial dimensioning of the members is completed, the mesh of finite elements is created. As a recommendation, elements should not be grater than 1/10 times the span length or 100 cm, whichever is the smallest. Additionally, the size of finite elements must be reduced at critical location (e.g slab-column connections, zones of concentrated loads).

Boundary conditions shall be correctly selected. Two approaches can be used to model boundary conditions. In the first approach, the columns below and above the slab are model using frame or three-dimensional elements in order to account for the flexural effects of the columns. For the second approach, either the column supports are modeled as pin or fixed supports, or as springs with finite elastic stiffness. When column supports are modeled using point supports, the area of the column should be modeled by inserting a thicker region in the

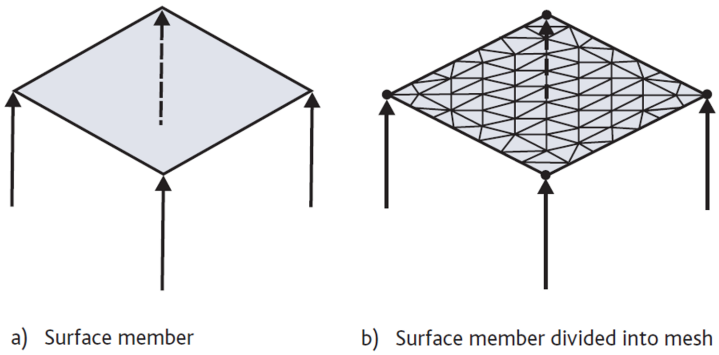

Figure 3.3: Typical slab meshing [23]

slab within the area of the column or by placing rigid arms between the column centerline and its perimeter [23].

The next step after setting up the model is to run the analysis. The output of the analysis is given in terms of bending moments in x and y direction and twisting moments. It is important that the software allows to incorporate the twisting moments in the design. Generally, twisting moments will be considered by most of FEM software using the Wood and Armer Method. This method is slightly conservative, and it considers the Johansen's yield criterion focusing on avoiding the yielding of the reinforcement in all directions. In general, results are presented by Wood Armer moments with four components, top (hogging) moments and bottom (sagging) moments in X and Y-directions.

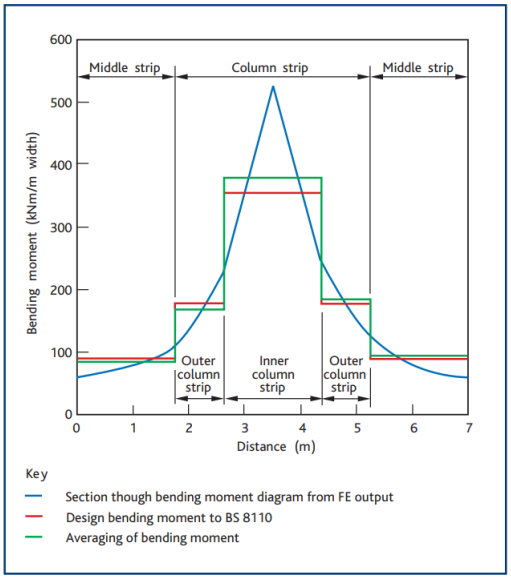

Figure 3.4: Distribution of output bending moments [23]

Finally, the results obtained cannot directly be used for the designing of the slab. Very large bending moment peaks can be spot at the column supports, the design of reinforcement for these huge bending moments should be avoided. Instead, and averaging of the bending moments acting in the finite elements over the width of column and middle strips must be done for designing.

For the evaluation of the punching shear, the reaction at the column where the slab is supported, is used to carry out the checks according to the provision inside the code of practice being used.

It is important to be aware that the Finite Element analysis will no produce lower results compared to another methods and when it is used correctly, FEM is a powerful tool to for analyzing any type of structural elements.

Chapter 4

Punching shear phenomenon

Generally, shear action in a slab-column connection is not critical when the slab is supported by beams or walls. However, in flat-slabs structures, shear can be critical around the vicinity of columns where concentrated forces are transferred. When the shear resistance is not enough to withstand the acting stresses a punching shear failure may occur.

Punching shear must be strictly avoided, since it is a brittle failure and it can lead to disastrous consequences. Punching shear failure (Fig. 4.1) is generated by the interaction between the column and the slab. Around the supporting columns, high values of shear are generated. The ultimate strength of flat slabs is usually determined by the punching shear failure load, which is generally smaller than the flexural failure load.

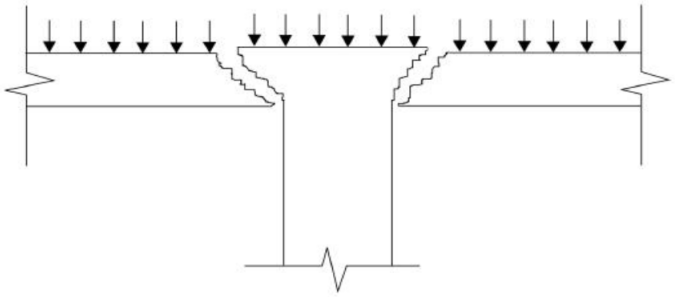

Figure 4.1: Punching shear failure

Most of the practical formulation to assess the shear strength of a flat slab-

column connection included in codes, are based primarily on experimental tests. The complexity of the failure pouching mechanism in the cracked slab makes impossible to rely the practical design on mechanical models that have been developed over the last years. Most relevant mechanical punching models and code provisions to evaluate the shear strength of a flat slab-connection are presented below.

4.1 Mechanical punching shear models

4.1.1 Kinnunen/Nylander

Based on tests carried out in 1960 on circular slabs with circular column stubs (Fig. 4.2), this model considers the formation of shear cracks, the deformation of elements and the expansion of the concrete and steel as its most important fundaments to predict the punching shear failure. Shear strength is calculated imposing equilibrium on a sector element which is limited at the sides by radial cracks and in the front by tangential shear cracks.

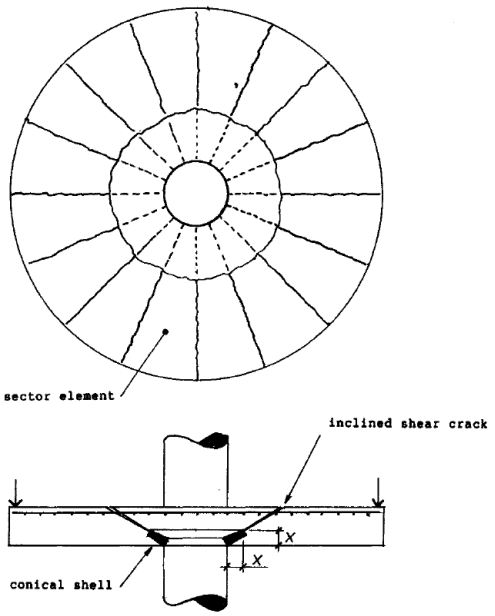

Figure 4.2: Kinnunen & Nylander punching shear model [24].

Kinnunen & Nylander [25] developed a formula to evaluate the punching strength of a slab-column connection, based on a rotational mechanical model (Fig. 4.3)

and assuming that the punching shear failure is reached for a given critical slab rotation ψ [26]. In this model, each sector element is assumed to act as a rigid body supported by a compressed imaginary conical shell. Therefore, failure criterion is defined by the ultimate tangential compressive strain of the concrete at the column face.

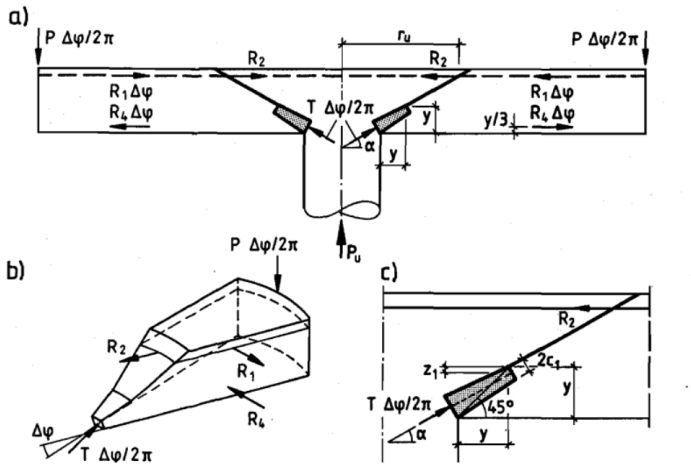

Figure 4.3: Mechanical model of Kinnunen & Nylander [27].

Although this model remains one of the best ones to describe the punching shear phenomenon, it has never been fully included in any building code because of its complexity.

4.1.2 Broms

In 1990, Broms [24] proposed a modification to the model of Kinnunen & Nylander [27]. Here, Broms introduced characteristic values for concrete properties, different compression zone heights in radial and tangential direction, more realistic position for the bottom of the stable shear crack and also, unsymmetrical punching shear and size effect related to the thickness of the slab.

For Broms, two different punching failure mechanism can occur in the vicinity of slab-column connections. Punching shear failure occurs when the concrete in compression near the column is distressed by either a high circumferential strain or a high radial stress (V_ε and V_σ denote the corresponding ultimate capacities respectively).

When the tangential concrete strain in the compression zone around the column

exceeds a critical value (Fig. 4.4), cracks will start to from parallel to the compression direction [27]. Therefore, shear cracks will propagate to the column face and cause punching shear mechanism failure. Critical tangential concrete strain ε_{cpu} is function of the concrete strength and the thickness of the compression zone according to the following equation:

$$\varepsilon_{cpu} = 0.0008 \left(\frac{150}{\alpha x_{pu}} \cdot \frac{25}{f'_c} \right)^{0.333} \tag{4.1}$$

Where:

150	is the diameter of a test cylinder specimen;
x_{pu}	is the high of the compression zone at flexure in tangential direction when punching occurs;
αx_{pu}	is the high of the equivalent rectangular stress block with the stress f'_c;
f'_c	is the concrete cylinder strength.

Once ε_{cpu} is determined, punching failure load V_ε, and the corresponding deformation can be computed based on linear elastic hypothesis [24]. Additionally, this calculation is carried out as a function of the reinforcement ratio to consider possible yielding or failure of the reinforcement.

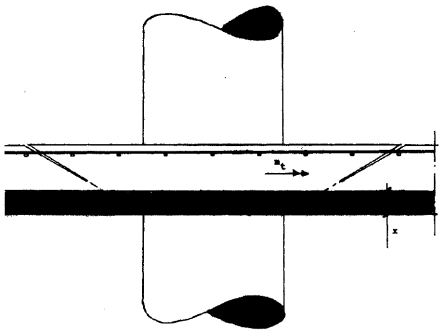

Figure 4.4: High tangential compression strain failure mechanism [24].

The second punching failure mechanism occurs when radial concrete compression stress, in an imaginary conical shell with a constant thickness and inclined 15°, reaches a value of 1.1 f'_c at the bottom of the shear crack (inclined 30°). The

factor 1.1 comes from the increase of concrete strength due to biaxial state of stresses.

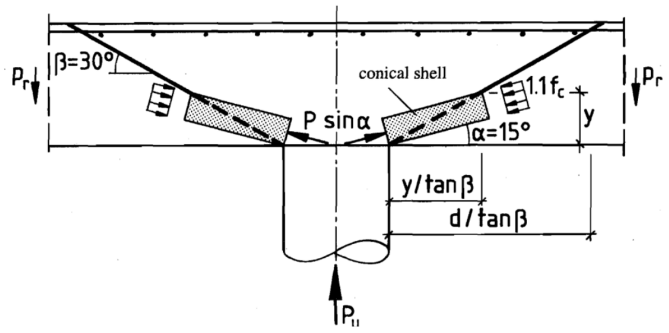

Figure 4.5: High radial compression stress failure mechanism at shear loading [27].

As a result, the punching load V_σ can be determined by equilibrium in the vertical direction according to Eq. (4.2). In this equation, size effects and height of compression zone in the radial direction are considered.

$$\underline{\sum V} : V_\sigma \approx 0.46 \cdot (b + 3.5y) \cdot y \cdot f'_c \cdot \left(\frac{150}{0.5y}\right)^{0.333} \tag{4.2}$$

Where:

150	is the diameter of a test cylinder specimen;
y	is the approximate thickness of conical shell:
b	diameter of the column;
f'_c	is the concrete cylinder strength

4.1.3 Muttoni

Based on the principal ideas of the Kinnunen & Nylander's model [25], Muttoni proposed a new failure criterion for punching shear strength [26]. This criterion describes the relationship between the punching shear strength and the rotation of the slab at failure (Fig. 4.6). This model accounts for size effects and it correctly describes the experimental evidence.

Muttoni found out that punching shear resistance decreases with increasing

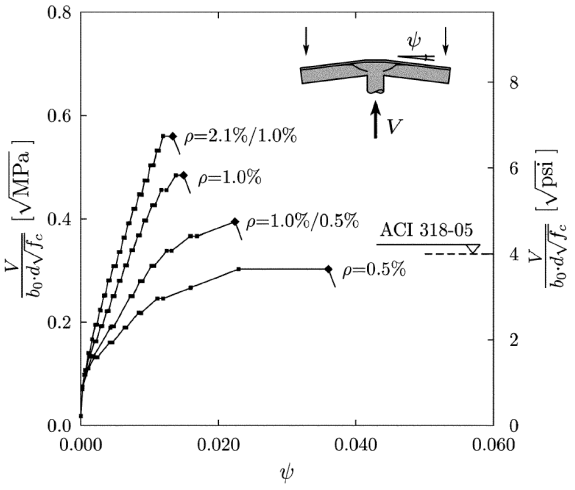

Figure 4.6: Load-rotation curves from tests by Kinnunen & Nylander [26]

rotation of the slab. This occurs due to the propagation of a critical shear cracks through the slab into the inclined compression strut carrying the shear force to the column (Fig. 4.7).

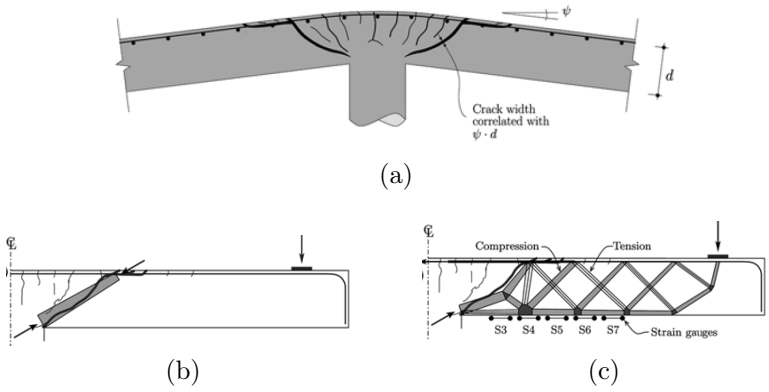

Figure 4.7: Mechanical model of Muttoni. (a) Cracking pattern of slab after failure;(b) theoretical strut developing across the critical shear crack; and (c) elbow-shaped strut. [26]

In this model, the width of the shear critical crack is assumed to be proportional to the slab effective depth d and to the rotation angle of the slab ψ (Fig. 4.7a). This assumption, first proposed by Muttoni and Schwartz in 1991 [28], helped to develop the following equation in which, the size effect and the rotation of the slab are included to determine the punching shear strength.

$$\frac{V_E}{b_0 d^3 \sqrt{f_c}} = \frac{1}{1 + \left(\frac{\psi d}{4mm}\right)^2} \quad (SI\ units) \tag{4.3}$$

Where:

- d is the average flexural depth of the slab;
- b_0 is the perimeter of the critical section located d/2 from the face of the column;
- ψ is the critical rotation;
- f_c is the specified concrete compressive strength

Later, this failure criterion was improved by himself in 2003. With this improvement, he took into consideration that the amount of shear that can be transferred across the critical shear cracks depend on the roughness of the crack (which is function of the maximum size of the aggregate), leading to the following equation:

$$\frac{V_R}{b_0 d\sqrt{f_c}} = \frac{3/4}{1 + 15\frac{\psi d}{d_{g0}+d_g}} \quad (SI\ units) \tag{4.4}$$

Where:

- d_g is the maximum aggregate size;
- d_{g0} is a reference size equal to 16 mm

This improvement in the failure criterion showed a good approximation to the experimental data (Fig. 4.8).

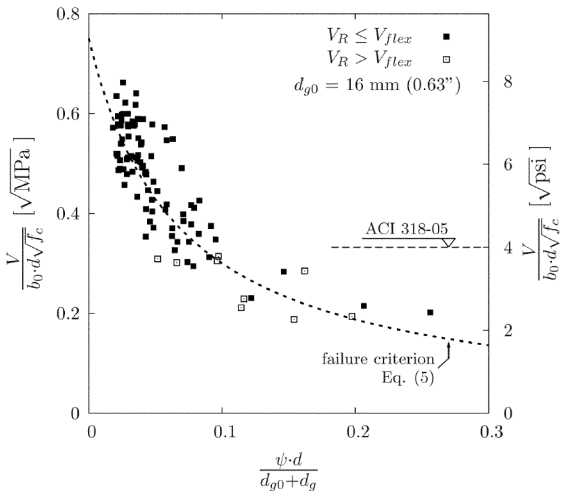

Figure 4.8: Failure criterion proposed by Muttoni [26]

In this model, punching shear failure occurs at the intersection of the failure criterion with the load rotation curve (Fig. 4.6). For practical design, he presented a simple formula to predict the load-rotation relationship. Once the load-rotation curved is defined, the intersection of this curve with the curve described by the failure criterion in Eq. (4.4), defines the critical load at punching shear failure Fig. 4.9.

$$\psi = 1.5 \frac{r_s}{d} \frac{f_y}{E_s} \left(\frac{V}{V_{flex}} \right)^{3/2} \tag{4.5}$$

Where:

r_s	is the radius of the isolated slab element;
d	is the effective depth of the slab;
f_y	is the yield strength of reinforcement;
E_s	is the modulus of elasticity of reinforcement;
V	is the shear force;
V_{flex}	shear force associated with flexural capacity of the slab

V_{flex} is computed according to the following equation:

$$V_{flex} = 2\pi m_R \frac{r_s}{r_q - r_c} \tag{4.6}$$

$$m_R = \rho \cdot f_y \cdot d^2 \left(1 - \frac{\rho \cdot f_y}{2 \cdot f_c} \right) \tag{4.7}$$

Where:

m_R	is the nominal moment capacity per unit width;
r_q	is the radius of the load introduction at the perimeter;
r_c	is the radius of a circular column;
f_c	is the average compressive strength of concrete (cylinder);
ρ	is the reinforcement ratio;

One of the biggest improvements of this model is that it allows to find the value of the rotation capacity of the slab and therefore, its ductility. Additionally, this

method takes into account the size effect and the slab depth in the computation of shear resistance. This method resulted to be really simple and powerful because it offers a good match with experimental results. Later, this model was named as the Critical Shear Crack Theory (CSCT).

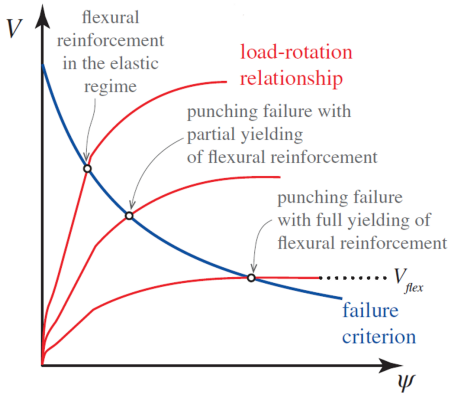

Figure 4.9: Potential punching shear failures [29]

Further studies were carried out by Muttoni et al. [29]. In 2018, they investigated and justified a power-law expression to characterize the failure criterion of the CSCT. When this criterion is used with a correct lead-deformation relationship, a close form expression for punching shear design for elements without shear reinforcement can be obtained. They provided a simple design approach for punching shear, which has been proved to be general and efficient. This formulation also takes into account size and strain effects in the slab.

According to these studies, the slab rotation can be determined according to the following equation:

$$\psi = k_{cs} \cdot k_m \frac{r_s}{d} \cdot \frac{f_y}{E_s} \left(\frac{V}{V_{flex}} \right)^{3/2} \tag{4.8}$$

$$k_{cs} = \left(0.08 \cdot \frac{m_R}{m_{cr}} \right)^{3/2} \leq 1 \tag{4.9}$$

Where:

m_{cr} is the cracking moment per unit length;

k_m is a factor depending on the level of refinement used to estimate the acting bending moment, 1.2 for refined analysis or 1.5 otherwise.

Thus, the punching shear resistance can be calculated as:

$$V_{Rc} = k_b \cdot \left(100\rho \cdot f_c \cdot \frac{d_{dg}}{k_{cs} \cdot r_s}\right)^{1/3} \cdot b_0 \cdot d \leq 0.55 \cdot b_0 \cdot d\sqrt{f_c} \tag{4.10}$$

$$k_b = \sqrt{8 \cdot a \cdot \frac{d}{b_0}} \geq 1 \tag{4.11}$$

Where:

b_0 is the length of control perimeter;

a is the ratio between acting shear force and average moment in the support strip, it can be taken 8 for inner columns

These closed form equations, which are derived from CSCT to calculate the shear resistance of slab-column connection without shear reinforcement, shows a good match with experimental results. Additionally, this formulation also considers in a correct way, the influence of different mechanical and geometrical properties of the element. For all of the above mentioned, this model is considered as one of the most simple and reliable models to be used in practical design.

4.2 Code provisions

4.2.1 Eurocode 2

No specific provision for the design of flat-slabs under seismic action as primary elements are given in Eurocode 8 [2]. Eurocode 2 [3] only considers the design of flat-slabs and punching verifications for the effects of gravity loads.

Because of the complexity of the punching shear problem, Eurocode 2 suggests a simplified procedure to verify the punching shear failure. Two basic verifications need to be performed, the first one at the face of the column and the second one at a basic control perimeter u_1. The model established by Eurocode 2 to evaluate punching failure at the Ultimate Limit State (ULS) is shown in Fig. 4.10.

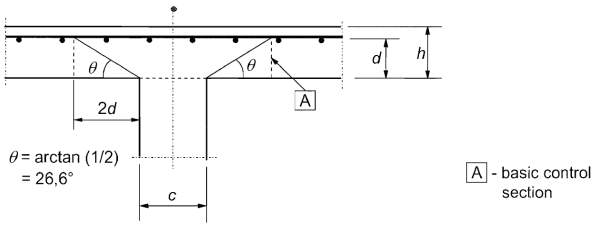

(a) Section

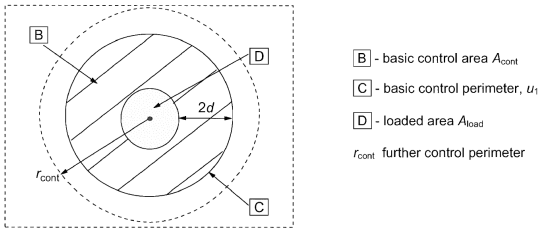

(b) Plan

Figure 4.10: Verification model for punching shear [3].

The basic control perimeter u_1 is defined according to the column geometry (Fig. 4.11). Usually, it may be taken to be at a distance $2d$ from the loaded area. Where d is the effective depth of the slab, and it is assumed to be constant.

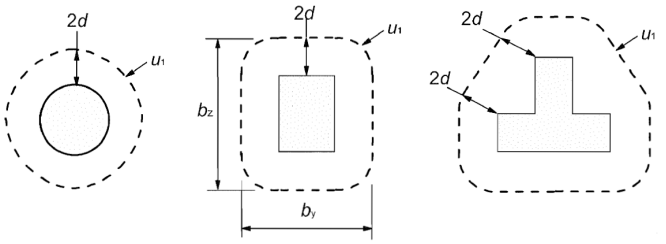

Figure 4.11: Basic control perimeters [3].

For a slab-column connection situated near an edge or corner, the control perimeter shall be taken as shown in the following figure:

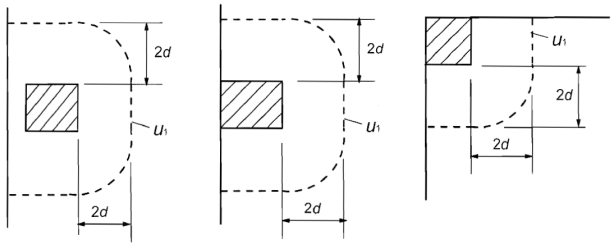

Figure 4.12: Basic control perimeters for slab-column connections [3].

At any control section, the shear resistance must be greater than the shear demand. According to Eurocode 2, the following checks should be carried out:

- At column face, the maximum resisting punching shear stress must not be exceeded.

$$v_{Ed} \leq v_{Rd,max} \tag{4.12}$$

Where:

v_{Ed}	is the maximum acting shear stress;
$v_{Rd,max}$	is the design value of the maximum punching shear resistance along the control section considered.

$v_{Rd,max}$ can be calculated as follows:

$$v_{Rd,max} = 0.4\nu f_{cd} \tag{4.13}$$

$$\nu = 0.6\left[1 - \frac{f_{ck}}{250}\right] \quad (f_{ck}\ in\ MPa) \tag{4.14}$$

Where:

f_{cd}	is the design value of concrete compressive strength;
f_{ck}	Characteristic compressive cylinder strength of concrete at 28 days.

- At the basic control perimeter, the resisting shear stress must be grater than the acting shear stress.

$$v_{Ed} \leq v_{Rd,c} \tag{4.15}$$

Where:

$v_{Rd,c}$	is the design value of the punching shear resistance of a slab without punching shear reinforcement along the control section considered.

Under horizontal loading or when the support reaction is eccentric with respect to the control perimeter, an unbalanced moment is generated at the slab-column node. This moment is transferred from the slab to the column, generating an increment in the demand of shear resistance. To consider the presence of an unbalanced moment, Eurocode 2 modifies the value of the acting shear by the factor β. In these cases, the maximum stress should be taken as:

$$v_{Ed} = \beta \frac{V_{Ed}}{u_1 d} \tag{4.16}$$

The value of β can be obtained as following:

$$\beta = 1 + k \frac{M_{Ed}}{V_{Ed}} \cdot \frac{u_1}{W_1} \tag{4.17}$$

Where:

V_{Ed} is the acting shear force;

M_{Ed} is the unbalanced moment transfer from the slab to the column;

k is a coefficient dependent on the ratio between the column dimensions: its value is a function of the proportions of the unbalanced moment transmitted by uneven shear and by bending and torsion (see Table 4.1)

V_{Ed} corresponds to a distribution of shear as illustrated in Table 4.1 and is a function of the basic control perimeter u_1:

$$W_i = \int_0^{u_1} |e| \, dl \tag{4.18}$$

Where:

dl is a length increment of the perimeter;

e is the distance of dl from the axis about which the moment M_{Ed} acts

For a rectangular column, the value of W_1 is shown in the following expression:

$$W_1 = \frac{c_1^2}{2} + c_1 c_2 + 4 c_2 d + 16 d^2 + 2\pi d c_1 \tag{4.19}$$

Where:

c_1 is the column dimension parallel to the eccentricity of the load;

c_2 is the column dimension perpendicular to the eccentricity of the load

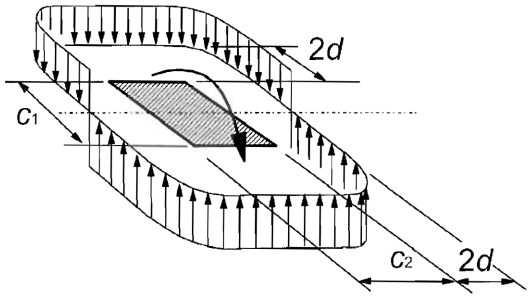

Figure 4.13: Shear distribution due to an unbalanced moment at a slab-internal column connection [3].

Values of k for rectangular loaded areas are reported in the following table:

Table 4.1: Values of k for rectangular loaded areas

$\mathbf{c_1/c_2}$	$\leq$**0.5**	**1**	**2**	$\geq$**3**
k	0.45	0.60	0.70	0.80

Approximate values of β can be used when the lateral stability of the structure does not depend on frame action between slabs and columns, and when the adjacent spans do not differ in length by more than 25%.

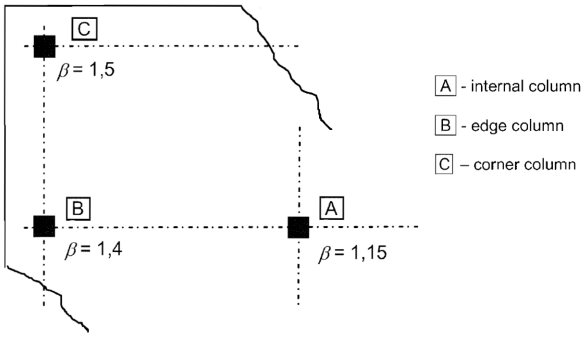

Figure 4.14: Recommended values for β [3].

At the basic control perimeter, the punching shear resistance of a slab without shear reinforcements shall be calculated as follows:

$$v_{rd,c} = C_{Rd,c} k \left(100 \rho_l \, f_{ck}\right)^{1/3} + k_1 \sigma_{cp} \;\geq\; \left(v_{min} + k_1 \sigma_{cp}\right) \quad (f_{ck} \; in \; MPa) \tag{4.20}$$

With:

$$k = 1 + \sqrt{\frac{200}{d}} \leq 2.0 \quad (d \; in \; mm) \tag{4.21}$$

$$\rho_l = \sqrt{\rho_{ly} \cdot \rho_{lz}} \;\leq\; 0.02 \tag{4.22}$$

$$\sigma_{cp} = \left(\sigma_{cy} + \sigma_{cz}\right)/2 \tag{4.23}$$

$$C_{Rd,c} = \frac{0.18}{\gamma_c} \tag{4.24}$$

$$v_{min} = 0.035 \cdot k^{3/2} {f_{ck}}^{1/2} \tag{4.25}$$

Where:

k_1	is a factor of recommended value of 0.1;
ρ_{ly}	is the steel ratio relate to the bonded tension steel in y direction. It should be calculated as a mean value taking into account a slab width equal to the column width plus 3d each side;
ρ_{lz}	is the steel ratio relate to the bonded tension steel in z direction. Same slab with as it was described above;
σ_{cy}	is the normal concrete stresses in the critical section in y direction;
σ_{cz}	is the normal concrete stresses in the critical section in z direction;
γ_c	is the partial factor for concrete.

4.2.2 ACI 318-19

The ACI 318-19 Building Code [30] contains provisions for the design of flat slab structures under seismic actions. This design can be carried out only when the flat slab system is not considered as part of the seismic-force-resisting system. The general procedure given by this code to verify punching shear effects on elements without shear reinforcement, is described below.

For any applicable load combination acting on the structure, the design strength must satisfy, in all the cases and at any critical section defined, the following expression.

$$\phi v_n \geq v_u \tag{4.26}$$

Where:

- ϕ is the strength reduction factor;
- v_n is the equivalent concrete stress corresponding to nominal strength
- v_u is the maximum factored shear stress calculated around the critical perimeter

According to ACI 318-19, the equivalent stress corresponding to a nominal shear strength of a slab without shear reinforcement is equal to:

$$v_n = v_c \tag{4.27}$$

Where:

- v_c is the stress corresponding to nominal shear strength provided by concrete

The maximum acting shear stress v_u is resisted by a section with a effective depth d and an assumed critical perimeter b_0 . The critical section is located at a distance not closer than $d/2$ from the column perimeter. For square or rectangular columns, the critical perimeter is permitted to be assume with straight sides.

The stress corresponding to nominal shear strength provided by concrete v_c,

can be calculated in accordance with the following equation:

$$v_c = min \begin{cases} 4\lambda_s \lambda \sqrt{f_c{}'} \\ \left(2 + \frac{4}{\beta}\right) \lambda_s \lambda \sqrt{f_c{}'} \\ \left(2 + \frac{\alpha_s d}{b_0}\right) \lambda_s \lambda \sqrt{f_c{}'} \end{cases} \quad (in\ US\ customary\ units : psi,\ in) \tag{4.28}$$

With:

$$\lambda_s = \sqrt{\frac{2}{1 + \frac{d}{10}}} \leq 1 \quad (in\ US\ customary\ units : psi,\ in) \tag{4.29}$$

Where:

- λ_s is the size effect modification factor;
- λ is the concrete weight factor. It is taken as 1 for normal weight concrete;
- β is the ratio of the long side to the short side of the column;
- $f_c{}'$ is the specified compressive strength of concrete;
- α_s is a value of 40 for interior columns, 30 for edge column and 20 for corner columns.

When a gravity, wind or earthquake load cause a transfer of moment between the slab and the column at the connection, a fraction of the moment resisted by the column at the join (M_{sc}) is transferred to the slab. At the end, the actual moment resisted by the column results as $\gamma_f M_{sc}$. γ_f is defined as follows:

$$\gamma_f = \frac{1}{1 + \left(\frac{2}{3}\right) \sqrt{\frac{b_1}{b_2}}} \tag{4.30}$$

Where:

b_1 is the dimension of the critical section b_0 measured in the direction of the span for which moments are determined;

b_2 is the dimension of the critical section b_0 measured in the direction perpendicular to b_1.

The fraction of the moment which is actually transferred can be expressed as $\gamma_v M_{sc}$. Thus, the factor γ_v results:

$$\gamma_v = 1 - \gamma_f \tag{4.31}$$

Therefore, the factored shear stress at the critical section v_u corresponds to a combination v_{uv} (factored shear stress on the slab critical section without moment transfer) and the shear stress produced by the transferred moment. The fraction of the moment, which is transferred, is applied to the centroid of the critical perimeter. The shear distribution for an interior and edge column is illustrated in Fig. 4.15.

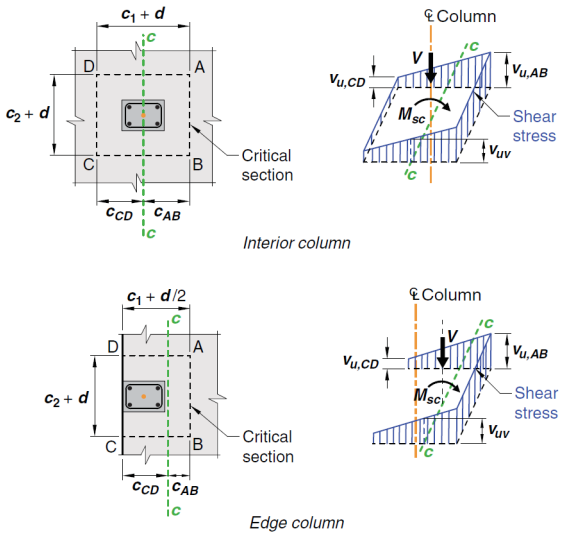

Figure 4.15: Assumed distribution of shear stress [30].

Finally, the maximum factored shear stress may be calculated as follows:

$$v_{u,AB} = v_{uv} + \frac{\gamma_v M_s c_{AB}}{J_c} \tag{4.32}$$

Or:

$$v_{u,CD} = v_{uv} - \frac{\gamma_v M_s c_{CD}}{J_c} \tag{4.33}$$

Where:

J_c is a property of the assumed critical section analogous to a polar moment of inertia.

Additional design recommendations for punching shear under seismic actions, are given in ACI 318-19 [30] and in ACI 421.2R-10 [22]. These recommendations are based on existing experimental data which have shown the detriment of the ultimate inter-story drift ratio when a slab-column connection is subjected to cyclic loading. It is important to mention that this considerations are only applicable to flat-slab structures with a lateral-force resistance system which can control the maximum lateral displacement. Inside this code, a limitation of the ultimate story drift ratio as a function of the gravity shear ratio is presented in order to reduce the probability of slab punching failure during lateral loading (see Fig. 4.16).

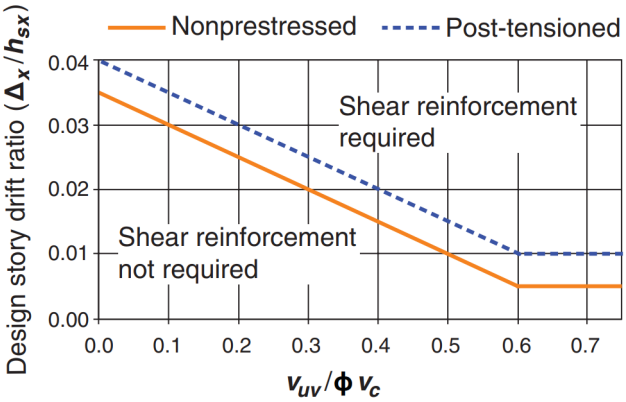

Figure 4.16: Requirement for shear reinforcement [30].

According to ACI 318-19, for flat slab-column connections, shear reinforcement is not necessary if the following conditions are satisfied.

$$\begin{cases} \Delta_x/h_{sx} \leq 0.035 - (1/20)(v_{uv}/\phi v_c) & for \ \ (v_{uv}/\phi v_c) \leq 0.6 \\ \Delta_x/h_{sx} \leq 0.005 & for \ \ (v_{uv}/\phi v_c) > 0.6 \end{cases} \tag{4.34}$$

Where:

Δ_x	is the design story drift of story x;
h_{sx}	is the story height for story x

In this case, v_{uv} should be calculated without induced moments and considering just gravity loads and the vertical component of earthquake loads according to the following load combination:

$$U = 1.2D + 1.0E + 1.0L + 0.2S \tag{4.35}$$

Where:

D	is the dead load;
E	is the earthquake load;
L	is the live load;
S	is the snow load.

Inside ACI 421.2R-10 an additional recommendation is provided. When the value $v_{uv}/\phi v_c$ is greater than 0.4, a minimum shear reinforcement should be provided to ensure enough ductility.

4.2.3 Model Code 2010

The fib Model Code 2010 [31] is based on the CSCT developed by Muttoni [26]. Simple design equations, which are verified with experimental result, are provided in this code.

The design punching shear force V_{Ed} is calculated as the sum of shear forces acting on a basic control perimeter b_1. The basic control perimeter is located at a distance of 0.5 times the effective depth d_v of the slab from the column face as is shown in the Fig. 4.17.

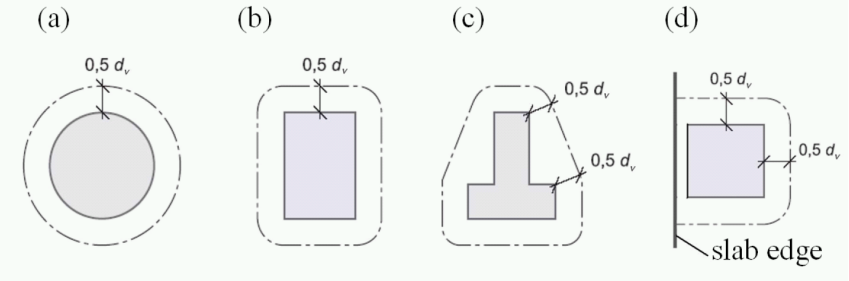

Figure 4.17: Basic control perimeter Model Code 2010 [31].

Additionally, this code contains some recommendations to define the basic control perimeter when the flat slab is supported by shear walls.

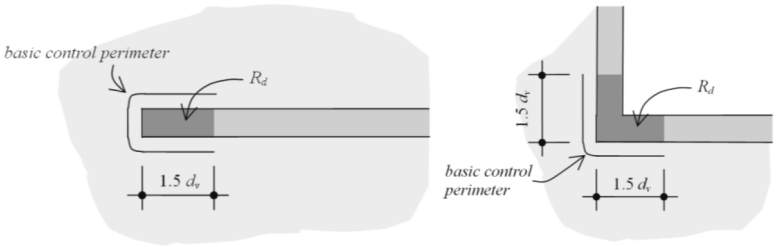

Figure 4.18: Basic control perimeter around walls Model Code 2010 [31].

The punching shear resistance is calculated at a shear-resistance control perimeter b_0. The perimeter b_0 considers the non-uniform distribution of shear forces along the perimeter b_1. When an unbalanced moment is transferred between the slab and the loaded area, this code proposes the Eq. (4.36) to take into account this effect.

$$b_0 = k_e \cdot b_{1,red} \tag{4.36}$$

Where:

k_e	is a coefficient of eccentricity;
$b_{1,red}$	is a reduced control perimeter which considers the presence of discontinuities or large supported areas

The coefficient of eccentricity can be computed as follows:

$$k_e = \frac{1}{1 + e_u/b_u} \tag{4.37}$$

Where:

e_u is the eccentricity of the resultant of shear forces with respect to the centroid of the basic control perimeter;

b_u is the diameter of a circle with the same surface as the region inside the basic control perimeter

The k_e factor can be approximated to the following values (Table 4.2) in cases where the adjacent spans do not differ in length more the 25% and the lateral stability does not depend on frame actions between slabs and columns.

Table 4.2: Values of k_e for columns and walls

Position	$\mathbf{k_e}$
Inner columns	0.90
Edge columns	0.70
Corner columns	0.65
Corner of walls	0.75

For a slab without punching shear reinforcement, the punching shear resistance force must satisfy the following condition:

$$V_{Rd} \geq V_{Ed} \tag{4.38}$$

According to this code, punching shear resistance is calculated as:

$$V_{Rd} = k_\psi \frac{\sqrt{f_{ck}}}{\gamma_c} b_0 d_v \tag{4.39}$$

Where:

f_{ck} is the characteristic value of compressive strength of concrete;

γ_c is the partial safety factor for concrete

With the parameter k_ψ depending on the rotation of the slab:

$$k_\psi = \frac{1}{1.5 + 0.9 k_{dg} \psi d} \leq 0.6 \tag{4.40}$$

$$k_{dg} = \frac{32}{16 + d_g} \geq 0.75 \tag{4.41}$$

Where:

ψ	is the rotation of the slab around the supported area;
d	is the mean value [in mm] of the effective depth for the x and y directions;
d	is the size of the maximum aggregate [in mm].

To determine ψ, Model Code 2010 introduces four different level of approximations. As the level of approximation increases, the value of ψ generally decreases due to the refinement of the calculations and thus, leading to the computation of a higher punching shear resistance force.

Level I of approximation

For a regular slab designed according to an elastic analysis, the rotation of the slab at failure can be calculated as:

$$\psi = 1.5 \cdot \frac{r_s}{d} \frac{f_{yd}}{E_s} \tag{4.42}$$

Where:

r_s	is the position where the radial bending moment is zero with respect to the support axis;
f_{yd}	is the design yield strength of reinforcing steel;
E_s	is the modulus of elasticity of reinforcing steel

Level II of approximation

This level of approximation is used when a significant moment redistribution is

considered in the design. Slab ration is calculated as follows:

$$\psi = 1.5 \cdot \frac{r_s}{d} \frac{f_{yd}}{E_s} \left(\frac{m_{Ed}}{m_{Rd}} \right)^{1.5} \tag{4.43}$$

Where:

m_{Ed} is the average moment per unit length of the flexural reinforcement in the support strip;

m_{Rd} is the design average flexural strength per unit length in the support strip.

Level III of approximation

In cases where r_s and m_{Ed} are calculated using a linear elastic model with uncracked elements , the coefficient 1.5 in Eq. (4.43) can be replaced by 1.2.

$$\psi = 1.2 \cdot \frac{r_s}{d} \frac{f_{yd}}{E_s} \left(\frac{m_{Ed}}{m_{Rd}} \right)^{1.5} \tag{4.44}$$

Level IV of approximation

This level of approximation considers the calculation of ψ using a nonlinear analysis.

Chapter 5

Study Case

The aim of this dissertation is to analyze the effects of the punching shear and its consequences in the design of a conventional flat-slab buildings under gravitational and seismic actions. To accomplish this objective, a series of different structures have been proposed. It is important to point out that the characteristics of the models of the structures proposed here, are based on the experimental work done by Coronelli et al. [1].

First, an initial model is proposed in order to compare numerical results with the experimental ones obtained from the tests on a real full-scale two-story flat-slab structure which were carried out at the ELSA laboratory of the European Commission's Joint Research Centre. Then, three additional models are presented to analyze the punching shear effects when different parameter of the structure are changed.

5.1 Description of the reference experimental test

5.1.1 Geometry of the specimen

The specimen tested by Cornelli et al. [1], is a full-scale reinforced concrete building with flat slabs supported by columns (Fig. 5.1) intended to represent a typical residential floor building.

The structure is a two-story flat-slab building with a story height of 3.20 m. The thickness of slab is 0.20 m and it has three by two bays.The spans are 4.50 m in transversal direction and, 4.50 m and 5.0 m and longitudinal direction. The total dimension of each floor is 14.50 m x 9.50 m. The slab is supported by twelve columns and the dimensions are 0.40 m x 0.40 m, 0.35 m x 0.35 m and 0.30 m x 0.30 m for interior, edge and corner columns respectively. Although in the test the shear walls were numerically simulated, it is important to mention that the dimensions of the cross-section of the wall reported, are 1.50 m x 0.32 m.

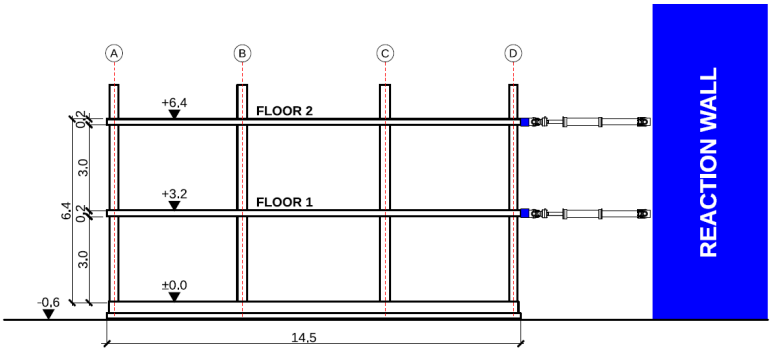

(a) Side view

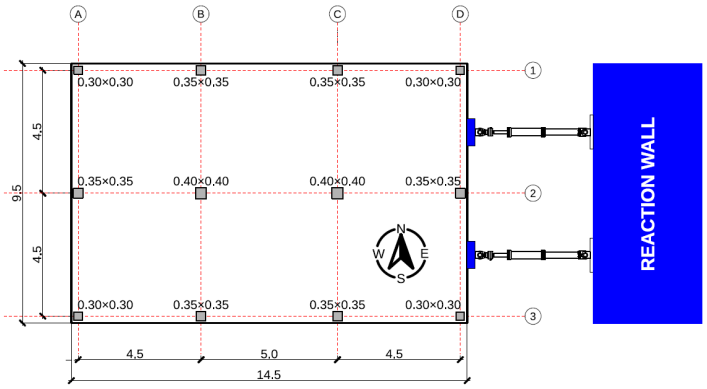

(b) Plan view

Figure 5.1: Geometry of the specimen [1]

5.1.2 Material characteristics of the specimen

The concrete used in the structure, was concrete Class C30/37 with a characteristic compressive cylinder strength of $f_{ck} = 30\,MPa$. Slab reinforcement with steel B450C was selected, the characteristic yield strength is $f_{yk} = 450\,MPa$. For columns, S500 Class B reinforcing steel with $f_{yk} = 500\,MPa$ was used except for

the column bases where steel B450C was selected. Steel with $f_{yk} = 500\,MPa$ was used for punching reinforcement studs.

5.1.3 Layout of reinforcements

The design of the structure was carried out according to the national design code NTC 2018 [32] and compatible with the provisions inside Eurocode 2 [2] and Eurocode 8 [3]. Columns and slabs were designed as secondary seismic elements whereas shear wall were designed as primary seismic elements. The location selected for seismic design was the city of Gemona, region of Friuli-Venezia Giulia, Italy. It is important to mentioned that the structure was conceived with primary seismic reinforced concrete walls, but they were numerically simulated during the tests.

A concrete cover of 15 mm was selected for the slabs whereas a concrete cover of 30 mm was used for the rest of the structure. Both slabs had the same reinforcement layout, and it was placed as it is described in the following paragraphs.

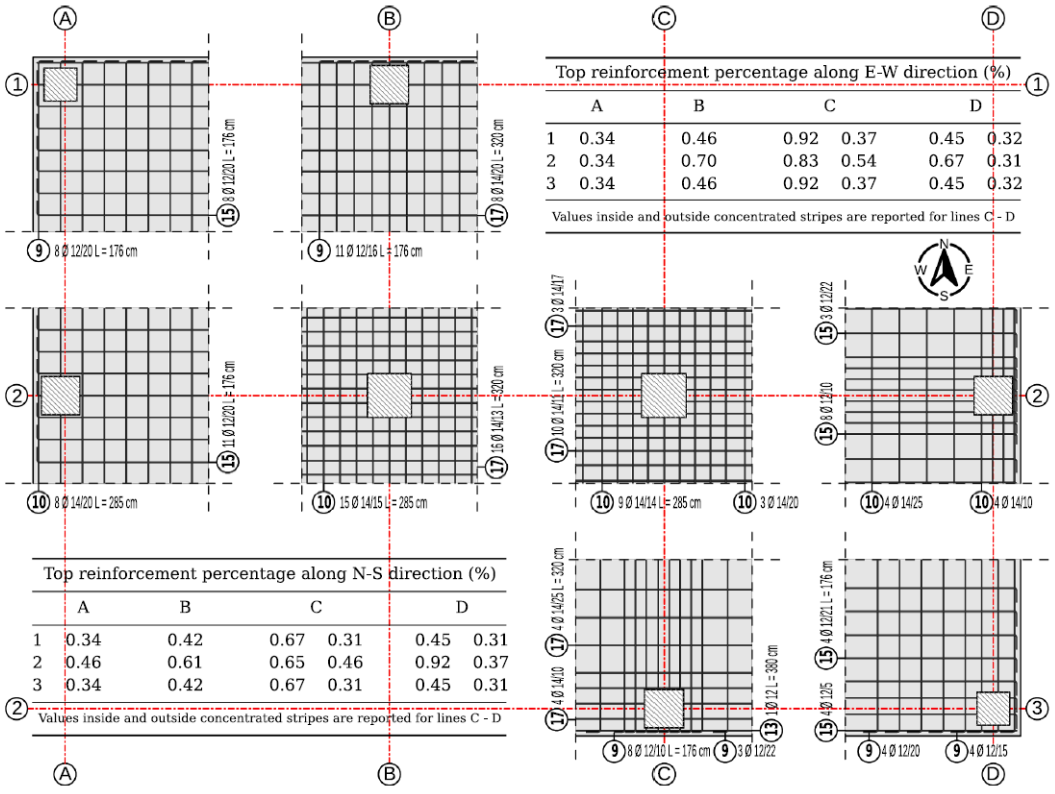

Figure 5.2: Top reinforcement in the slab [1]

For the bottom reinforcement, a uniform layout, in both directions, with bars of 12 mm diameter with a spacing of 25 cm was placed except for column centerlines, where a spacing of 20 cm was used.

Regarding to the top reinforcement, two different configurations of rebars arrangement were used. For the part of the slab along East direction, a concentration of reinforcement in slab column connection zone was placed following the recommendations inside Eurocode 2. For the part of the slab along West direction, a smeared reinforcement in slab column connection was used. The Fig. 5.2 described the top reinforcement of the slabs.

Headed studs were use at the second floor. These studs were not required by the design, but they were placed to carry out tests to evaluate the performance of slab-column connection with punching shear reinforcement. The slab-column connection at the first floor were not reinforced against punching shear at the begging of the study. Nevertheless, punching shear reinforcement was post installed after the slab-column connections at first floor were damaged during the tests.

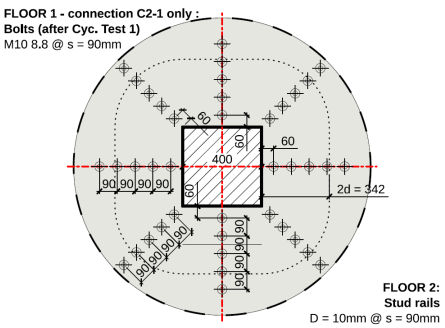

(a) Interior columns

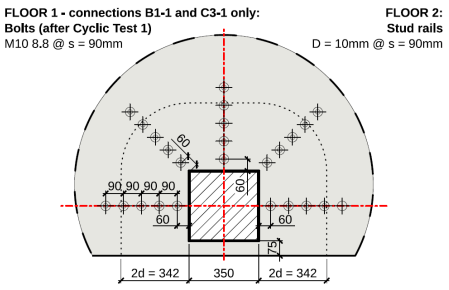

(b) Edge columns

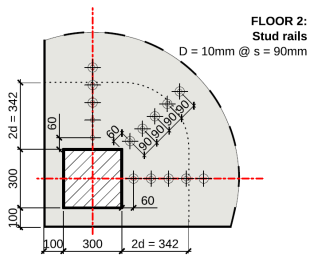

(c) Corner columns

Figure 5.3: Punching shear reinforcement layout of slab-column connections at second floor and at first floor after damage of connections [1].

The column reinforcement placed, was design to ensure the formation of plastic hinges at the base of columns and to avoid premature failure of the structure due to the lack of ductility. With this reinforcement used, it was also ensured that the resisting moment of the column framing into the slab was bigger than the transferred moment from the slab.

It should be noted that the three different types of columns in the structure share the same longitudinal reinforcement arrangement as is shown in Fig. 5.4.

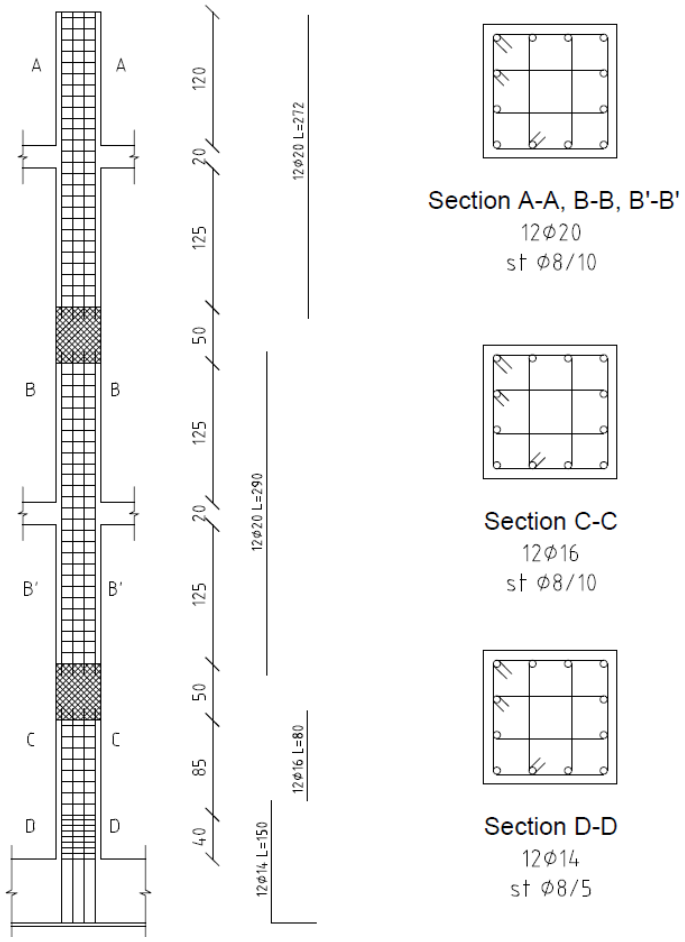

Figure 5.4: Schematic representation of reinforcement in 30x30, 35x35 and 40x40cm columns.

5.1.4 Test programme

Four different tests were carried out. The two first tests were intended to evaluate the performance of the structure under the design seismic actions. The last two tests were performed to evaluate the performance of the structure beyond

the design displacements.

The first and second test were pseudo-dynamic tests. The first one was used to evaluate the serviceability limit state (SLS) of the structure whereas the second one was used to evaluate the ultimate limit state (ULS). In these two tests, shear walls were numerically simulated.

The two last tests were two subsequently cyclic queasy-static tests. No shear walls numerical simulated were present in these tests. The third test was performed to reach a progressive and controlled damage of slab-column connections. With this test, the response of the structure until punching shear failure of the first floor was studied. After this test was carried out, slab-column connection of first floor were strengthened. The aim of the second test was to evaluate the performance of the structure at its ultimate capacity.Table 5.1 summarized the tests carried out.

Table 5.1: Test programme

#	**Test id.**	**Type of test**	**Maximum action**
1	SEIS-SLS	Pseudo-Dynamic	SLS (PGA=0.884 m/s^2)
2	SEIS-ULS	Pseudo-Dynamic	ULS (PGA=2.498 m/s^2)
3	CYC-1	Cyclic	2.5% drift ratio
4	CYC-2	Cyclic	6.0% drift ratio

5.1.5 Loads applied in the tests

Apart from the self-wight of the structure, additional vertical loads were added using water tanks at first floor, and concrete blocks at the second floor. This was done to simulate additional distributed loads which are present in a real structure. For the test SEIS-SLS and SESIS-ULS, 48 water tanks of 10 KN were placed on the first floor. For tests CYC-1, 24 water tanks of 10 KN and another 24 water tanks of 4.5 KN each one were used on the first floor. For test CYC-2, 32 water tanks of 10 KN were placed on the first floor. In all tests, blocks of 66 KN weight were placed on the second floor. Fig. 5.5 shows how additional loads were placed on the structure during each test.

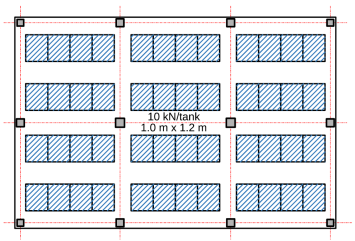

(a) First floor test SEIS-SLS and SEIS ULS

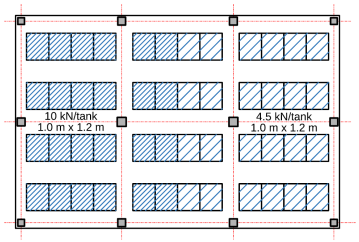

(b) First floor for test CYC-1

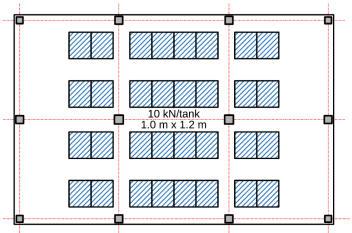

(c) First floor for test CYC-2

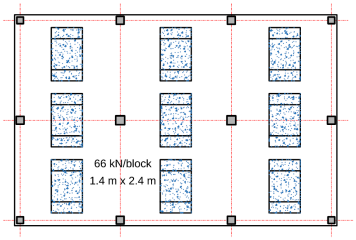

(d) Second floor for all test

Figure 5.5: Additional gravity loads. [1]

For lateral loading, the input selected for the seismic test was the Y component of signal 007142ya recorded from an MW 6.3 earthquake in Bingöl the first of May of 2003 (Fig. 5.6a). The original Peak Ground Acceleration (PGA) registered of 2.92 m/s^2, was reduced in order to match the site elastic response spectra for ULS and SLS design. PGA was scale at 31% and 87% for tests SEIS-SLS and SEIS-ULS respectively. The pseudo-acceleration response spectra and the design spectra used in the tests at ULS and SLS are shown in Fig. 5.6b.

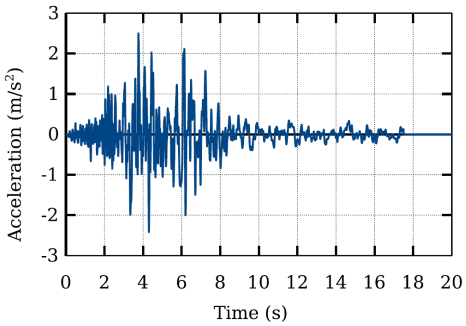

(a) Time-history of the selected accelerogram.

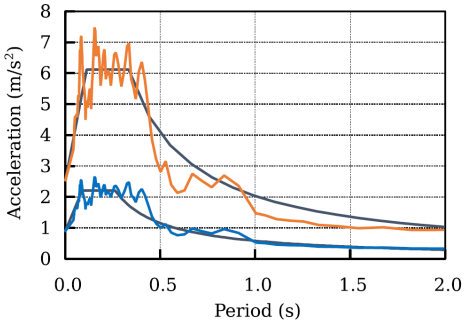

(b) Pseudo-acceleration response spectra at SLS (blue) and ULS (red).

Figure 5.6: Inputs of seismic tests [1].

For the cyclic tests, a displacement history was enforced on the second floor and half of the measured horizontal force at second floor was also imposed on the first floor. The cycling displacement was performed using gradually increasing steps. For test CYC-1, seven sets of three cycles were used (Fig. 5.7a). For test CYC-2, five increasing single cycles were performed (Fig. 5.7b).

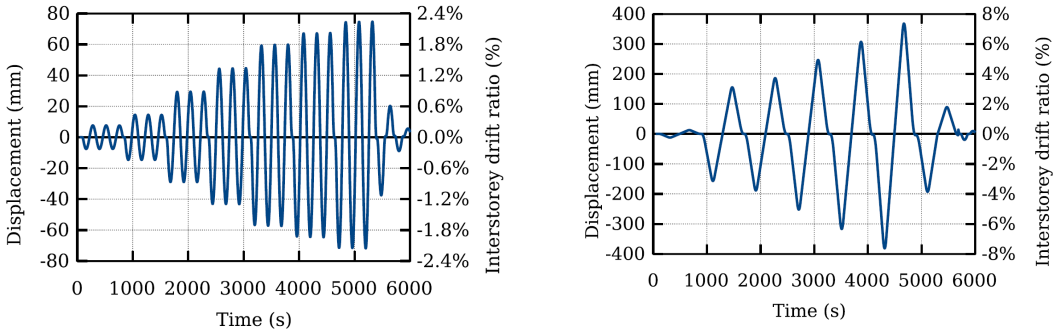

(a) Test CYC-1.

(b) Test CYC-2.

Figure 5.7: Displacement history for tests CYC-1 and CYC-2 [1].

The mechanical system used to imposed the displacements to each floor was composed of a pair of hydraulic actuators connected to the ELSA reaction wall.

5.1.6 Experimental results

For what concerns this thesis, only the experimental results obtained from the two first tests are meaningful for this dissertation. The reason of this, is because the design and analysis of the structures carried out here are based on a linear elastic analysis and also, because in all the models here, shear walls are present as primary seismic elements.

Test SEIS-SLS

The behavior of the structure under this test resulted to be essentially linear, as it was expected. The maximum inter-story drifts registered were 0.1% at first floor and 0.13% at second floor. No substantial damage of the structure was observed. Complete history of lateral displacements is reported in Fig. 5.8a. The response of the structure in terms of shear forces and global drift ration is shown in Fig. 5.9a.

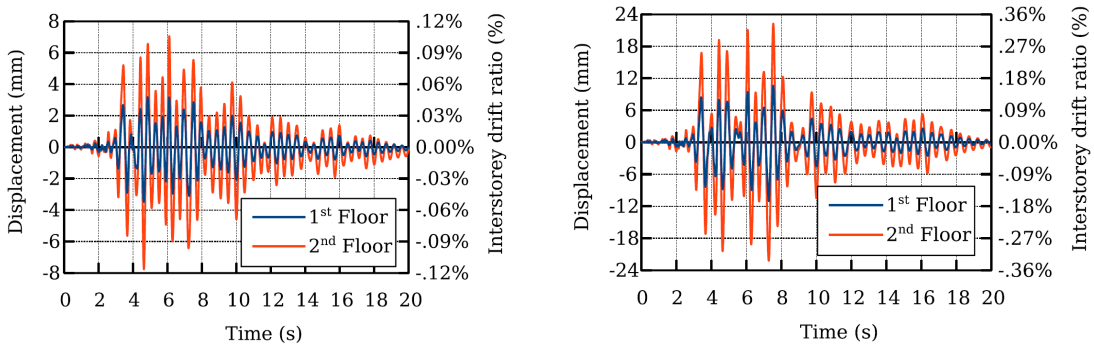

(a) SEIS-SLS test (b) SEIS-ULS test

Figure 5.8: Recorded lateral displacements [1]

Test SEIS-ULS

Maximum inter-story drift recorded during the tests, were 0.34% at first floor and 0.36% at second floor. The maximum displacement measured at the second floor was 22 mm with a global drift ratio of 0.35%. The complete history of lateral displacements is reported in Fig. 5.8b. This test indicated that the flat-slab frame with lateral primary resisting shear walls have a nearly elastic response with very limited damage. The response of the structure in terms of shear forces and global drift ration is shown in the Fig. 5.9b.

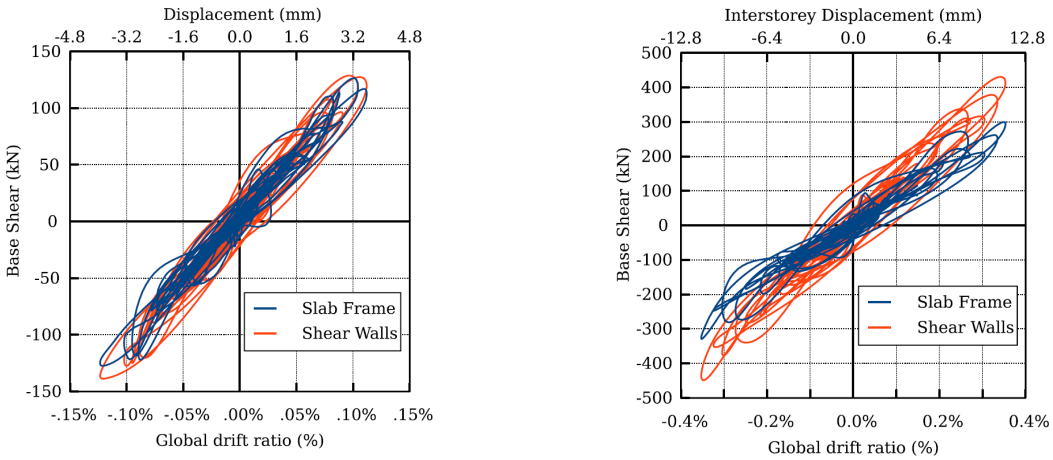

(a) SEIS-SLS test (b) SEIS-ULS test

Figure 5.9: Base shear versus global drift ratio [1]

The fundamental vibration period obtained, in the direction of the walls, was $T_1 = 0.315s$.

5.2 Description of proposed models

Unless otherwise specified, the material properties and the value of the loads applied for the analysis and design of each structure, are the same for all the models described here.

5.2.1 Materials characteristics

Concrete

The same concrete used in the experimental tests, C30/37, was selected. The mechanical characteristics of this concrete class , according to Eurocode 2, are listed below.

Table 5.2: Concrete properties

Property	Symbol	Value
Characteristic cylindrical compression strength	f_{ck}	30 MPa
Mean tensile strength	f_{ctm}	2.9 MPa
Elastic modulus	E_{cm}	33 GPa
Specific weight	γ_{cls}	25 KN/m^3
Partial safety factor	γ_c	1.5

Steel

The steel selected for the reinforcement is of class B40C. Material properties are given in the following table.

Table 5.3: Steel properties

Property	Symbol	Value
Characteristic yield strength	f_{yk}	450 MPa
Elastic modulus	E_s	20 GPa
Partial safety factor	γ_c	1.15

5.2.2 Applied loads and load combinations

Vertical loads

All the structures are intended to represent a typical residential building. Therefore, and according to Eurocode 1 [33], the following vertical loads are applied to the models.

- *Dead loads.* The self-weight of the structure, which is calculated using an specific weight of concrete equal to 25 KN/m^3. As well as an additional non-structural load of 3 KN/m^2 on each floor.

- *Live loads.* According to Eurocode 1, all the structures analyzed here, are classified as building of category of use A. For this reason, a live load of 2 KN/m^2 is considered on each floor of the structures.

For ultimate limit state, the fundamental combination of action established by Eurocode 0 [34] is given below:

$$\sum \gamma_{G,j} G_{k,j} \text{ “+” } \gamma_P P \text{ “+” } \gamma_{Q,1} Q_{k,1} \text{ “+” } \sum \gamma_{Q,i} \psi_{0,i} Q_{k,i} \tag{5.1}$$

Where:

$\gamma_{G,j}$	is the partial factor for permanent action j;
$G_{k,j}$	is the characteristic value of permanent action j;
γ_P	is the partial factor for prestressing actions;
P	is the representative value of a prestressing action;
γ_Q	is the partial factor for variable actions;
$Q_{k,1}$	is the characteristic value of the leading variable action 1;
$\gamma_{Q,i}$	is the partial factor for variable action i;
$\psi_{0,i}$	is the factor for combination value of a variable action ;
$Q_{k,i}$	is the characteristic value of the accompanying variable action i.

Therefore, the fundamental combination at ultimate limit state results:

$$1.35G + 1.5Q \tag{5.2}$$

Where:

G	is the dead load;
Q	is the live load.

Seismic actions

Apart from the vertical loads, the only additional considered for the design is the seismic action. A dynamic analysis will be performed to evaluate the seismic effects in the structures, for this reason it is important to correctly define the response spectrum. The elastic response spectrum for ULS and SLS was generated according to NTC 2018 [32] because the location selected for the building, was the same location used for the experimental tests (Gemona, region of Friuli-Venezia Giulia, Italy).

Following the indications inside NTC 2018, some initial consideration are set in order to get the parameters to build the Elastic Response Spectrum.

- Ground type: A.
- Topographic category: T1.
- Importance class of the building: II.

Hence, the parameters required to define the Elastic Response Spectrum for ULS are indicated in the following table.

Table 5.4: Elastic Response Spectrum parameters for ULS

Parameter	**Symbol**	**Value**
Return period for ULS	T_R	450 years
Peak ground acceleration	a_g	0.259g
Viscous damping ratio	ξ	0.05
Amplification Factor	F_0	2.408
Period of initial constant acceleration	T_B	0.110 s
Period of initial constant velocity	T_c^*	0.331 s
Period of initial constant displacement	T_D	2.636 s

In the same way, the parameters required to define the Elastic Response Spectrum for SLS are listed below.

Table 5.5: Elastic Response Spectrum parameters for SLS

Parameter	Symbol	Value
Return period for SLS	T_R	50 years
Peak ground acceleration	a_g	0.092g
Viscous damping ratio	ξ	0.05
Amplification Factor	F_0	2.450
Period of initial constant acceleration	T_B	0.086 s
Period of initial constant velocity	T_c^*	0.258 s
Period of initial constant displacement	T_D	1.968 s

The Elastic Response Spectrum used to analyse and design all the structure for ULS and SLS are shown in Fig. 5.10

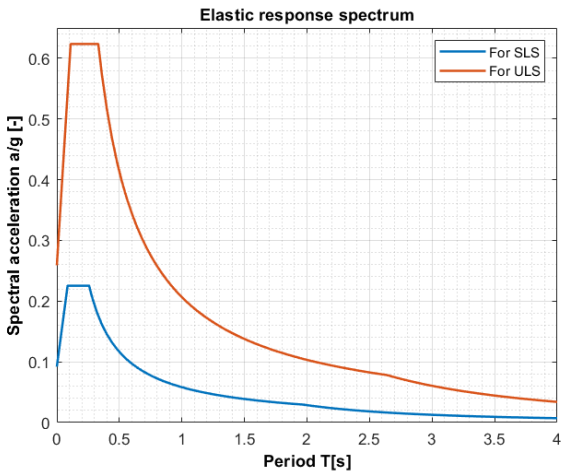

Figure 5.10: Elastic Response Spectrum for ULS and SLS.

According to Eurocode 0, the combination of actions for seismic design situation at ULS shall be as follows:

$$\sum G_{k,j} \text{ “+” } P \text{ “+” } A_{Ed} \text{ “+” } \sum \psi_{2,i} Q_{k,i} \tag{5.3}$$

Where:

A_{Ed}	is the design value of seismic action;
$\psi_{2,i}$	is the factor for quasi-permanent value of a variable action.

For this case, the combination of action for seismic design situation at ULS results:

$$1.0G \text{ “+” } E + 0.3Q \tag{5.4}$$

Where:

E	is the seimic action affects;

Horizontal components of the seismic action shall be considered as acting simultaneously. Eurocode 8 allows the combination of horizontal components using the 30% rule:

$$E_{Edx} \text{ “+” } 0.30E_{Edy} \tag{5.5}$$

$$0.3E_{Edx} \text{ “+” } E_{Edy} \tag{5.6}$$

Where:

E_{Edx}	is the action effects due to the application of the seismic action along axis x of the structure;
E_{Edy}	is the action effects due to the application of the seismic action along axis y of the structure.

Accidental eccentricities, which may produce accidental torsional effects must be also considered in Eq. (5.4). To account for accidental eccentricities in the location of masses during seismic motion, the center of mass at each floor should be considered as being displaced in each direction by the following distance:

$$e_{ai} = \pm 0.05 L_i \tag{5.7}$$

Where:

e_{ai} is the accidental eccentricity of storey mass i from its nominal location, applied in the same direction at all floors;

L_i is the floor-dimension perpendicular to the direction of the Seismic action.

For inertial effects, the design seismic action shall be evaluated by accounting the masses associated with all gravity loads appearing in the following expression:

$$\sum G_{k,j} \text{ “+” } \sum \psi_{E,i} Q_{k,i} \tag{5.8}$$

$$\psi_{E,i} = \varphi \psi_{2i} \tag{5.9}$$

Where:

$\psi_{E,i}$ is the combination coefficient for variable action i;

φ is a factor which considers the importance and the use of the structure.

For all the structures modeled here, the load combination to determine the inertial effects, results as it is shown in the following expression:

$$1.0G + 0.15Q \tag{5.10}$$

5.2.3 Model 0

The principal aim of this model is to validate the modelling of the other structures proposed in this thesis, using as a reference the experimental data previously described. In this way, some parameters were calibrated in order to better analyzed and represent the behavior of the flat-slab structures under lateral loads.

The geometry of this model is exactly the same as the specimen tested by Coronelli et al [1]. The only difference is that, in this model, shear walls are explicitly included. The dimensions of the cross-section of the walls are 1.50m x 0.32m. Additionally, it is also important to point out that in this model the vertical

loads applied were the same vertical loads as they are described in Section 5.1.5.

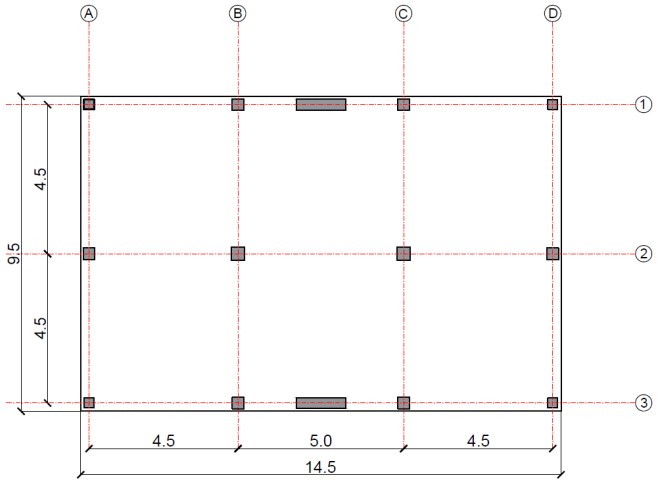

Figure 5.11: Plan view of Model 0

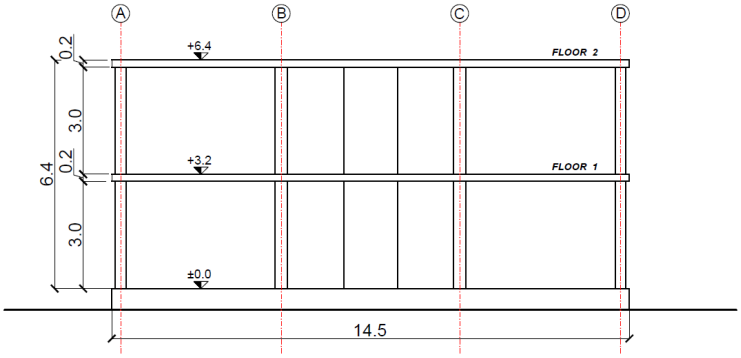

Figure 5.12: Side view of Model 0

The software midas Gen Midas 2020 (v2.3) was used to modeled all the fictitious structures analyzed here. This software uses the Finite Element Method (FEM) to analyze structural elements. Columns are modeled as beam elements; floor slabs are modeled by a mesh of plate elements and shear walls are modeled using the shear wall element inside the software.

Fixed supports were assumed at the base of the columns and walls. For this model, it is important to mention that joints between slab and column are restrained by simple supports to not allow the displacement in Y-direction in such a way that this model better represent the experimental tests carried out where the movement of the structure in Y-direction was also restricted.

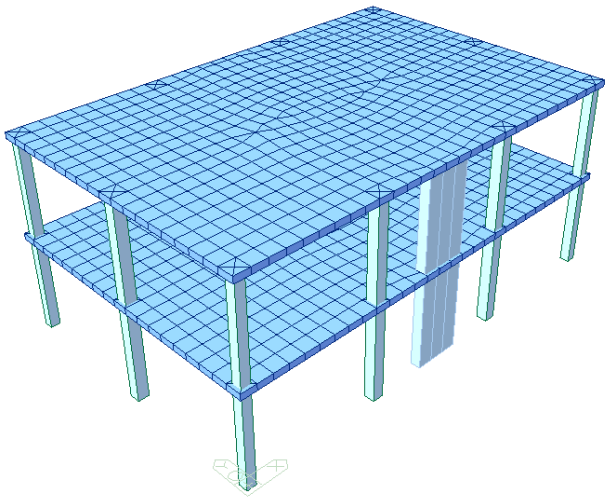

Figure 5.13: Structural Model 0

As it was mentioned before, this model was used to calibrate certain parameters of modeling. One of these, was the lateral stiffness reduction of the flat-slab under lateral loading. When a structure is subjected to lateral loads, a stiffness reduction of the elements is expected in the structure due to cracking of concrete. Currently, this is a topic that is still not well studied. Some authors [35] [36] have recommended some values for stiffness reduction factors for flat-slabs. In this thesis, the values of the stiffness reduction factor were selected based on the recommendations in literature and they were validated using the results in the experimental tests.

The stiffness reduction factors for columns and walls are taken from FEMA 356 [37]. The ones for flat slabs were selected based on the work done by Han et al. [35] and Setiawan et al. [36]. The following table summarizes the values used for the stiffness reduction due to cracking of concrete. These values were used for all the models.

Table 5.6: Effective Stiffness Values

Rigidity	**Columns**	**Walls**	**Flat slab**
Flexural	0.50	0.50	-
Shear	0.40	0.40	0.40
Flexural out of plane	-	-	0.25
Tosion out of plane	-	-	0.125
Shear out of plane	-	-	0.40

These values were selected because they showed a good match between the period of vibration and the displacements of the tested structure and the results from the numerical model.

5.2.4 Model I

The goal of this model is to analyze the behavior of punching shear in the flat slab-column connections when the dimension in X-direction of the structure in model 0 is increased. Compared to the first model, this one adds shear walls in Y-direction in order to carry out a complete seismic analysis and design in both directions.

The building modeled here is a two-story flat-slab structure with a story height of 3.20 m. The spans between columns remain the same respect to model 0, 4.50 m and 5.00 m in the longitudinal direction and 4.50 m in the transversal one. Slabs are supported by a total of twelve columns and the dimensions are 0.40 m x 0.40 m, 0.35 m x 0.35 m and 0.30 m x 0.30 m for interior, edge, and corner columns respectively. An additional bay was added in X-direction, so that the floor is composed of four by two bays. The thickness of the slab remains the same 0.20 m. Two pairs of shear walls are present in both directions; the cross sections of the shear walls are 2.00 m x 0.32 m in Y and X-direction.

The total dimension of the structure is 19.50 m x 9.50 m. The following figures illustrate the geometry of the structure modeled.

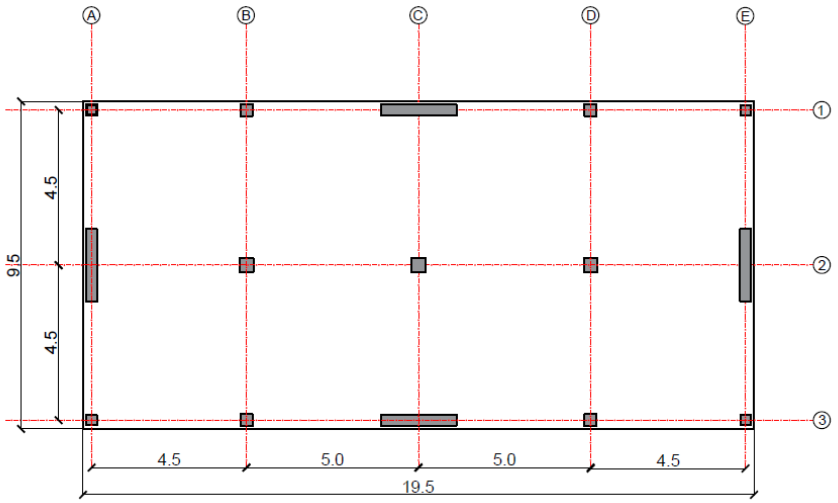

Figure 5.14: Plan view of Model I

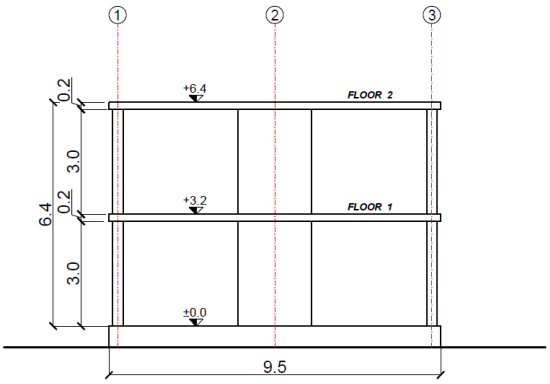

Figure 5.15: Side view of Model I. Y-direction

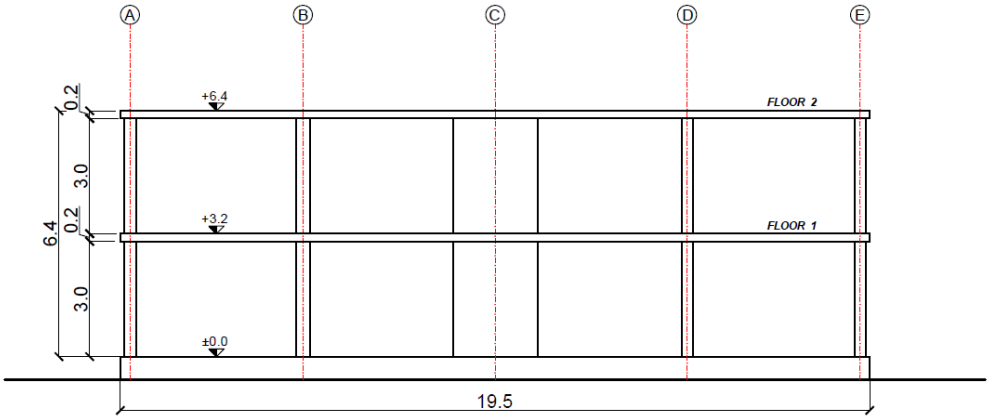

Figure 5.16: Side view of Model I. X-direction

The same modeling criteria as the one described in model 0 was used except that in this model, the only restrains added to the structure were those at the base of columns and walls to fixed the structure to the ground. For seismic analysis the stiffness reduction factor assigned to the structural elements are those described in Table 5.6.

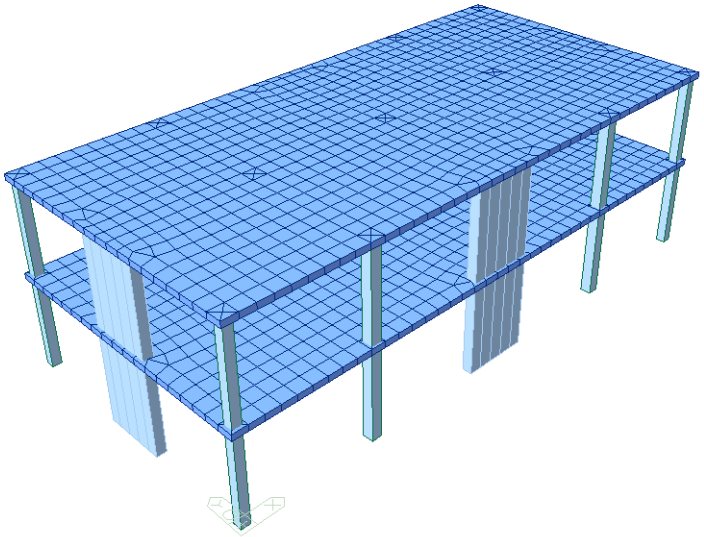

Figure 5.17: Structural Model I

5.2.5 Model II

This model is intended to analyze the effects of the punching shear at the slab-column connections when the model 0 is modified in such a way that the dimension in X and Y-direction are greatly increased but maintaining the same dimensions for the bays.

The story height of the building is 3.20 m. As mentioned earlier, the spans between columns do not change with reference to model 0, the correspondent distance between columns is presented in Fig. 5.18. The slabs are supported by 38 columns and 7 shear walls, the dimensions are 0.40 m x 0.40 m, 0.35 m x 0.35 m and 0.30 m x 0.30 m for interior, edge, and corner columns respectively. The cross-section dimensions of the shear walls are 2.40 m x 0.32m and 2.60 m x 0.32 m in X and Y-direction respectively.

The total dimension of the structure is 39.50 m x 19.50 m. The following figures illustrate the geometry of the structure modeled.

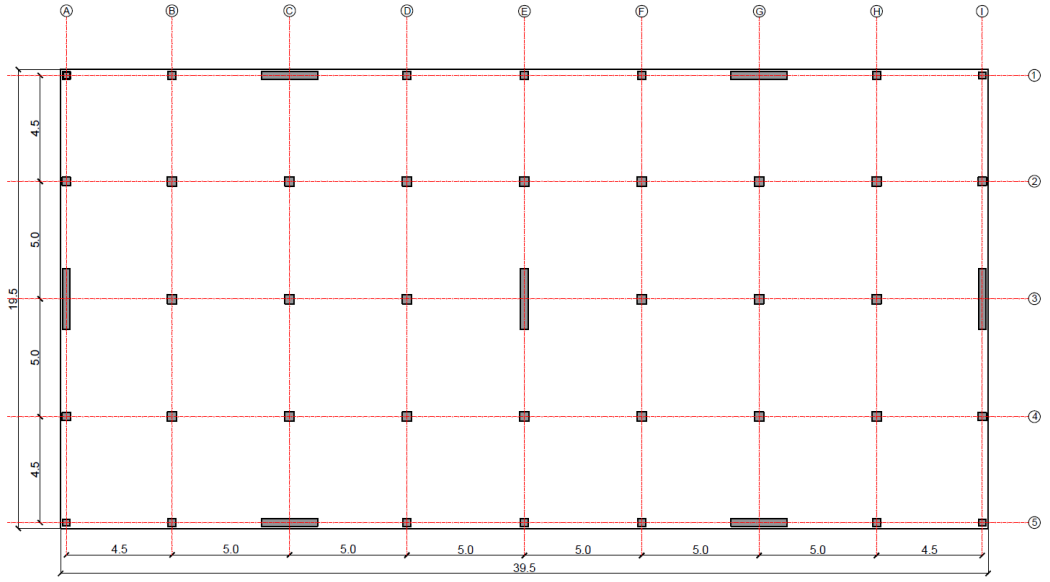

Figure 5.18: Plan view of model II

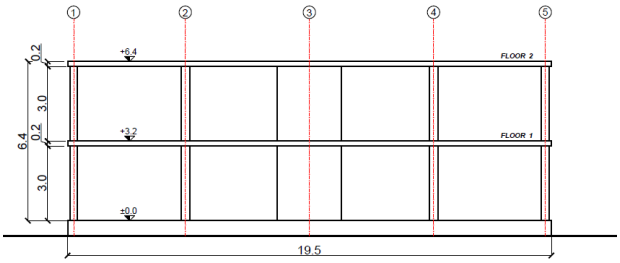

Figure 5.19: Side view of Model II. Y-direction

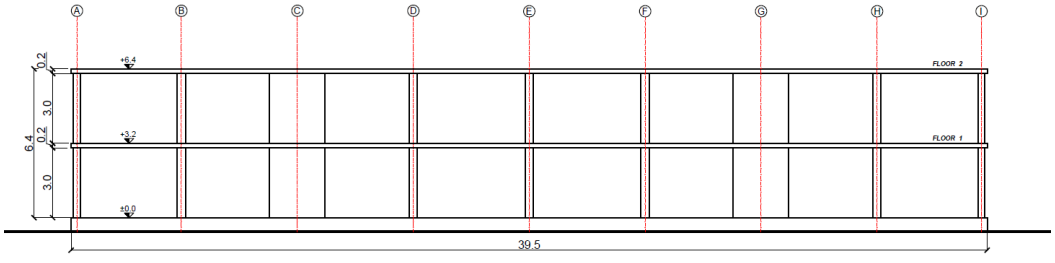

Figure 5.20: Side view of Model II. X-direction

The structure was modeled as it is described for model I. For seismic analysis, the effective lateral stiffness used for the structural elements are those described in Table 5.6.

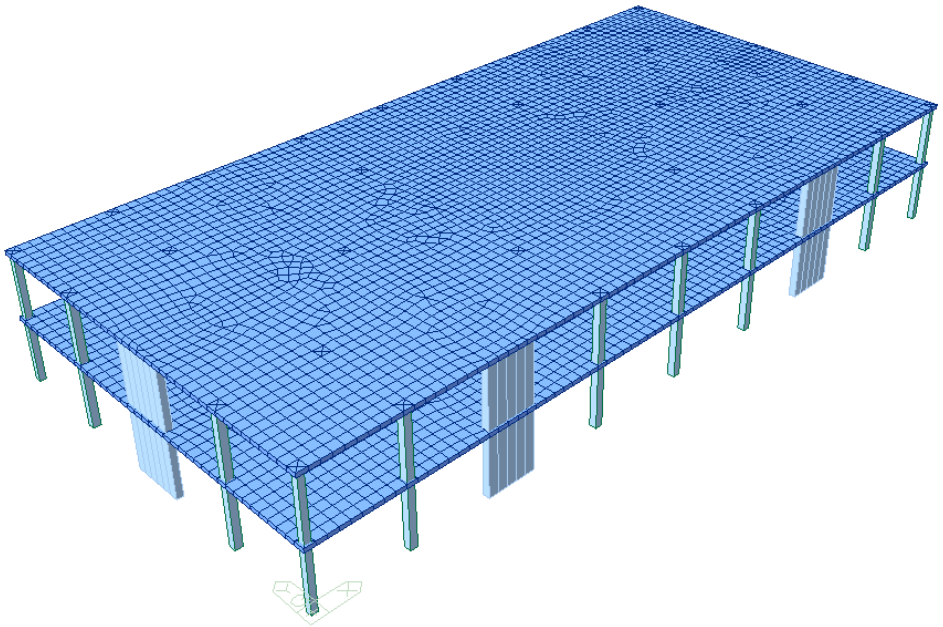

Figure 5.21: Structural Model II

5.2.6 Model III

Previous models were proposed to analyze the impact of increasing the plan dimensions of the building in the punching shear behavior in the slab-column connections. Although in these mentioned models the plan dimensions were increased, the same dimensions and aspect ratio for the bays of the structure were maintained to match the ones from the structure experimentally tested.

Differently form the other models, Model III was proposed to analyze the punching shear in slab-column connections when the dimensions of the bays from model 0 are modified. The thickness of the slabs remains the same 0.20 m, and the structure has seven by two bays. The slabs are supported by 14 columns and 10 shear walls. The distance between columns and shear walls is described in Fig. 5.22. Column dimensions are 0.40 m x 0.40 m, 0.35 m x 0.35 m and 0.30 m x 0.30 m for interior, edge, and corner columns respectively. The cross-section dimensions of the shear walls are 1.70 m x 0.32m and 1.80 m x 0.32 m in X and Y-direction respectively.

The structure modeled is a two-story building with a story height of 3.20 m. The total plan dimension of the structure is 37.90 m x 11.30 m. The following

figures illustrate the geometry of the structure modeled.

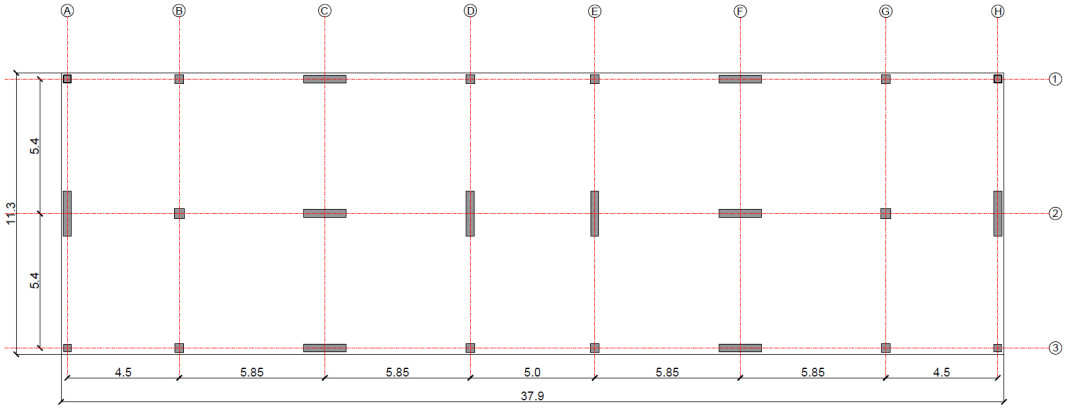

Figure 5.22: Plan view of Model III

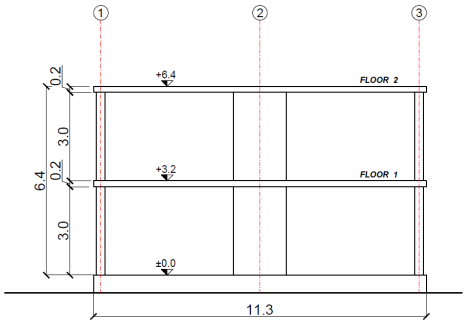

Figure 5.23: Side view of Model III. Y-direction

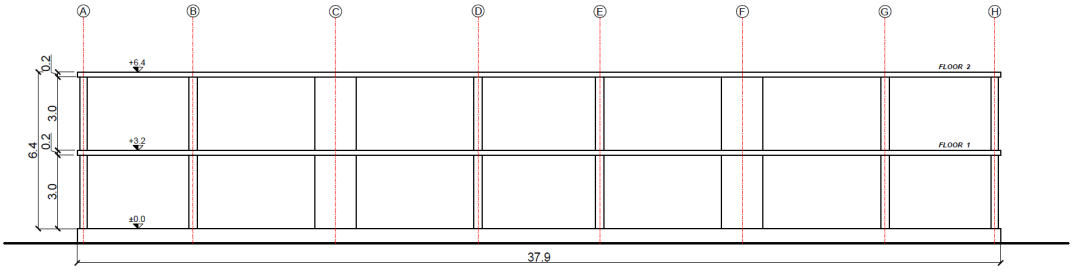

Figure 5.24: Side view of Model III. X-direction

The structure was modeled using the same criteria as previous models. For seismic analysis, the effective lateral stiffness used for the structural elements are those indicated in Table 5.6.

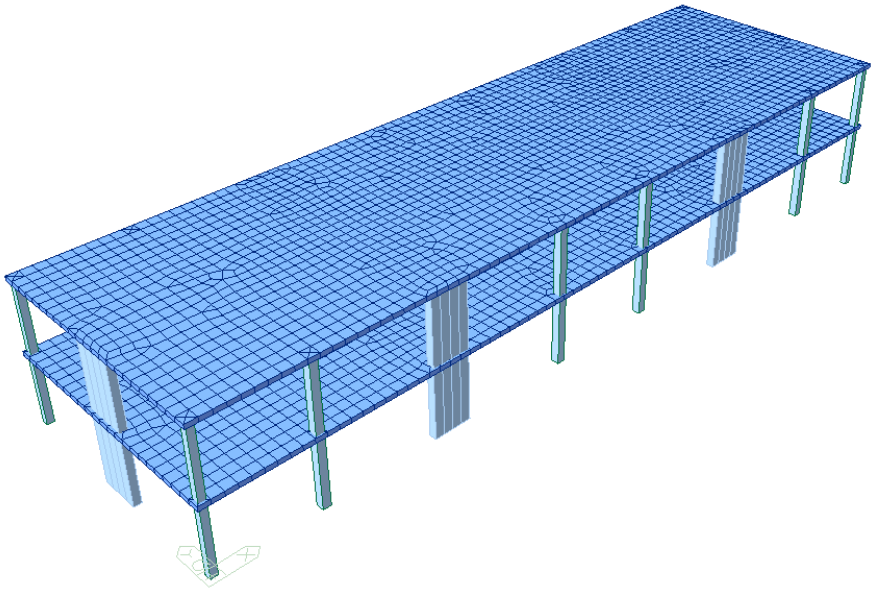

Figure 5.25: Structural Model III

Chapter 6

Results

In this chapter, a detailed analysis of the results is presented. After setting up all the proposed structures inside midas Gen software, the structural analysis was performed for each of the buildings to evaluate the behavior of the structure under the imposed loads and consequently, to carry out the design of the structural elements.

The design of all the structures was carried out according to the current code provisions, at the moment this dissertation was written, of Eurocode 2 and Eurocode 8 for a structure of Ductility Class High (DCH). In all the cases for seismic design, the structures were conceived as secondary flat slab frames inside a structure with primary seismic resistant walls.

As a consequence, for each structure analyzed, two numerical sub-models were used to design the structure under seismic action. According to Eurocode 8, the total contribution of lateral stiffness of all secondary elements must be lower than the 15% of the whole system. If this condition is satisfied, the stiffness and the strength of the secondary elements against seismic actions can be neglected and they may be design according to the provisions in Eurocode 2, the only additional requirement is that, secondary elements must have the capacity to withstand the lateral deformations imposed by the primary elements. Due to the lack of information and guidance to design flat slabs as primary seismic elements, they were considered as secondary elements.

As it was mentioned before, in order to carry out the design of primary an secondary seismic elements two different numerical models are needed. The first

sub-model of each structure considers only the contribution of the shear walls to resist the seismic effects neglecting secondary elements. The second one considers the contribution of the whole structure but just to resist the gravity loads. Therefore, the results of the two models in question, are combined in order to get the correct values of the actions in the secondary structural elements.

It is important to highlight that in this chapter, only the design for the members under the most unfavorable actions for each structure are presented. Please refer to Appendix A and Appendix B to consult the results for the designing of the rest of the structural members of each structure.

6.1 Model 0

6.1.1 Structural Analysis

Different modelling characteristics and options offered by the software were explored using this model. The most relevant parameter calibrated was the stiffness reduction factor of structural elements due to cracking of concrete. After several analysis ran, the best values for the stiffness reduction of elements are those in Table 5.6.

6.1.1.1 Modal analysis

First, a modal analysis considering cracked sections was performed. According to Eurocode 8, all modes with effective modal masses greater than 5% of the total mass shall be considered. The sum of the effective modal masses of all the modes considered must be at least 90% of the total mass of the structure. The following table summarizes the modes of the structure computed:

Table 6.1: Modal properties. Model 0

Mode	Mass Tran-X[%]	Sum Mx[%]	Period T[s]
1	79.61	79.61	0.331
2	20.35	99.96	0.058

It is worth noting that the value of the period of the first mode $T_1 = 0.322s$, is very close to the first period obtained during the experimental tests ($T_1 = 0.315s$).

6.1.1.2 Lateral displacements

To evaluate the lateral displacements at ULS under earthquake action, a behavior factor $q = 4$ was considered. The Fig. 6.1 shows the Design Response Spectrum used.

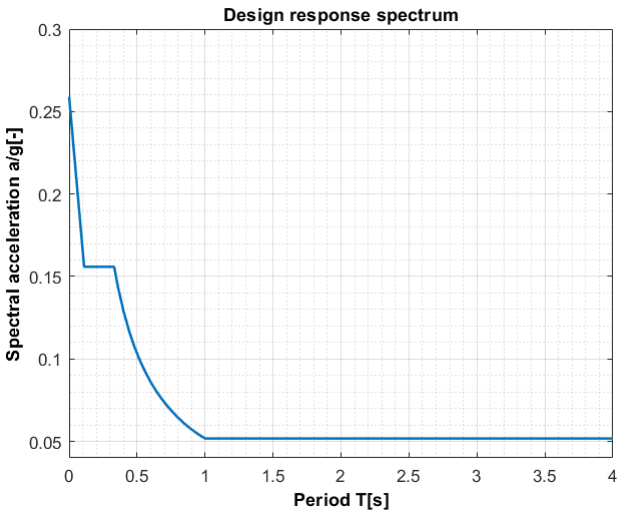

Figure 6.1: Design response spectrum. Model 0

After performing a dynamic analysis, the lateral displacements obtained are shown in the Table 6.2.

Table 6.2: Lateral displacements. Model 0

Level	**Lateral displacement d[mm]**	**Inter-story drift ratio [%]**	**Global drift ratio [%]**
First floor	6.6	0.21	-
Second floor	20.1	0.42	0.31

The maximum lateral displacement reached at the top floor of the structure under the seismic action, resulted equal to 19.5 mm. Thus, a drift ratio of 0.31%

is obtained which results similar to the drift ratio of 0.35% registered in the test performed to the real structure.

6.1.1.3 Base shear force

The shear force at the base of the structure under seismic action is summarize in Table 6.3.

Table 6.3: Base shear force. Model 0

Element	**Shear Force [KN]**	**[%]**
Slab-column frame	37.12	10
Walls	335.85	90
Total	372.97	100

The total shear base is similar to the maximum value registered in the SEIS-ULS test (see Fig. 5.9b).

6.1.2 Discussion

The model 0 presented in this section, can represent accurately the behavior of the structure tested by Coronelli et al. during the test SEIS-ULS. Thus, the same philosophy of modeling is used for analysis and design of the other proposed structures.

The stiffness reduction factor listed in Table 5.6 were selected because the numerical results obtained of the displacements and period of Model 0 are very close to the values obtained during the experimental tests.

Although the design of the slab-column frame for the specimen tested was carried out as secondary seismic elements, when a simple analysis of a model accounting for the lateral stiffness of the columns and the slabs is performed, it is demonstrated that the contribution of the of the columns and the slabs is around 36%. Hence, the design of this elements should have been carried out as primary elements, according to recommendations inside Eurocode 8.

6.2 Model I

6.2.1 Structural Analysis

For analyzing and designing the structure inside model I, two different sub-models were used. The first sub-model disregards the contribution of the stiffness and the strength of secondary elements, which in this case, are the columns and the slabs. This model was used to carry out the modal and the seismic analyses. For all other actions (e.g. gravity loads), another sub-model which considers the contribution of the secondary elements was used.

6.2.1.1 Modal analysis

To perform the modal analysis, the model including only the contribution of primary elements was used considering also, cracked sections for the primary elements. The following table summarizes the modes of the structure:

Table 6.4: Modal properties. Model I

Mode	Mass Tran-X[%]	Sum Mx[%]	Mass Tran-Y[%]	Sum My[%]	Period T[s]
1	78.11	78.11	0.00	0.00	0.296
2	0.00	78.11	78.11	78.11	0.296
3	0.00	78.11	0.00	78.11	0.180
4	21.89	100.00	0.00	78.11	0.050
5	0.00	100.00	21.89	100.00	0.050

The fundamental period of the structure corresponds to a translational mode equal to $T_1 = 0.296s$ in X-direction. The second mode is also a translational mode equal to the first one but in Y-direction and the third mode resulted to be a torsional mode.

6.2.1.2 Lateral displacements

Under SLS situation, the maximum displacements obtained are listed below:

Table 6.5: Lateral displacements at SLS. Model I

Level	**Lateral displacement $d_{x,SLS}$[mm]**	**Inter-story drift ratio X[%]**	**Lateral displacement $d_{y,SLS}$[mm]**	**Inter-story drift ratio Y[%]**
First floor	1.7	0.05	1.8	0.06
Second floor	5.4	0.12	5.7	0.12

Results of displacements at SLS comply with the regulations inside Eurocode 8 which suggests a limit of 0.5% inter-story drift for buildings having brittle non-structural elements.

To evaluate the lateral displacements at ULS under earthquake action, a behavior factor $q = 4$ was considered, this value was determined according to the specifications inside Eurocode 8. The Fig. 6.1 shows the Design Response Spectrum used. The maximum displacements obtained at seismic ULS are listed in Table 6.6.

Table 6.6: Lateral displacements at ULS. Model I

Level	**Lateral displacement $d_{x,ULS}$[mm]**	**Inter-story drift ratio X[%]**	**Global drift ratio X[%]**	**Lateral displacement $d_{y,ULs}$[mm]**	**Inter-story drift ratio Y[%]**	**Global drift ratio Y[%]**
First floor	5.9	0.18	–	6.4	0.20	–
Second floor	18.3	0.39	0.29	20.0	0.43	0.31

Maximum inter-story drifts in this model are very similar to the ones obtained through the experimental tests. The average stiffness of the structure under seismic action, resulted equal to 25 160 KN/m and 24 240 KN/m in X and Y-direction respectively. In the model where all the elements are included with their corresponding lateral stiffness, the distribution of the total lateral stiffness between the structural elements is listed below.

Table 6.7: Stiffness distribution. Model I

Element	X [%]	Y [%]
Slab-column frame	13.0	11.3
Walls	87.0	88.7
Total	100	100

6.2.1.3 Base shear force

For seismic analysis at Ultimate Limit State, the distribution of shear forces at the base of the walls is shown in the following table.

Table 6.8: Base shear force. Model I

Element	Shear Force [KN]
Walls X-direction	460.19
Walls Y-direction	460.19

For only comparison purpose, when all the structure is consider as primary, the following distribution of base shear forces under seismic analysis is obtained.

Table 6.9: Base shear force Model I as a whole primary system.

Element	Shear Force X-direction [KN]	X-direction [%]	Shear Force Y-direction [KN]	Y-direction [%]
Slab-column frame	21.30	5	21.80	5
Walls	439.10	95	433.6	95
Total	460.40	100	455.4	100

6.2.2 Design

Design of all the structural elements is carried out according to Eurocode 8 and Eurocode 2. As mentioned previously, to perform the seismic design, the structure

was considered as a secondary flat slab frame in a building with primary seismic resisting walls. The design was carried out for ULS and SLS for seimic situations and ULS for gravity loads.

Regarding to the secondary elements, they were designed for seismic actions using a combination of the results obtained from the two sub-models previously described. A description of how this combination is performed is given below.

Secondary elements are introduced inside the model, in which their stiffness and strength is neglected, with a fictitious elastic modulus E. This fictitious elastic modulus is equal to the real elastic modulus affected by a reduction factor α as it is shown in the following equation.

$$E = \alpha E_{real} \tag{6.1}$$

The value of α was assumed equal to 1/1000 for the modeling of all the structures. Once the the secondary elements were introduced with the fictitious elastic modulus in the model, the seismic analysis of the structure was carried out. From this analysis, the values of internal actions in secondary elements are obtained.

The next step is to find out the internal action produced by the deformation inflicted by the primary elements due to the seismic design action. To achieve this, the internal actions, previously computed, are amplified by the factor q/α and reduced by the corresponding effective stiffness reduction factor. Finally, they are added to the internal actions obtained from the model in which all the elements are introduced with the correct elastic modulus under the quasi-permanent combination for gravitational loads.

Therefore, the design moment and shear resistance determined according to Eurocode 2, must not be, in any case, less than the internal actions derived from the deformation imposed by the primary elements in the seismic design situation.

6.2.2.1 Shear walls

For the sake of simplicity, a general description of the procedure carried out to design the elements as well as the design of only the most unfavorable element is provided here.

The dimensions of each wall can be found in the following table. These dimensions comply with all the requirements specified in Eurocode 8.

Table 6.10: Shear walls dimensions. Model I

Element	L_w [m]	b_w [m]	h_w [m]
Wall A2	2.00	0.32	6.40
Wall C1	2.00	0.32	6.40
Wall C3	2.00	0.32	6.40
Wall E2	2.00	0.32	6.40

After ruining the analysis, the actions in the elements were extracted from the software and then, the design actions were computed according to the recommendations inside Eurocode 8. The design envelope of bending moments acting in the most unfavorable shear walls C1 is illustrated in Fig. 6.2.

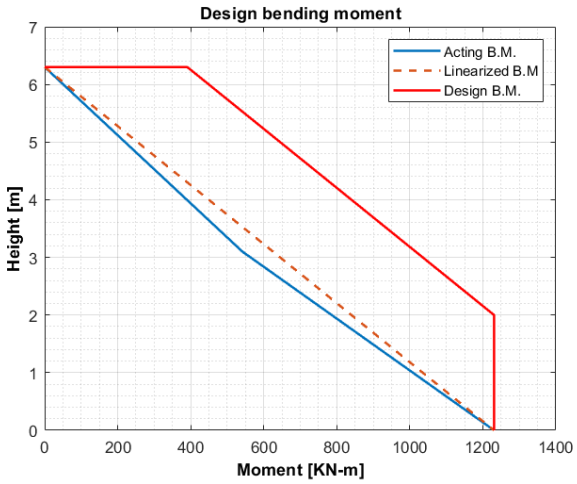

Figure 6.2: Design bending moment for wall C1. Model I

In the same way, the design envelope of acting shear in the most unfavorable shear wall C1 is shown in the following figure:

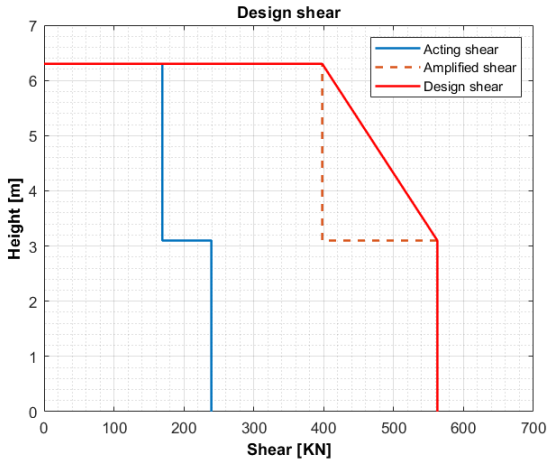

Figure 6.3: Design shear for wall C1. Model I

In summary, the design internal actions for the wall C1 are listed in Table 6.11.

Table 6.11: Design loads for wall C1. Model I

Height [m]	$\mathbf{N_{Ed}}$ **[KN]**	$\mathbf{M_{Ed}}$ **[KN-m]**	$\mathbf{V_{Ed}}$ **[KN]**
0.0	285.4	1230.7	563.0
2.0	285.4	1230.7	563.0
3.2	130.1	1015.8	563.0
6.4	130.1	390.8	398.0

Axial force

According to Eurocode 8 for DCH, the value of the normalized axial force v_d shall not exceed 0.35. Since the cross section of each wall does not change along the height, the normalized axial force is only verified at the base of the wall.

$$v_d = \frac{N_{Ed}}{A_c f_{cd}} \tag{6.2}$$

Where:

N_{Ed} is the axial force from the analysis for the seismic design situation;

A_c is the area of section of concrete member;

f_{cd} is the design value of concrete compressive strength.

Table 6.12: Normalized axial force in walls. Model I

Height [m]	$\mathbf{N_{Ed}}$ **[KN]**	$\mathbf{v_d}$ **[-]**	$\mathbf{v_d < 0.35}$ **[-]**
0.0	285.4	0.02	Ok

Bending resistance

The acting bending moment must be computed with the least favorable value of axial force coming from the analysis in the seismic design situation. In order to ensure a proper ductility at the base of the wall, a sufficient confinement in the compressed zone should be provided inside the critical region of the element. This confinement must be defined over the height h_{cr} of the critical zone and a length l_c of the cross section (Fig. 6.4). In accordance with Eurocode 8, l_c should be not smaller than $0.15l_w$ or $1.5b_w$.

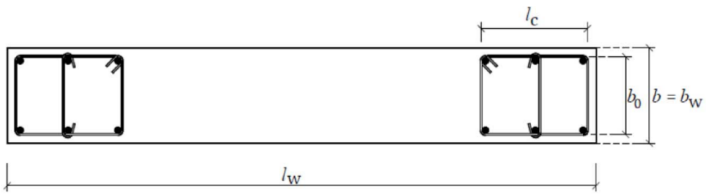

Figure 6.4: Wall confinement

Length l_c is measured from the extreme compression fiber of the wall up to the point where unconfined concrete may spall due to large compressive strains (Fig. 6.5).

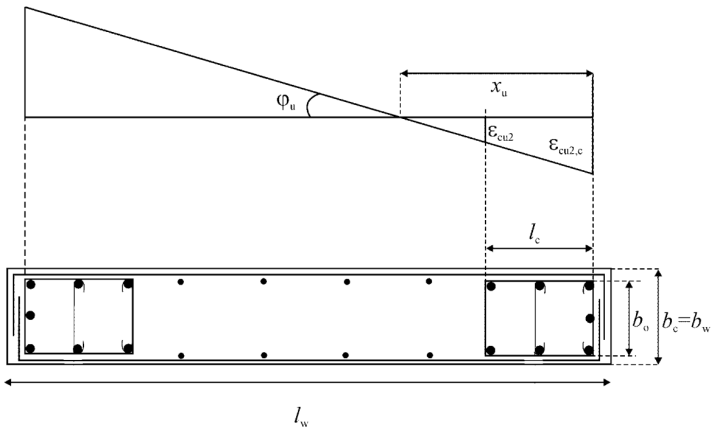

Figure 6.5: Confined boundary element [2].

Where:

$\varepsilon_{cu2} = 0.0035$	is the ultimate strain of unconfined concrete;
$\varepsilon_{cu2,c} = 0.0035 + 0.1\alpha\omega_{wd}$	is the ultimate strain of confined concrete;
α	is the confinement effectiveness factor;
ω_{wd}	is the mechanical volumetric ratio of confining reinforcement;
x_u	is the neutral axis depth.

Over the critical height h_{cr}, the mechanical volumetric ratio of confining ω_{wd} should be at least equal to 0.12 and:

$$\alpha\omega_{wd} \geq 30\mu_\phi \left(v_d + \omega_v\right) \cdot \varepsilon_{sy,d} \cdot \frac{b_c}{b_0} - 0.035 \tag{6.3}$$

$$\omega_{wd} = \frac{volume\ of\ confining\ hoops}{volume\ of\ concrete\ core} \cdot \frac{f_{yd}}{f_{cd}} \tag{6.4}$$

$$\alpha = \alpha_n \alpha_s \tag{6.5}$$

$$\alpha_n = 1 - \sum_n \frac{{b_i}^2}{6 b_0 l_o} \tag{6.6}$$

$$\alpha_s = \left(1 - \frac{s}{2b_0}\right)\left(1 - \frac{s}{2l_0}\right) \tag{6.7}$$

Where:

μ_ϕ	is the curvature ductility factor;
ω_v	is the mechanical ratio of vertical web reinforcement;
$\varepsilon_{sy,d}$	is the design value of steel strain at yield ;
bi	is the distance between consecutive engaged bars.

Unless a more exhaustive method to determine μ_ϕ is used, the value μ_ϕ should be at least equal to:

$$\mu_\phi = 2q_0 \frac{M_{Ed}}{M_{Rd}} - 1 \qquad if\ \ T_1 \geq T_c \tag{6.8}$$

$$\mu_\phi = 1 - 2\left(q_0 \cdot \frac{M_{Ed}}{M_{Rd}} - 1\right) \cdot \frac{T_c}{T_1} \qquad if\ \ T_1 < T_c \tag{6.9}$$

Assuming vertical equilibrium and the same yielded amount of reinforcement steel over l_c at both ends, the neutral axis can be approximated using the following expression:

$$x_u = (v_d + \omega_v)\,\frac{l_w b_c}{b_0} \tag{6.10}$$

Taking into consideration all the above mentioned, the vertical designed reinforcement is shown in the following table:

Table 6.13: Vertical reinforcement of wall C1. Model I

	Boundary element	**Web**
Concrete cover, c$[mm]$	30	30
Bar diameter, $\phi[mm]$	12	12
# of bars	12	14
Area of vertical reinforcement, A_{sv} $[mm^2]$	1357	1583
Vertical reinforcement ratio ρ_v	0.008	0.005

In the same way, horizontal reinforcement for the confined zones is listed below.

Table 6.14: Horizontal reinforcement of wall C1. Model I

	Boundary element
Concrete cover, c$[mm]$	30
Bar diameter, $\phi[mm]$	8
# of arms	2
Spacing, $s_w[mm]$	50
Area of horizontal reinforcement, A_{sv} $[mm^2]$	101
Horizontal reinforcement ratio ρ_h	0.006

Once the vertical reinforcement has been determined, it is verified that in every section of the wall, the following condition is fulfilled :

$$M_{Rd} \geq M_{Ed} \tag{6.11}$$

The Table 6.15 contains the design moment resistance of the wall along its height.

Table 6.15: Bending resistance wall C1. Model I

Height [m]	$\mathbf{M_{Ed}}$ **[KN-m]**	$\mathbf{M_{Rd}}$ **[KN-m]**	$\mathbf{M_{Rd} > M_{Ed}}$ **[-]**
0.0	1230.7	1720	Ok
2.0	1230.7	1720	Ok
3.2	1015.8	1610	Ok
6.4	390.8	1610	Ok

Since all the walls have the same geometry and the internal actions are similar, the same reinforcement is used for all the walls. The following figure shows the $M - N$ interaction diagram for all the shear walls in this model.

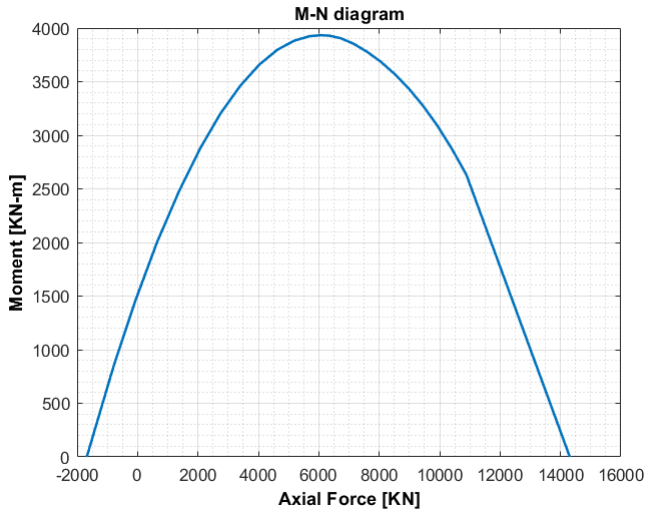

Figure 6.6: M-N interaction diagram for all the walls. Model I

The corresponding check for ductility at the base of the wall C1, is verified below.

Table 6.16: Ductility check wall C1. Model I

Element	$\mathbf{l_c}$ **[m]**	μ_ϕ **[-]**	$\omega_\mathbf{v}$ **[-]**	$\mathbf{x_u}$ **[m]**	$\alpha\omega_{\mathbf{wd,min}}$ **[-]**	α **[-]**	$\omega_\mathbf{wd}$ **[-]**	$\alpha\omega_\mathbf{wd}$ **[-]**	
Wall C1	0.48	5.19	0.099	0.30	0.12	0.659	0.190	0.125	Ok

Shear resistance

In every section of the wall, the shear capacity of the element should be greater than the shear acting force. Shear resistance shall be computed according to recommendations inside Eurocode 8 as follows:

Diagonal compression failure of the web

Outside the critical region, the shear resistance must be computed according to the following equation:

$$V_{Rd,max} = b_w z \nu_1 f_{cd} \cdot \frac{1}{\cot\theta + \tan\theta} \tag{6.12}$$

Where:

b_w	is the minimum width between tension and compression chords;
z	is the inner lever arm;
ν_1	is the strength reduction factor for concrete cracked in shear;
θ	is the angle of the concrete compression strut.

Inside the critical region, the same formulation previously described is used to calculate the shear resistance, but the value shall be reduced to 40%.

Diagonal tension failure of the web

For the tension shear resistance, the following value of the shear ratio α_s is introduced.

$$\alpha_s = \frac{M_{Ed}}{V_{Ed}\, l_w} \tag{6.13}$$

If the ratio $\alpha_s \geq 2.0$, shear resistance shall be calculated as follows:

$$V_{Rd,s} = \frac{A_{sw}}{s} z f_{ywd} \cot\theta \tag{6.14}$$

Where:

A_{sw}	is the cross-sectional area of the shear reinforcement;
s	is the spacing of the stirrups;
$f_{yw,d}$	is the design yield strength of the shear reinforcement.

If the ratio $\alpha_s < 2.0$, the following inequalities must be cheeked. The first in-

equality concerns the horizontal web bars, it must be satisfied that:

$$V_{Ed} \leq V_{Rd,c} + 0.75\rho_h f_{yd,h}\, b_{wo}\, \alpha_s\, l_w \tag{6.15}$$

With:

$$V_{rd,c} = \left[C_{Rd,c} k \left(100\rho_l\, f_{ck}\right)^{1/3} + k_1\sigma_{cp}\right] b_w d \;\geq\; \left(v_{min} + k_1\sigma_{cp}\right) b_W d \tag{6.16}$$

Where:

ρ_h	is the reinforcement ratio of horizontal web bars;
$f_{yw,h}$	is the design value of the yield strength of the horizontal web reinforcement.
k	$= 1 + \sqrt{\frac{200}{d}} \leq 2.0 \quad (d\, in\, mm)$;
ρ_l	$= \frac{A_{sl}}{b_w d} \;\leq\; 0.02$
A_{sl}	is the area of the tensile reinforcement;
σ_{cp}	$= N_{Ed}/A_c < 0.2 f_{cd}$
A_c	is the area of concrete cross section;
$C_{Rd,c}$	$= \frac{0.18}{\gamma_c}$
v_{min}	$= 0.035 \cdot k^{3/2} {f_{ck}}^{1/2}$
γ_c	is the partial factor for concrete.

The second inequality considers the vertical web bars anchored and joined along the height of the wall:

$$\rho_h f_{yd,h} b_{wo} z \leq \rho_v f_{yd,v} b_{wo} z + min N_{Ed} \tag{6.17}$$

Where:

ρ_v	is the reinforcement ratio of vertical web bars;
$f_{yw,v}$	is the design value of the yield strength of the vertical web reinforcement.

Sliding shear failure

To prevent a potential sliding shear failure within the critical region of the wall, the design value of shear resistance against sliding of the wall $V_{Rd,S}$ must be greater than the acting shear at the base of the element.

The value of $V_{Rd,S}$ is determined by the following equation:

$$V_{Rd,S} = V_{dd} + V_{id} + V_{fd} \tag{6.18}$$

With:

$$V_{dd} = min \begin{cases} 1.3 \cdot \sum A_{sj} \cdot f_{yd} \sqrt{f_{cd} \cdot f_{yd}} \\ 0.25 \cdot f_{yd} \cdot \sum A_{sj} \end{cases} \tag{6.19}$$

$$V_{id} = \sum A_{si} \cdot f_{yd} \cdot \cos \varphi \tag{6.20}$$

$$V_{fd} = min \begin{cases} \mu_f \cdot [(\sum A_{sj} \cdot f_{yd} + N_{Ed}) \cdot \xi + M_{Ed}/z] \\ 0.5\eta \cdot f_{cd} \cdot \xi \cdot l_w \cdot b_{w0} \end{cases} \tag{6.21}$$

Where:

V_{dd}	is the dowel resistance of the vertical bars;
V_{id}	is the shear resistance of inclined bars;
V_{fd}	is the friction resistance;
A_{sj}	is the sum of the areas of the vertical bars of the web and of additional bars arranged for resistance against sliding;
A_{si}	is the sum of the areas of all inclined bars in both directions;
φ	is the angle of the potential sliding plane;
μ_f	is the concrete-to-concrete friction coefficient under cyclic actions;
ξ	is the normalised neutral axis depth;
η	$= 0,6(1 - f_{ck}(MPa)/250)$

Summarizing, the designed reinforcement in the web to resist the shear action is presented in Table 6.17.

Table 6.17: Horizontal reinforcement for shear of wall C1. Model I

	Web
Concrete cover, c$[mm]$	30
Bar diameter, $\phi[mm]$	10
# of arms	2
Spacing, $s_w[mm]$	100
Area of horizontal reinforcement, A_{sv} $[mm^2]$	157
Vertical reinforcement ratio ρ_h	0.005

The following table shows the shear resistance values of wall C1:

Table 6.18: Shear strength wall C1. Model I

Height [m]	$\mathbf{V_{Ed}}$ **[KN]**	$\mathbf{V_{Rd,max}}$ **[KN]**	α_s **[-]**	$\mathbf{V_{Rd,s}}$ **[KN]**	**Eq. (6.15)** **[-]**	**Eq. (6.17)** **[-]**	$\mathbf{V_{Rd,S}}$ **[KN]**
0.0-3.2	563.0	1081	1.09	1029	Ok	Ok	829
3.2-6.0	563.0	2703	0.90	853	Ok	Ok	–

Final steel reinforcement of wall C1 is shown in the following figure.

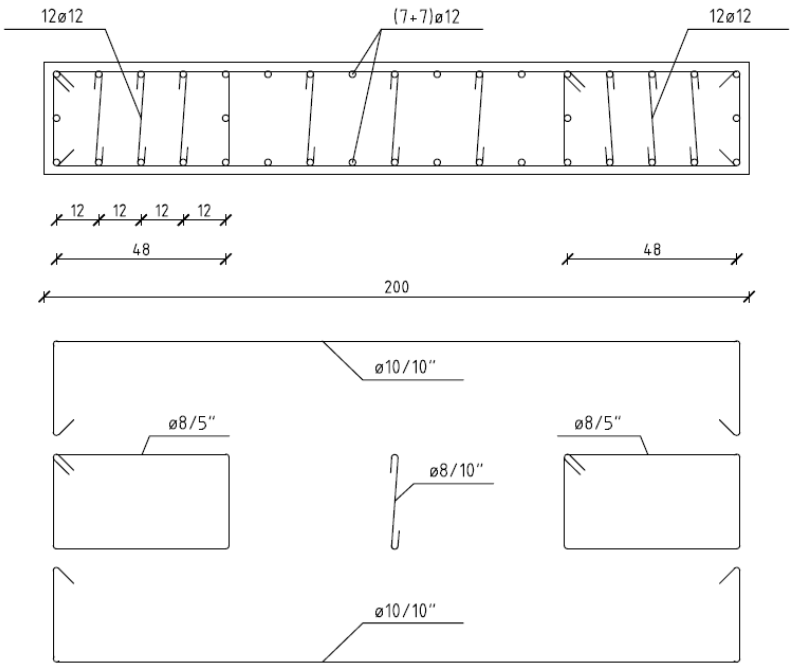

Figure 6.7: Steel reinforcement Wall C1. Model I

6.2.2.2 Columns

As previously mentioned, columns are considered as secondary seismic elements and therefore, they are designed according to the provision inside Eurocode 2. Columns are elements that can be significantly influenced by second order effects. They may be ignored if the slenderness of the element is below a certain value:

$$\lambda < \lambda_{lim} \tag{6.22}$$

$$\lambda = \frac{l_0}{i} \tag{6.23}$$

$$\lambda_{lim} = 20 \cdot A \cdot B \cdot C \cdot \frac{1}{\sqrt{n}} \tag{6.24}$$

Where:

A	$= 1/(1 + 0.2\varphi_{ef}$ (if φ_{ef} is not known, $A = 0.7$ may be used);
B	$= \sqrt{1 + 2\omega}$ (if ω is not known, $B = 1.1$ may be used);
C	$= 1.7 - r_m$ (if r_m is not known, $C = 0.7$ may be used);
φ_{ef}	is the effective creep ratio;
ω	is the mechanical reinforcement ratio;
n	$= N_{Ed}/\left(A_c f_{cd}\right)$; is the relative normal force;
r_m	M_{01}/M_{02}; is the moment ratio;
M_{01}, M_{02}	are the first order end moments;
l_o	is the effective length;
i	is the radius of gyration of the uncracked section.

Table 6.19: Column slenderness. Model I

Element	$\mathbf{N_{Ed,max}}$ **[KN]**	$\mathbf{v_d}$ **[-]**	λ **[-]**	$\lambda_{\mathbf{lim}}$ **[-]**	
Corner column	257.8	0.143	22.5	26.2	No slender
Edge column	306.4	0.147	19.3	28.1	No slender
Internal column	754.2	0.277	16.9	20.4	No slender

For all the columns of the structure, second order effects are neglected.

Bending resistance

At every cross-section of the members, the resistance moment capacity must be grater than the maximum acting moment coming from the analysis. An additional moment due to accidental eccentricity in the section is added to the design bending moment.

For the sake of simplification, the same reinforcement steel designed for the most unfavorable action of each column, is extended along the two stories of the building. Results are shown in Table 6.20.

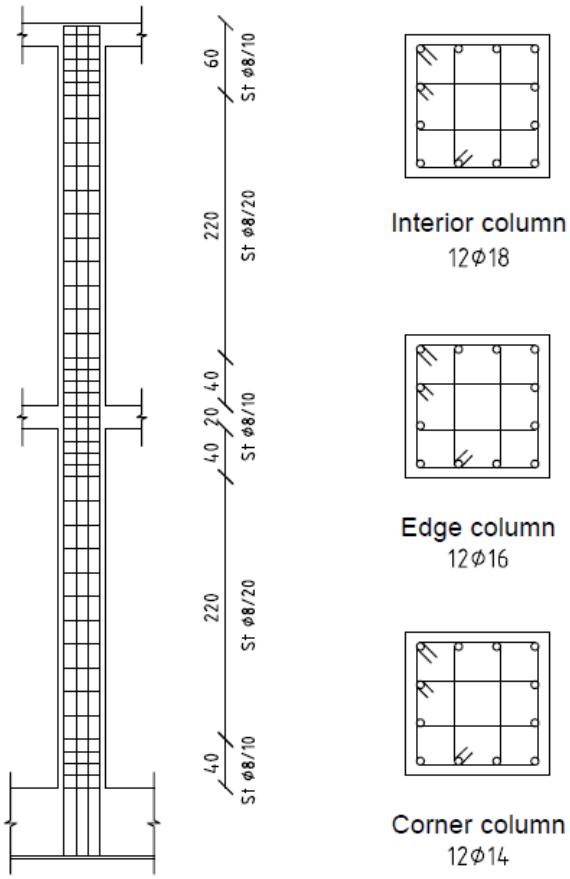

Figure 6.8: Steel reinforcement for columns. Model I

A schematic representation of the designed steel reinforcement in columns is shown in fig Fig. 6.8.

Table 6.20: Bending moment resistance columns. Model I

Element	N_{Ed} [KN]	$M_{Ed,y}$ [KN-m]	$M_{Ed,z}$ [KN-m]	Bar diameter [mm]	# of bars [-]	$M_{Rd,y}$ [KN-m]	$M_{Rd,z}$ [KN-m]
Corner column	131.1	45.4	60.1	14	12	52.0	68.0
Edge column	155.8	67.9	80.9	16	12	82.0	102.0
Interior column	372.8	80.2	77.7	18	12	125.0	121.0

The interaction axial force-bending moment curve for corner columns is shown in the following figure.

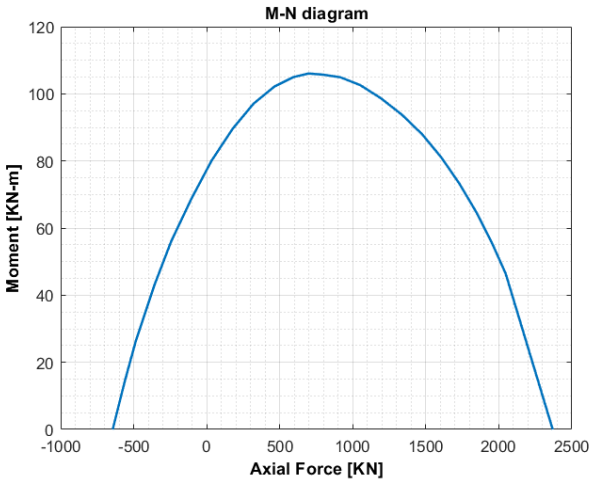

Figure 6.9: M-N interaction diagram for corner columns. Model I

Shear resistance

Shear resistance shall be grater than the acting shear computed in the analysis of the structure for the most unfavorable load combination. Shear strength is calculated according to the expressions in Eq. (6.12) and Eq. (6.14). The reinforcement selected and the values of the design shear resistance force for the columns are listed in Table 6.21.

Table 6.21: Shear reinforcement in columns. Model I

Element	$V_{Ed,y}$ [KN]	$V_{Ed,z}$ [KN]	$V_{Rd,max}$ [KN]	Spacing, s [mm]	Bar diameter [mm]	Arms [-]	$V_{Rd,s}$ [KN]	Spacing column ends [mm]
Corner column	27.8	21.9	342.1	200	8	2	42.4	100
Edge column	41.5	31.2	482.3	200	8	2	51.3	100
Interior column	34.9	35.7	646.3	200	8	2	60.1	100

6.2.2.3 Slab

The design of slabs was carried out using the values of actions coming from the analysis of the finite element model. The values of internal actions obtained by the software, follow the Wood-Armer criterion in which the twisting moment is explicitly incorporated in the design moment.

The design procedure is based on Eurocode 2 and on the recommendation inside the technical report "How to design reinforced concrete flat slabs using finite element analysis" [23] for finite element modeling of flat slabs.

Bending moment

To design the amount of steel reinforcement for bending, the slab is divided into different strips along both directions (see Fig. 6.10). Then the values of acting bending moment obtained in each finite element from the analysis, are distributed inside these strips by averaging them over the length over the column and middle strips.

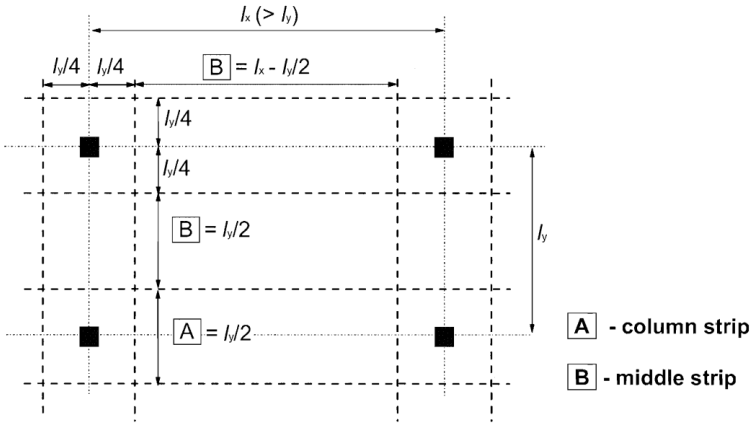

Figure 6.10: Division of panels in flat slabs [3]

In this section, only the design for maximum actions are listed. For maximum negative bending moment, the top reinforcement at slab-column connection C2 of the strip column along axis number 2 (see Fig. 6.11) is described. For maximum positive bending moment, the design for bottom reinforcement at mid-span between A2-C2 inside the same strip is shown here. The same reinforcement arrangement is used for both slabs.

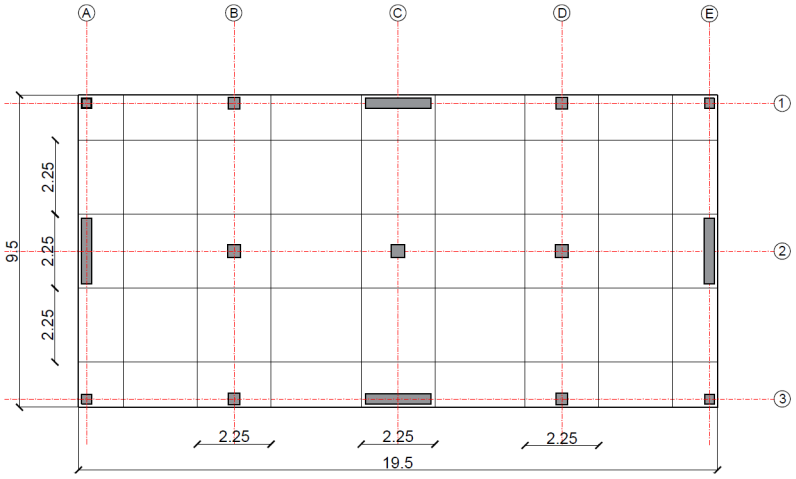

Figure 6.11: Division of panels. Model I

It is important to mentioned that the bottom reinforcement is the same in all the slab, except for the slab column connection where at least two bars must pass through the column. This was done in order to maintain a certain simplicity in the arrangement of steel reinforcement.

Top reinforcement for maximum negative bending moment at slab-column connection C2 is listed below.

Table 6.22: Maximum top reinforcement. Model I

Parameter	**Value**
Strip width, $b[mm]$	2250
Slab depth, $h[mm]$	200
Concrete cover, $c[mm]$	30
Bar diameter, $\phi[mm]$	16
# of bars	16
Area of steel, A_s $[mm^2]$	3217
Acting moment $M_{Ed,x}$	123
Resisting moment $M_{Rd,x}$	138

The following table shows the bottom reinforcement used for the span A2-C2. A uniform mesh of bars #12 spaced at 25 cm was selected for whole slab except at the slab-column connection where the spacing is 20 cm.

Table 6.23: Bottom reinforcement. Model I

Parameter	Value
Strip width, $b[mm]$	2250
Slab depth, $h[mm]$	200
Concrete cover, $c[mm]$	30
Bar diameter, $\phi[mm]$	12
# of bars	10
Area of steel, A_s $[mm^2]$	1131
Acting moment $M_{Ed,x}$	57
Resisting moment $M_{Rd,x}$	67

Complete arrangement of steel reinforcement can be found in Appendix B.

Punching shear resistance

Punching shear resistance was determined according to Eurocode 2 (see Section 4.2.1). Two basic verification are performed in order to evaluate the punching shear in the slab column connection.

The first verification is performed at the column face perimeter U_0 . The results obtained are shown in the following table:

Table 6.24: Punching shear at column face. Model I

Parameter	Corner column	Edge column	Interior column
Column Dimensions, $[mm]$	300x300	350x350	400x400
Slab depth, $h[mm]$	200	200	200
Concrete cover, $c[mm]$	30	30	30
Effective depth, $d[mm]$	158	156	156
β	1.5	1.4	1.15
Control perimeter, $U_0[mm]$	474	818	1600
$V_{Ed}[KN]$	59.82	144.58	365.80
$v_{Ed}[MPa]$	1.20	1.59	1.69
$v_{Rd,max}[MPa]$	4.22	4.22	4.22

From the values reported in the table above, no punching shear problem at column face are present. The second verification is performed at the basic control perimeter. Basic control perimeter U_1 is determined according to Fig. 4.11 and Fig. 4.12. Results are listed in Table 6.25.

Table 6.25: Punching shear at basic control perimeter. Model I

Parameter	**Corner column**	**Edge column**	**Interior column**
Column Dimensions, $[mm]$	300x300	350x350	400x400
Slab depth, $h[mm]$	200	200	200
Concrete cover, $c[mm]$	30	30	30
Effective depth, $d[mm]$	158	156	156
β	1.5	1.4	1.15
ρ_l	0.0051	0.0078	0.0099
Basic control perimeter, $U_1[mm]$	1296	2230	3560
$V_{Ed}[KN]$	54.42	134.68	351.4
$v_{Ed}[MPa]$	0.399	0.542	0.728
$v_{Rd}[MPa]$	0.596	0.686	0.743

It is concluded then, that no punching shear reinforcement in the slab-column connections is needed at ULS for vertical loads.

Although no further provisions are given in Eurocode 8 for the seismic design of flat slabs as secondary elements, they must be able to carry the gravity loading and to withstand the displacement imposed by the primary elements. For this reason, an additional checks is suggested to evaluate the drift capacity of the flat slab system.

Ramos et al. [38] proposed a simple formula, based on the ACI 318 prescriptive approach and on the available existing experimental data in Europe, to determine the values of the ultimate drift of the a flat-slab structure. This approach evaluates the performance of a slab column connection based on a relationship between the ultimate drift and the gravity shear ratio GSR. Gravity shear ratio is defined as the ratio between the acting shear under gravity loads during a seismic action and the nominal shear resistance of the slab.

Hence, the ultimate drift ratio d_r, can be obtained through the following equation:

$$d_r = 4.82 \cdot 10^{-0.83 \cdot GSR} - 0.71 \tag{6.25}$$

$$GSR = \frac{V_g}{V_0} \tag{6.26}$$

Where:

V_g is the slab shear force due to gravitational loads under seismic ULS design;

V_0 is the nominal shear strength of the slab-column connection at the basic control perimeter.

The following table summarizes the ultimate drift capacity of each type of slab column connection:

Table 6.26: Ultimate inter-story drift Model I. Ramos et al.

Parameter	**Corner column**	**Edge column**	**Interior column**
$V_{Ed}\,[KN]$	35.9	82.7	218.0
$v_{Ed}\,[MPa]$	0.263	0.333	0.451
$v_{Rd}\,[MPa]$	0.596	0.686	0.743
GSR	0.44	0.48	0.61
$d_r[\%]$	1.37	1.20	0.79

The ultimate inter-story drift ratios that a slab-column connection can reach under lateral loading, obtained through this formulation, resulted bigger than the inter-story drift ratio produced by the seismic action. Thus, the failure of the structure due to punching shear under seismic action is avoided.

Additional checks using the ACI 318-19 (see Section 4.2.2) and the draft for the second generation of Eurocode 2 are carried out. The following equations which were extracted from [4], were used to calculate the shear performance according to the second generation of Eurocode 2.

$$V_{Rd,c} = \frac{3.8}{\gamma_v} b_{0,5}^{1/2} \cdot d^{3/2} \left(100 \rho_{hog} f_{ck} \frac{d_{dg}}{d\sqrt{L/\left(36 \cdot d\right)}} \right)^{1/3} \tag{6.27}$$

Where:

γ_v is the partial safety factor for shear (proposed as 1.40);

$b_{0,5}$ is the length of control perimeter located at a distance of 0.5 d from the face of the column;

d is the effective depth of the slab;

ρ_{hog} is the hogging reinforcement ratio;

d_{dg} $= d_g + 16mm$; is a dimension which describes the roughness of the critical shear crack;

d_g is the aggregate size;

L is the slab span.

For not slender columns, slab rotation can be approximated to the inter-story drift. The rotation capacity of the slab can calculated using the following expression:

$$\psi_{slab,R} = 0.60\% \cdot \left(\frac{b_{0,5}}{10 \cdot d} \cdot \frac{1}{100 \cdot \rho_{hog}}\right)^{3/4} \cdot \left(\frac{10 \cdot d_{dg}}{d} \cdot \frac{L}{36 \cdot d}\right)^{1/2} \cdot f\left(GSR\right) \quad (6.28)$$

With:

$$f\left(GSR\right) = 1 - \left(2 \cdot GSR - 1\right)^{3/2} \qquad for \;\; 0.50 \leq GSR \leq 1.00 \quad (6.29)$$

$$f\left(GSR\right) = 1 + 1.2 \cdot \left(1 - 2 \cdot GSR\right)^{3/2} \cdot \left(\frac{\rho_{hog}}{\rho_{sag}}\right)^{4/3} \leq 2 \;\; for \; 0.20 \leq GSR < 0.50 \quad (6.30)$$

Where:

GRS is the gravity shear ratio;

ρ_{sag} is the sagging reinforcement ratio. $\rho_{hog}/\rho_{sag} \leq 2$

The inter-story drift capacity of the flat-slab system according to ACI-318 and the draft of the second generation of Eurocode 2, are summarized in the following tables:

Table 6.27: Ultimate inter-story drift Model I. ACI 318-19

Parameter	**Corner column**	**Edge column**	**Interior column**
$v_u\,[MPa]$	0.299	0.488	0.934
$v_c\,[MPa]$	1.818	1.818	1.818
$v_u/\phi v_c$	0.219	0.357	0.685
d_r [%]	2.40	1.71	0.50

Table 6.28: Ultimate inter-story drift Model I. Draft 2^{nd} generation of Eurocode 2

Parameter	**Corner column**	**Edge column**	**Interior column**
$v_{Ed}\,[MPa]$	0.288	0.394	0.696
$v_{Rd}\,[MPa]$	1.703	1.561	1.381
GSR	0.17	0.25	0.50
$\psi_{slab,R}$ [%]	1.65	1.75	1.02

In both cases, the flat slab structure is able to withstand the inter-story drifts imposed by the primary elements without the necessity of punching shear reinforcement in the slab-column connection.

No guidance is given by Eurocode 2 or Eurocode 8 for the evaluation of punching shear in shear walls connections. Nevertheless, a punching shear check is performed here according to the provision inside Model Code 2010 (see Section 4.2.3) for defining the control perimeter and according to the draft for the second generation of Eurocode 2 (see Eq. (6.28) and Eq. (6.29)) for the evaluation of punching shear resistance.

Table 6.29: Punching shear at basic control perimeter wall C1. Model I

Parameter	**Wall C1 connection**
Wall dimensions, $[mm]$	2000x320
Slab depth, $h[mm]$	200
Concrete cover, $c[mm]$	30
Effective depth, $d[mm]$	158
ρ_l	0.0043
Basic control perimeter, $U_1[mm]$	771
$V_{Ed}[KN]$	105.5
$v_{Ed}[MPa]$	0.960
$v_{Rd}[MPa]$	1.760

According to the draft of the second generation of Eurocode 2, the maximum rotation that the slab can develop at the corner of the wall is shown in the following table:

Table 6.30: Ultimate inter-story drift wall C1 Model I.
Draft 2^{nd} generation of Eurocode 2

Parameter	**Wall C1 connection**
$v_{Ed}\,[MPa]$	0.566
$v_{Rd}\,[MPa]$	1.7596
GSR	0.32
$\psi_{slab,R}\,[\%]$	1.13

The slab-wall connection is able to withstand the drift developed by the ULS design seismic actions.

6.2.3 Discussion

The reinforcement designed for the all the structural elements of this structure (see Appendix A and Appendix B) is very similar to the reinforcement used for

structure tested. Especially the reinforcement arrangement proposed for the slab, resulted the same as the one Coronelli et. al. used in the specimen during the test. These similarities in the amount of steel can be explain by the fact that the geometry of this structure is still very similar to the reference specimen. Therefore, not a big variation of internal actions is present and the same dimensions and steel configuration used in the building studied, can be also used to resist the actions acting in the structure modeled here.

It is important to be noted that some variation in the values of acting shear stresses in the slab-column connection between the structure modeled here and the experimental one are present. Coronelli et al. stated that the the specimen tested was design for a GSR between 0.3 - 0.4. Nevertheless, when the design of the structure modeled here was carried out, a maximum GSR of 0.61 for interior columns was obtained. The increase of the GSR can be explained by means of the change of the concrete cover. For this structure, a concrete cover of 30 mm was proposed for the slab whereas in the structure tested, a concrete cover of 15 mm was used. The increment of the concrete of cover for the slab resulted in a reduction of the effective depth leading to the consequent reduction of the basic control perimeter for the evaluation of the punching shear. So then, an increment of shear stress occurs due to the reduction of the basic control perimeter.

Although an increment of the shear stress occurred in the slab, no punching shear problems were present. Every slab-column connection is able to resist the acting punching shear at ULS for gravitational and lateral loads. However, an obvious decrement in the drift capacity of slab-column under lateral loading is observed due to the increased of the GSR. This is also supported on the results given by Coronelli et al., in which the maximum inter-story drift reached by the structure (which in fact, it is very similar to the specimen tested) was around 2.5%, before punching shear damage was observed.

Punching capacity of the shear walls connections with the slab was also verified. No punching problems were present using the configuration of shear walls proposed. Although a punching verification around shear walls was performed, no specific provision are given in Eurocode 2 for this purpose. It is evident the necessity of developing a correct procedure to determine and check the punching shear around shear walls.

Additionally, column cross-section dimensions were reduced 5 cm in each direc-

tion in order to evaluate if the dimensions of columns used during the experimental test were optimal or not. After reducing the dimension of the cross-section of all the columns, punching shear failure was predicted for interior an corner columns, Thus, the dimension of the cross-section used in the specimen were the optimal dimension to bear the punching shear with the length of the slab panels used.

6.3 Model II

6.3.1 Structural Analysis

The structural analysis was carried out using two models as it is described in Section 6.2.1 for model I. According to Eurocode 8, the behaviour factor corresponding to the structural typology of this building (uncoupled walls system with more than two wall per horizontal direction) is $q = 4.4$. Therefore, the design response spectrum is given in Fig. 6.12.

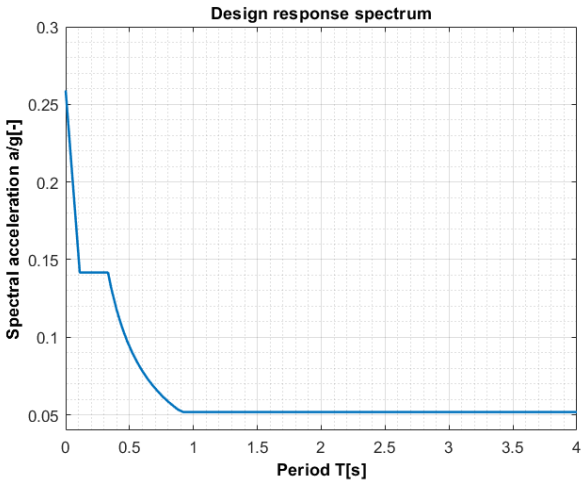

Figure 6.12: Design response spectrum. Model II

6.3.1.1 Modal analysis

After ruining a modal analysis and considering the sections of primary elements cracked, the modes of the structure obtained are listed in the Table 6.31.

The fundamental period of the structure corresponds to a translational mode

Table 6.31: Modal properties. Model II

Mode	Mass Tran-X[%]	Sum Mx[%]	Mass Tran-Y[%]	Sum My[%]	Period T[s]
1	0.00	0.00	79.17	79.17	0.340
2	78.80	78.80	0.00	79.17	0.327
3	0.00	78.80	0.00	79.17	0.233
4	0.00	78.80	20.82	100.00	0.067
5	21.19	100.00	0.00	100.00	0.061

equal to 0,340 s in Y-direction. The second mode is also a translational mode in X-direction and the third mode resulted to be a torsional mode.

6.3.1.2 Lateral displacements

At serviceability limit state seismic design situation, the inter-story drift obtained are below the limit established by Eurocode 8 (0.5%).

Table 6.32: Lateral displacements SLS. Model II

Level	Lateral displacement $d_{x,SLS}$[mm]	Inter-story drift ratio X[%]	Lateral displacement $d_{y,SLS}$[mm]	Inter-story drift ratio Y[%]
First floor	2.0	0.06	2.2	0.07
Second floor	6.0	0.18	6.8	0.21

The lateral displacements obtained from the ULS seismic design situation are listed in the following table.

Table 6.33: Lateral displacements. Model II

Level	Lateral displacement $d_{x,ULS}$[mm]	Inter-story drift ratio X[%]	Global drift ratio X[%]	Lateral displacement $d_{y,ULS}$[mm]	Inter-story drift ratio Y[%]	Global drift ratio Y[%]
First floor	7.0	0.22	–	8.0	0.25	–
Second floor	21.1	0.44	0.33	24.4	0.51	0.38

Lateral displacements still resulted very similar to the ones recorded during the

structure tested by Coronelli et al. The average lateral stiffness of the structure under seismic action is 78 830 KN/m and 66 590 KN/m in X and Y-direction respectively.

Using the model were all the elements are included with their correct value of elastic modulus, the contribution of secondary and primary elements to the lateral stiffness of the structure can be found in the following table:

Table 6.34: Stiffness distribution. Model II

Element	**X [%]**	**Y [%]**
Slab-column frame	11.4	13.2
Walls	88.6	86.8
Total	100	100

6.3.1.3 Base shear force

The distribution of the shear base under seismic action between the primary seismic elements is listed in the following table:

Table 6.35: Base shear force. Model II

Element	**Shear Force [KN]**
Walls X-direction	1663.4
Walls Y-direction	1625.0

When all the structure is considered as primary elements, the distribution of the shear base is presented in the table below.

Table 6.36: Base shear force Model II as a whole primary system.

Element	Shear Force X-direction [KN]	X-direction [%]	Shear Force Y-direction [KN]	Y-direction [%]
Slab-column frame	115.1	6.3	150.9	8.3
Walls	1705.2	93.7	1670.8	91.7
Total	1820.3	100	1821.7	100

6.3.2 Design

The design of the structural elements was carried out as follows. The shears walls, which constitute the primary resisting system for earthquake motion are design according to recommendations inside Eurocode 8 for DCH structures. Columns and slabs were design following the provisions of Eurocode 2 and with the ability to resist the displacements impose by the primary system during seismic actions. Same procedure as described in Section 6.2.2 was followed here.

6.3.2.1 Shear walls

In this part, only the design shear wall under the most unfavorable actions is carried presented. Results for the design of the other elements can be found in Appendix A. The dimensions selected for each shear wall are listed in the following table:

Table 6.37: Shear walls dimensions. Model II

Element	L_w [m]	b_w [m]	h_w [m]
Wall A3	2.60	0.32	6.40
Wall C1	2.40	0.32	6.40
Wall C5	2.40	0.32	6.40
Wall E3	2.60	0.32	6.40
Wall G1	2.40	0.32	6.40
Wall G5	2.60	0.32	6.40
Wall I3	2.40	0.32	6.40

The wall with the most unfavorable internal actions is the wall A3. The following two figures show the design envelope of bending moment and shear acting in the shear wall A3.

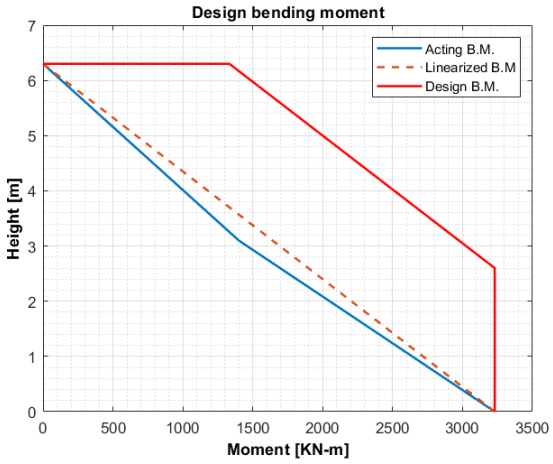

Figure 6.13: Design bending moment for wall A3. Model II

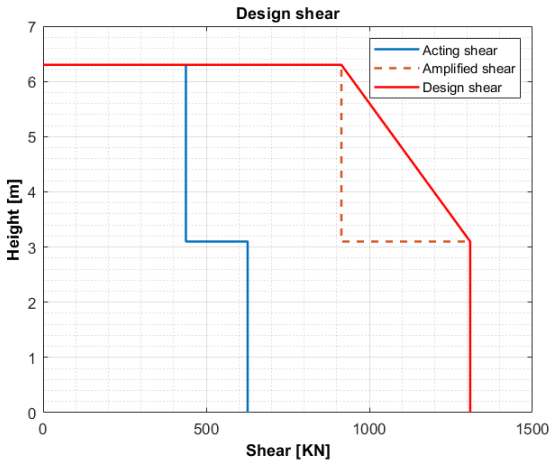

Figure 6.14: Design shear for wall A3. Model II

Summarizing, the design actions for wall A3 are listed in the following table:

Table 6.38: Design loads for wall A3. Model II

Height [m]	$\mathbf{N_{Ed}}$ **[KN]**	$\mathbf{M_{Ed}}$ **[KN-m]**	$\mathbf{V_{Ed}}$ **[KN]**
0.0	288.0	3230.0	1309.0
2.0	288.0	3230.0	1309.0
3.2	130.0	2974.0	1309.0
6.4	130.0	1333.1	914.4

Axial force

According to Eurocode 8 for DCH, the value of the normalized axial force v_d shall not exceed 0.35. Table 6.39 shows the corresponding check for the normalized axial force of wall A3.

Table 6.39: Normalized axial force in wall A3. Model II

Height [m]	$\mathbf{N_{Ed}}$ **[KN]**	$\mathbf{v_d}$ **[-]**	$\mathbf{v_d < 0.35}$ **[-]**
0.0	288	0.02	Ok
2.0	288	0.02	Ok
3.2	130	0.01	Ok
6.4	130	0.01	Ok

Bending resistance

The vertical reinforcement designed for this wall is shown in the following table:

Table 6.40: Vertical reinforcement wall A3. Model II

	Boundary element	**Web**
Concrete cover, c[mm]	30	30
Bar diameter, ϕ[mm]	16	14
# of bars	14	20
Area of vertical reinforcement, A_{sv} [mm^2]	2815	3079
Vertical reinforcement ratio ρ_v	0.013	0.007

In the same way, horizontal reinforcement for the confined zones is listed below.

Table 6.41: Horizontal reinforcement Wall A3. Model II

	Boundary element
Concrete cover, c$[mm]$	30
Bar diameter, $\phi[mm]$	10
# of arms	2
Spacing, $s_w[mm]$	50
Area of horizontal reinforcement, A_{sv} $[mm^2]$	101
Horizontal reinforcement ratio ρ_h	0.010

The corresponding bending resisting check, along the height of the wall, is presented in Table 6.42.

Table 6.42: Bending resistance wall A3. Model II

Height [m]	$\mathbf{M_{Ed}}$ **[KN-m]**	$\mathbf{M_{Rd}}$ **[KN-m]**	$\mathbf{M_{Rd} > M_{Ed}}$ **[-]**
0.0	3230	3700	Ok
2.0	3230	3700	Ok
3.2	2974	3590	Ok
6.4	1333	3590	Ok

The Fig. 6.15 shows the M-N interaction diagram for wall A3.

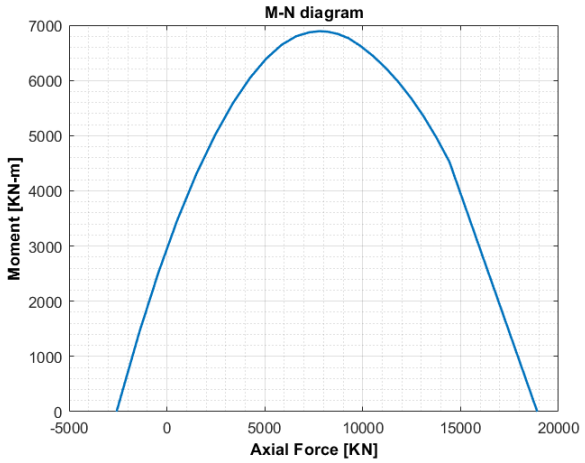

Figure 6.15: M-N interaction diagram for wall A3. Model II

In order to comply with the ductility needed in the base of the walls for DCH structures, the following check for wall A3 is performed.

Table 6.43: Ductility check wall A3. Model II

Element	$\mathbf{l_c}$ [m]	μ_ϕ [-]	$\omega_\mathbf{v}$ [-]	$\mathbf{x_u}$ [m]	$\alpha\omega_{\mathbf{wd,min}}$ [-]	α [-]	$\omega_\mathbf{wd}$ [-]	$\alpha\omega_\mathbf{wd}$ [-]	
Wall C1	0.60	6.68	0.14	0.51	0.12	0.68	0.275	0.187	Ok

Shear resistance

Following the same procedure describe in Section 6.2.2.1 for the shear resistance of the walls, the horizontal reinforcement in the web of wall A3 to resist the shear action is listed in the following table:

Table 6.44: Horizontal reinforcement for shear wall A3. Model II

	Web
Concrete cover, c$[mm]$	30
Bar diameter, $\phi[mm]$	8
# of arms	2
Spacing, $s_w[mm]$	50
Area of horizontal reinforcement, A_{sv} $[mm^2]$	101
Vertical reinforcement ratio ρ_h	0.006

The corresponding checks for shear resistance for the aforementioned wall are summarized in Table 6.41.

Table 6.45: Shear strength wall A3. Model II

Height [m]	$\mathbf{V_{Ed}}$ **[KN]**	$\mathbf{V_{Rd,max}}$ **[KN]**	α_s **[-]**	$\mathbf{V_{Rd,s}}$ **[KN]**	**Eq. (6.15)** **[-]**	**Eq. (6.17)** **[-]**	$\mathbf{V_{Rd,S}}$ **[KN]**
0.0-3.2	1309	1406	0.95	1467	Ok	Ok	1545
3.2-6.0	1309	3514	0.87	1351	Ok	Ok	–

The following figure shows the reinforcement steel of wall A3:

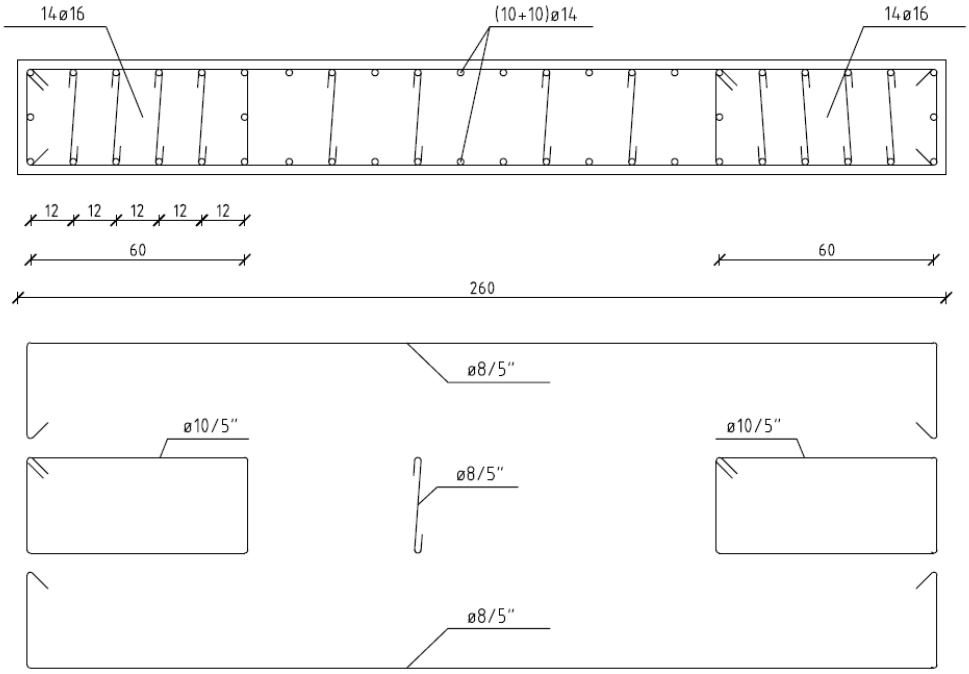

Figure 6.16: Steel reinforcement Wall A3. Model II

6.3.2.2 Columns

Columns are designed according to Eurocode 2 following the same procedure describe in Section 6.2.2.2. The first step is to determine the slenderness of the element, so then it can be known if second order effects will affect or not the design

of the columns. Table 6.46 shows that second order effects can be disregarded in the design.

Table 6.46: Column slenderness. Model II

Element	$\mathbf{N_{Ed,max}}$ **[KN]**	$\mathbf{v_d}$ **[-]**	λ **[-]**	$\lambda_{\mathbf{lim}}$ **[-]**	
Corner column	159.7	0.089	22.5	33.3	No slender
Edge column	372.9	0.152	19.3	25.47	No slender
Internal column	737.9	0.231	16.9	20.69	No slender

Bending resistance

For the sake of simplicity, the same longitudinal reinforcement for each type of column will be placed along the two stories of the building. The moment resistant check and the longitudinal reinforcement selected for every column are summarized in the following table.

Table 6.47: Bending moment resistance columns. Model II

Element	$\mathbf{N_{Ed}}$ **[KN]**	$\mathbf{M_{Ed,y}}$ **[KN-m]**	$\mathbf{M_{Ed,z}}$ **[KN-m]**	**Bar diameter [mm]**	**# of bars [-]**	$\mathbf{M_{Rd,y}}$ **[KN-m]**	$\mathbf{M_{Rd,z}}$ **[KN-m]**
Corner column	74.6	48.8	53.5	14	12	55.0	61.0
Edge column	195.3	88.9	97.1	16	12	92.0	101.0
Interior column	224.3	98.9	126.2	18	12	133.0	151.0

A schematic representation of the arrangement of steel reinforcement in columns is shown in the following figure.

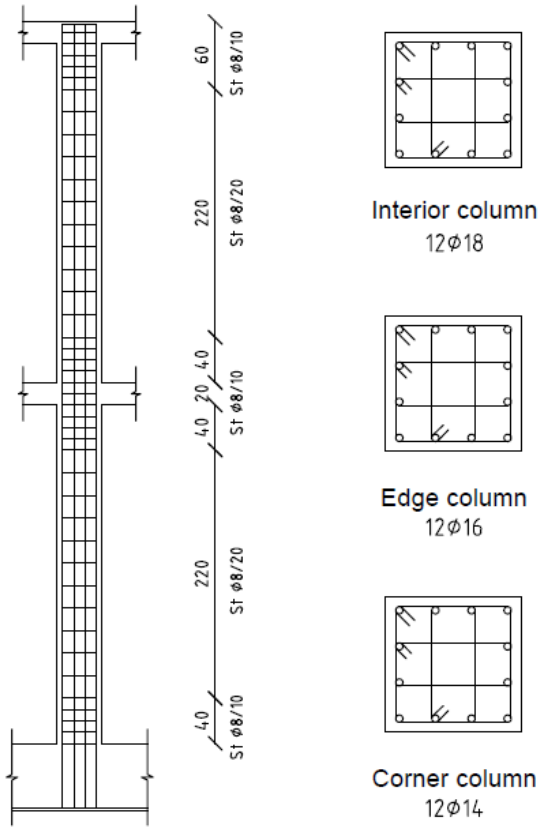

Figure 6.17: Steel reinforcement for columns. Model II

The interaction axial force-bending moment curve for corner columns is shown in the figure below.

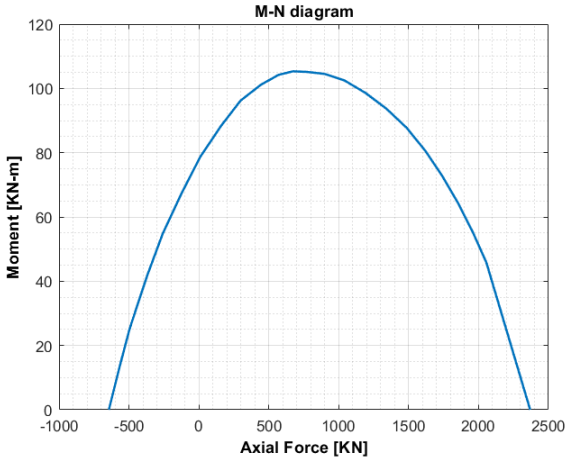

Figure 6.18: M-N interaction diagram for corner columns. Model II

Shear resistance

Shear strength is calculated in the same way as it is described in Section 6.2.2.2. Shear strength shall be greater than most unfavorable action coming for the worst combination of loads. Table 6.48 summarizes the resistance checks for columns.

Table 6.48: Shear reinforcement columns. Model II

Element	$V_{Ed,y}$ [KN]	$V_{Ed,z}$ [KN]	$V_{Rd,max}$ [KN]	Spacing, s [mm]	Bar diameter [mm]	Arms [-]	$V_{Rd,s}$ [KN]	Spacing at beam ends [mm]
Corner column	26.3	24.1	342.1	200	8	2	42.4	100
Edge column	46.8	43.4	482.3	200	8	2	51.3	100
Interior column	57.2	45.1	646.3	200	8	2	60.1	100

6.3.2.3 Slab

The design of the slabs was carried out following the procedure described in Section 6.2.2.3. It is important to point out that the reinforcement of both slabs is the same because the internal action in the slab at first and second floor are very similar.

Bending moment

For the design, the slabs was divided in different strips as it is shown in Fig. 6.19. Then the values of acting bending moment obtained in each finite element from the analysis, are distributed inside these strips by averaging them over the length over the column and middle strips.

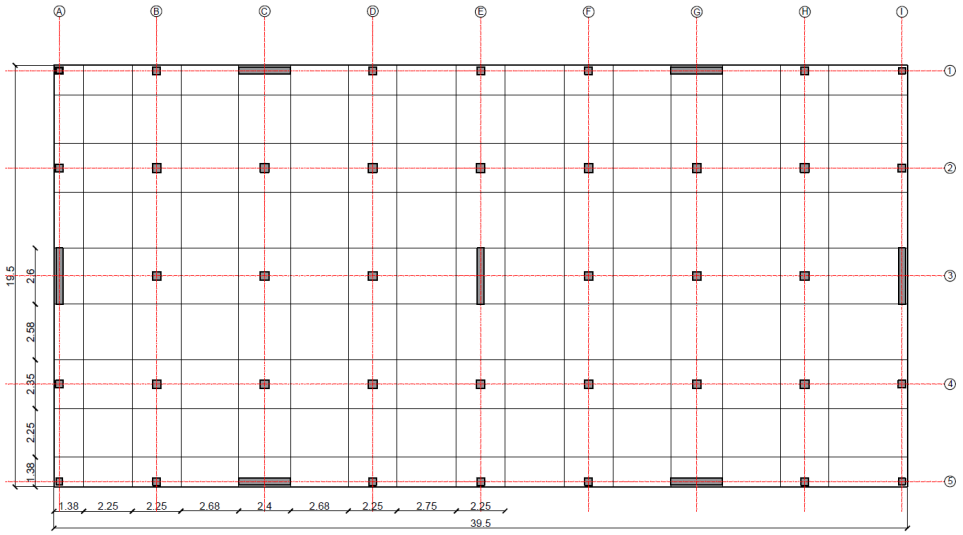

Figure 6.19: Division of panels. Model II

Top reinforcement at slab-column connection E4 in Y-direction is listed in Table 6.49. Here the maximum negative moment is developed.

Table 6.49: Maximum top reinforcement. Model II

Parameter	**Value**
Strip width, $b[mm]$	2250
Slab depth, $h[mm]$	200
Concrete cover, $c[mm]$	30
Bar diameter, $\phi[mm]$	20
# of bars	17
Area of steel, A_s $[mm^2]$	5340
Acting moment $M_{Ed,y}$	182
Resisting moment $M_{Rd,y}$	230

It has to be noted that the bottom reinforcement is the same in all the slab, except at the slab column connection where at least two bars must pass through the column. This was done in order to avoid a very complex arrangement of steel reinforcement.

The following table shows the bottom reinforcement used for the span A3-C3 in X-direction, where it is present the maximum positive bending moment. A uniform mesh of bars #12 spaced at 25 cm was selected for whole slab except at the slab column connection where the spacing is 20 cm.

Table 6.50: Bottom reinforcement. Model II

Parameter	**Value**
Strip width, $b[mm]$	2600
Slab depth, $h[mm]$	200
Concrete cover, $c[mm]$	30
Bar diameter, $\phi[mm]$	12
# of bars	12
Area of steel, A_s $[mm^2]$	1357
Acting moment $M_{Ed,x}$	63
Resisting moment $M_{Rd,x}$	78

Punching shear resistance

Punching shear resistance was determined according to Eurocode 2 (see Section 4.2.1). Two basic verification are performed in order to evaluate the punching shear in the slab column connection.

The first verification is performed at the column face. The results obtained are shown in the following table:

Table 6.51: Punching shear at column face. Model II

Parameter	**Corner column**	**Edge column**	**Interior column**
Column Dimensions, $[mm]$	300x300	350x350	400x400
Slab depth, $h[mm]$	200	200	200
Concrete cover, $c[mm]$	30	30	30
Effective depth, $d[mm]$	158	154	153
β	1.5	1.4	1.15
Control perimeter, $U_0[mm]$	474	812	1600
$V_{Ed}[KN]$	71.92	158.68	357.10
$v_{Ed}[MPa]$	1.44	1.78	1.68
$v_{Rd,max}[MPa]$	4.22	4.22	4.22

The second verification is performed at the basic control perimeter. Results are listed below.

Table 6.52: Punching shear at basic control perimeter. Model II

Parameter	**Corner column**	**Edge column**	**Interior column**
Column Dimensions, $[mm]$	300x300	350x350	400x400
Slab depth, $h[mm]$	200	200	200
Concrete cover, $c[mm]$	30	30	30
Effective depth, $d[mm]$	158	154	153
β	1.5	1.4	1.15
ρ_l	0.0058	0.0111	0.0179
Basic control perimeter, $U_1[mm]$	1296	2217	3522
$V_{Ed}[KN]$	66.52	148,78	342.7
$v_{Ed}[MPa]$	0.487	0.610	0.731
$v_{Rd}[MPa]$	0.623	0.772	0.905

After performing the two verification, it is shown that the slab-column connections can resist the acting punching shear at ULS for vertical loads without any punching shear reinforcement.

According to Ramos et al. (see Eq. (6.26)), the ultimate inter-story drift ratios that the slab-columns connections can developed are listed in Table 6.53.

Table 6.53: Ultimate inter-story drift Model II. Ramos et al.

Parameter	**Corner column**	**Edge column**	**Interior column**
$V_{Ed}\,[KN]$	42.4	93.2	215.0
$v_{Ed}\,[MPa]$	0.311	0.382	0.459
$v_{Rd}\,[MPa]$	0.623	0.772	0.905
GSR	0.5	0.49	0.51
$d_r[\%]$	1.15	1.16	1.12

The slab-column connections are able to withstand the displacements imposed by the shear wall during design seismic actions. The inter-story drifts reached by the structure under the design seismic excitation (Table 6.33) are smaller than the ultimate inter-story drift of the slab column-connections.

Additional checks are performed in order to evaluate the performance of slab-column connections under lateral loads. In any of these cases punching shear reinforcement is needed. Inter-story drift ratios for the seismic design action are below the ultimate inter-story drift ratios that the slab-column connections can develop according to ACI 318-19 and the draft of the second generation of Eurocode 2.

Table 6.54: Ultimate inter-story drift Model II. ACI 318-19

Parameter	**Corner column**	**Edge column**	**Interior column**
$v_u\,[MPa]$	0.369	0.577	0.893
$v_c\,[MPa]$	1.818	1.818	1.818
$v_u/\phi v_c$	0.270	0.423	0.655
$d_r\,[\%]$	2.15	1.38	0.50

Table 6.55: Ultimate inter-story drift Model II.
Draft 2^{nd} generation of Eurocode 2

Parameter	**Corner column**	**Edge column**	**Interior column**
$v_{Ed}\,[MPa]$	0.313	0.447	0.704
$v_{Rd}\,[MPa]$	1.780	1.750	1.675
GSR	0.18	0.25	0.42
$\psi_{slab,R}$ [%]	1.52	1.37	0.80

A punching shear analysis of slab-wall connection is performed here according to the provision inside Model Code 2010 (see Section 4.2.3) for defining the control perimeter and according to the draft of second generation of Eurocode 2 (see Eq. (6.28) and Eq. (6.29)) for the evaluation of punching shear resistance.

Table 6.56: Punching shear at basic control perimeter for walls. Model II

Parameter	**Wall C1 connection**	**Wall A3 connection**	**Wall E3 connection**
Wall dimensions, $[mm]$	2400x320	2600x320	2600x320
Slab depth, $h[mm]$	200	200	200
Concrete cover, $c[mm]$	30	30	30
Effective depth, $d[mm]$	158	158	156
ρ_l	0.0043	0.0049	0.0108
Basic control perimeter, $U_1[mm]$	771	771	1033
$V_{Ed}[KN]$	122.7	127.3	260.5
$v_{Ed}[MPa]$	1.007	1.045	1.616
$v_{Rd}[MPa]$	1.760	1.838	2.022

Maximum rotation that the slab can develop at the corner of the wall is shown in the following table:

Table 6.57: Ultimate inter-story drift for walls Model II. Draft 2^{nd} generation of Eurocode 2

Parameter	**Wall C1 connection**	**Wall A3 connection**	**Wall E3 connection**
$v_{Ed}\,[MPa]$	0.655	0.679	1.018
$v_{Rd}\,[MPa]$	1.760	1.838	2.022
GSR	0.372	0.370	0.504
$\psi_{slab,R}$ [%]	1.01	0.95	0.56

The slab-wall connection is able to withstand the drift developed by the ULS design seismic situation.

6.3.3 Discussion

It can be observed that the amount of the steel used for columns, is the same as the one used for the design of the structure in model I. Nevertheless, an increment in the concentration of top steel in the slab near columns was necessary in order to resist the acting bending moments coming from the analysis. The increase of the values of the internal actions in the slabs, is the result of increasing the dimensions of the building.

Despite the fact that the dimensions of the building were greatly increasing in both directions with respect to the dimensions of structure experimentally tested, no punching shear problems at slab-column connections are present. In fact, the values of the acting shear are almost equal to the values obtained in the previous model. This is explained by the fact that the spans between the columns remain the same as the ones used for the specimen tested and the structure of model I.

Another important aspect that can be pointed out from the analysis of this model, is the increment of the punching shear resistance of the slabs. This increment is caused by the increment of the top reinforcement concentration at the slab-column connections, increasing also, the drift capacity of the connections.

Lateral displacements and inter-story drifts obtained after performing the analysis, are still similar to the experimental results. This occurs because the di-

mensions of the spans between the columns are the same dimensions as the ones used in the reference structure and also, because the shear wall are restricting the lateral displacements even though the total dimension of the structure are much bigger than the original one.

Using the provisions inside Model Code 2010 and the Draft of the Second Generation of Eurocode 2, no punching shear problems at walls were detected. However, the results obtained for wall E3 shows that the maximum capacity drift of the slab-wall connection is very close to the maximum drift at ULS seismic situation.

6.4 Model III

6.4.1 Structural Analysis

The structural analysis for the model III was carried out following the same procedure used for the other models. The behaviour factor for this structure resulted equal to 4.4. Hence, the design response spectrum is the same as the one used for the model II (see Fig. 6.12).

6.4.1.1 Modal analysis

The results of the modal analysis with cracked sections are presented in the following table:

Table 6.58: Modal properties. Model III

Mode	Mass Tran-X[%]	Sum Mx[%]	Mass Tran-Y[%]	Sum My[%]	Period T[s]
1	0.00	0.00	77.93	77.93	0.365
2	77.79	77.79	0.00	77.93	0.324
3	0.00	77.79	0.00	77.93	0.294
4	0.00	77.79	22.07	100.00	0.057
5	22.21	100.00	0.00	100.00	0.049

The fundamental period is equal to 0.365 s in Y-direction. The second mode is also a translational mode in X-direction, and the third mode corresponds to a torsional mode.

6.4.1.2 Lateral displacements

At SLS seismic design situation, the inter-story drift obtained are below the limit established by Eurocode 8 (0.5%).

Table 6.59: Lateral displacements SLS. Model III

Level	**Lateral displacement $d_{x,SLS}$[mm]**	**Inter-story drift ratio X[%]**	**Lateral displacement $d_{y,SLS}$[mm]**	**Inter-story drift ratio Y[%]**
First floor	1.8	0.06	2.4	0.08
Second floor	5.9	0.18	7.8	0.24

At ULS for the seismic design situation, the lateral displacements obtained from the analysis are presented in the following table:

Table 6.60: Lateral displacements. Model III

Level	**Lateral displacement $d_{x,ULS}$[mm]**	**Inter-story drift ratio X[%]**	**Global drift ratio X[%]**	**Lateral displacement $d_{y,ULS}$[mm]**	**Inter-story drift ratio Y[%]**	**Global drift ratio Y[%]**
First floor	6.5	0.20	–	8.8	0.28	–
Second floor	20.8	0.45	0.33	27.9	0.60	0.44

The average lateral stiffness of the structure under seismic action is 45 270 KN/m and 30 960 KN/m in X and Y-direction respectively.

The contribution of secondary and primary elements to the lateral stiffness of the structure can be found in the following table:

Table 6.61: Stiffness distribution. Model III

Element	X [%]	Y [%]
Slab-column frame	13.2	14.8
Walls	86.8	85.2
Total	100	100

6.4.1.3 Base shear force

The distribution of the maximum shear base under seismic action between the primary seismic elements is listed in the following table:

Table 6.62: Base shear force. Model III

Element	Shear Force [KN]
Walls X-direction	944.5
Walls Y-direction	862.6

If all the structure were considered as primary elements, the distribution of the shear base is presented in the table below.

Table 6.63: Base shear force Model III as a whole primary system.

Element	Shear Force X-direction [KN]	X-direction [%]	Shear Force Y-direction [KN]	Y-direction [%]
Slab-column frame	15.1	1.6	20.1	2.2
Walls	929.4	98.4	899.9	97.8
Total	944.5	100	920.0	100

6.4.2 Design

Shear walls are design as primary seismic elements following the specifications given by Eurocode 8 for DCH structures. On the contrary, columns and flat slabs

are design as secondary seismic elements. The design is performed according to Section 6.2.2.

6.4.2.1 Shear walls

The dimensions selected for each shear walls are listed in the following table:

Table 6.64: Shear walls dimensions. Model III

Element	L_w [m]	b_w [m]	h_w [m]
Wall A2	1.80	0.32	6.40
Wall C1	1.70	0.32	6.40
Wall C2	1.70	0.32	6.40
Wall C3	1.70	0.32	6.40
Wall D2	1.80	0.32	6.40
Wall E2	1.80	0.32	6.40
Wall F1	1.70	0.32	6.40
Wall F2	1.70	0.32	6.40
Wall F3	1.70	0.32	6.40
Wall H2	1.80	0.32	6.40

The element under the most unfavorable actions is the shear wall A2. The following two figures show the design bending moment and shear for wall A2.

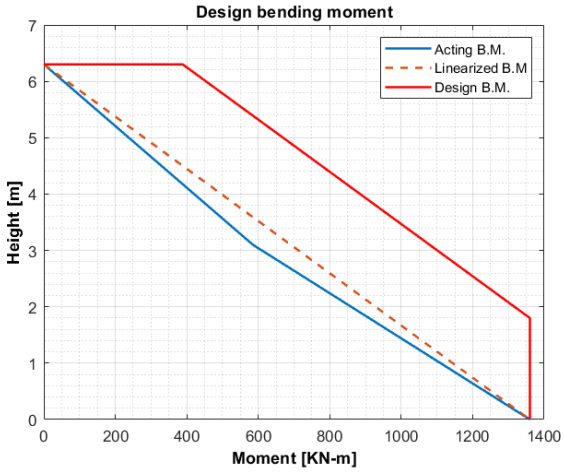

Figure 6.20: Design bending moment for wall A2. Model III

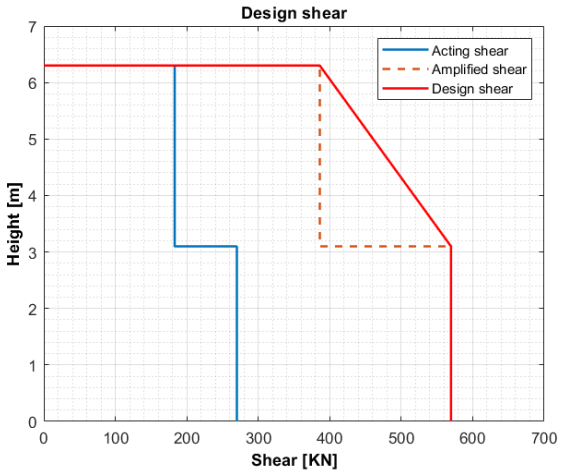

Figure 6.21: Design shear for wall A2. Model III

Summarizing, the design actions for wall A2 are listed in the following table:

Table 6.65: Design loads for wall A2. Model III

Height [m]	$\mathbf{N_{Ed}}$ **[KN]**	$\mathbf{M_{Ed}}$ **[KN-m]**	$\mathbf{V_{Ed}}$ **[KN]**
0.0	294.0	1360.0	570.0
2.0	294.0	1360.0	570.0
3.2	137.0	1079.0	570.0
6.4	137.0	388.7	386.1

Axial force

The corresponding check for the normalized axial force in the wall is provided in the table below.

Table 6.66: Normalized axial force in wall A2. Model III

Height [m]	$\mathbf{N_{Ed}}$ **[KN]**	$\mathbf{v_d}$ **[-]**	$\mathbf{v_d < 0.35}$ **[-]**
0.0	294.0	0.03	Ok
2.0	294.0	0.03	Ok
3.2	137.0	0.01	Ok
6.4	137.0	0.01	Ok

Bending resistance

The vertical reinforcement for wall A2 is listed in the following table:

Table 6.67: Vertical reinforcement wall A2. Model III

	Boundary element	**Web**
Concrete cover, c[mm]	30	30
Bar diameter, ϕ[mm]	14	14
# of bars	12	8
Area of vertical reinforcement, A_{sv} [mm^2]	1847	1232
Vertical reinforcement ratio ρ_v	0.012	0.005

In the same way, horizontal reinforcement for the confined zones is listed below.

Table 6.68: Horizontal reinforcement wall A2. Model III

	Boundary element
Concrete cover, c[mm]	30
Bar diameter, ϕ[mm]	8
# of arms	2
Spacing, s_w[mm]	50
Area of horizontal reinforcement, A_{sv} [mm^2]	101
Horizontal reinforcement ratio ρ_h	0.006

The resistance bending moment along the height and the corresponding resisting check is presented in the next table:

Table 6.69: Bending resistance wall A2. Model III

Height [m]	$\mathbf{M_{Ed}}$ **[KN-m]**	$\mathbf{M_{Rd}}$ **[KN-m]**	$\mathbf{M_{Rd} > M_{Ed}}$ **[-]**
0.0	1360	1500	Ok
2.0	1360	1500	Ok
3.2	1079	1390	Ok
6.4	389	1390	Ok

The M-N interaction diagram for the geometry and vertical reinforcement of the wall A2 is illustrated in the following figure:

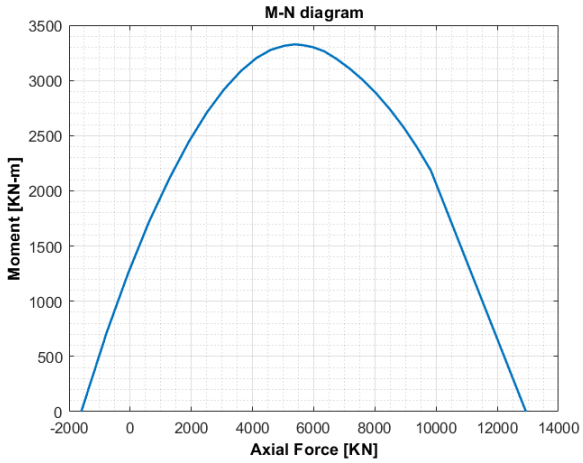

Figure 6.22: M-N interaction diagram for wall A2. Model III

For DCH structures a certain level of ductility must be ensured at the base of the wall, Table 6.70 shows the ductility check for wall A2.

Table 6.70: Ductility check wall A2. Model III

Element	$\mathbf{l_c}$ **[m]**	μ_ϕ **[-]**	$\omega_\mathbf{v}$ **[-]**	$\mathbf{x_u}$ **[m]**	$\alpha\omega_{\mathbf{wd,min}}$ **[-]**	α **[-]**	$\omega_\mathbf{wd}$ **[-]**	$\alpha\omega_\mathbf{wd}$ **[-]**	
Wall C1	0.48	6.98	0.097	0.27	0.12	0.66	0.19	0.125	Ok

Shear resistance

Following the same procedure describe in Section 6.2.2.2 for the shear resistance of the walls, the horizontal reinforcement in the web for the wall A2 to resist the worst shear action coming from the analysis, is presented in the following table:

Table 6.71: Horizontal reinforcement for shear wall A2. Model III

	Web
Concrete cover, c$[mm]$	30
Bar diameter, $\phi[mm]$	8
# of arms	2
Spacing, $s_w[mm]$	100
Area of horizontal reinforcement, A_{sv} $[mm^2]$	101
Vertical reinforcement ratio ρ_h	0.003

The corresponding checks for shear resistance for the aforementioned wall are summarized in the table below.

Table 6.72: Shear strength wall A2. Model III

Height [m]	$\mathbf{V_{Ed}}$ **[KN]**	$\mathbf{V_{Rd,max}}$ **[KN]**	α_s **[-]**	$\mathbf{V_{Rd,s}}$ **[KN]**	**Eq. (6.15)** **[-]**	**Eq. (6.17)** **[-]**	$\mathbf{V_{Rd,S}}$ **[KN]**
0.0-3.2	570	973	1.33	723	Ok	Ok	853
3.2-6.0	570	2433	1.05	576	Ok	Ok	–

The following figure shows the reinforcement steel of wall A2:

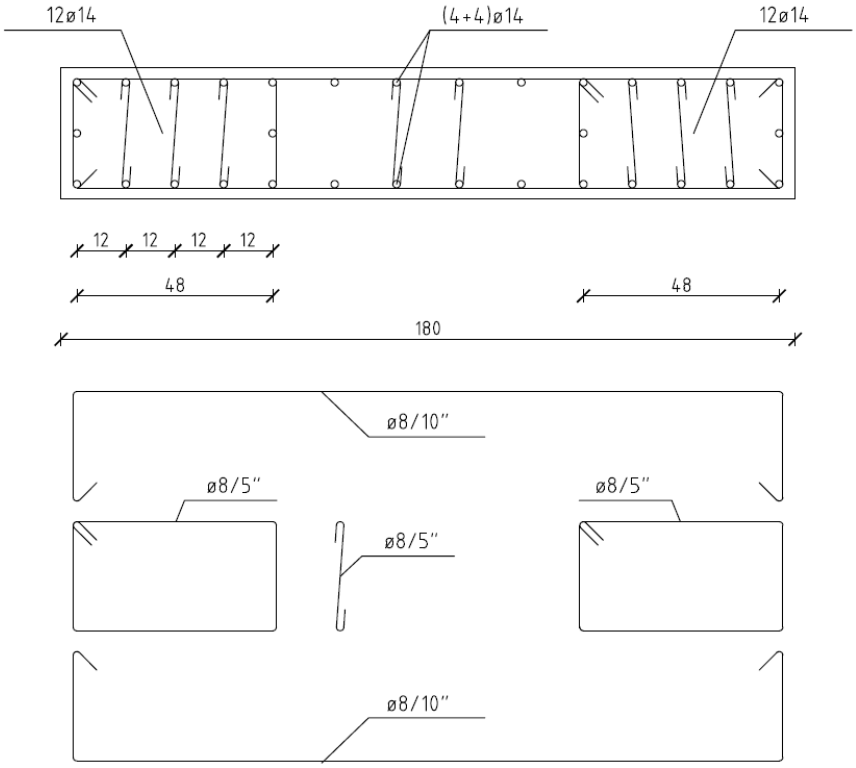

Figure 6.23: Steel reinforcement Wall A2. Model III

6.4.2.2 Columns

Columns are designed according to Eurocode 2 following the procedure describe in Section 6.2.2.2 for the design of columns. The first step is to determine the

slenderness, so then it can be known if second order effects affect or not the design of the columns. Table 6.73 shows that second order effects can be disregarded.

Table 6.73: Column slenderness. Model III

Element	$\mathbf{N_{Ed,max}}$ **[KN]**	$\mathbf{v_d}$ **[-]**	λ **[-]**	$\lambda_{\mathbf{lim}}$ **[-]**	
Corner column	270.1	0.15	22.5	25.7	No slender
Edge column	502.3	0.21	19.3	21.9	No slender
Internal column	909.9	0.33	16.9	18.6	No slender

Bending resistance

The same longitudinal reinforcement for each type of column is placed along the two stories of the building. The moment resistant check and the longitudinal reinforcement selected for every column are summarized in Table 6.74.

Table 6.74: Bending moment resistance columns. Model III

Element	$\mathbf{N_{Ed}}$ **[KN]**	$\mathbf{M_{Ed,y}}$ **[KN-m]**	$\mathbf{M_{Ed,z}}$ **[KN-m]**	**Bar diameter [mm]**	**# of bars [-]**	$\mathbf{M_{Rd,y}}$ **[KN-m]**	$\mathbf{M_{Rd,z}}$ **[KN-m]**
Corner column	137.1	51.4	83.0	16	12	55.0	89.0
Edge column	258.9	77.1	131.8	18	12	85.0	144.0
Interior column	385.9	102.8	118.7	18	12	145.0	161.0

A schematic representation of steel reinforcement of columns is shown in the following figure:

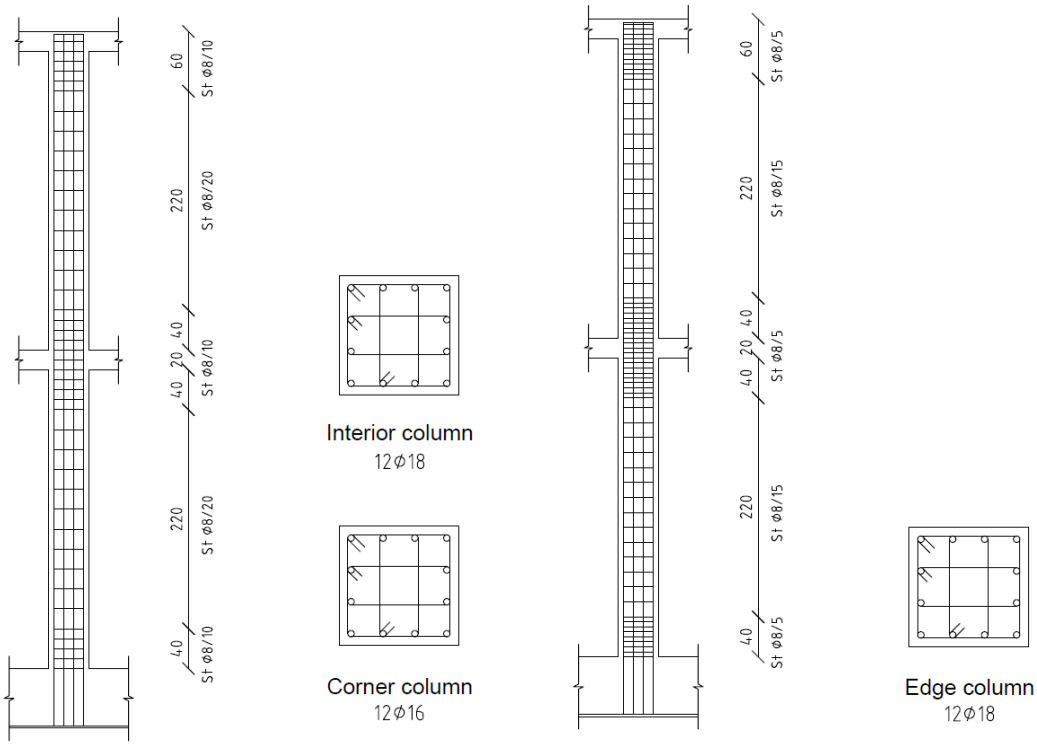

(a) Interior and corner columns (b) Edge columns

Figure 6.24: Steel reinforcement for columns. Model III

The interaction axial force-bending moment curve for corner columns is shown in the following figure.

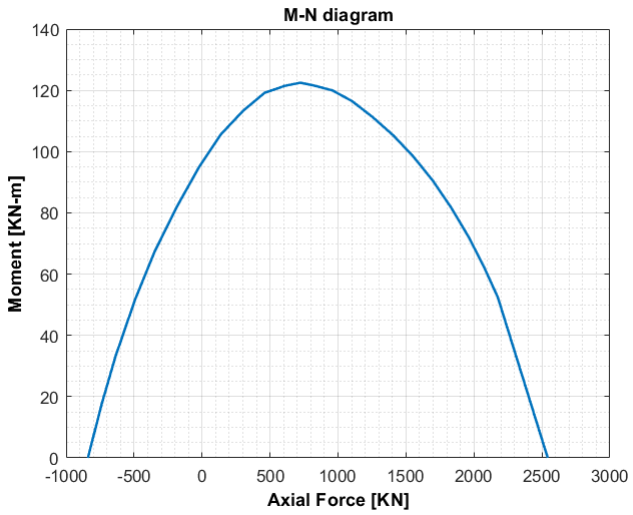

Figure 6.25: M-N interaction diagram for corner columns. Model III

Shear resistance

Shear strength is calculated in the same way as it is described in Section 6.2.2.2. Shear strength shall be greater than most unfavorable action coming for the worst combination of loads. Table 6.48 shows the reinforcement place to resist shear acting forces and the corresponding strength checks.

Table 6.75: Shear reinforcement in columns. Model III

Element	$V_{Ed,y}$ [KN]	$V_{Ed,z}$ [KN]	$V_{Rd,max}$ [KN]	Spacing, s [mm]	Bar diameter [mm]	Arms [-]	$V_{Rd,s}$ [KN]	Spacing at beam ends [mm]
Corner column	39.3	25.0	342.1	200	8	2	42.4	100
Edge column	62.6	34.8	482.3	150	8	2	68.4	50
Interior column	54.3	46.8	646.3	200	8	2	60.1	100

6.4.2.3 Slab

The design of the slabs was accomplished following the same procedure described in Section 6.2.2.3. The same reinforcement layout is used for the two slabs because the internal actions in both slabs are similar.

Bending moment

For the bending moment design, the slabs was divided in different strips as it is shown in Fig. 6.26. Then the values of acting bending moment obtained in each finite element from the analysis, are distributed inside these strips by averaging them over the length over the column and middle strips.

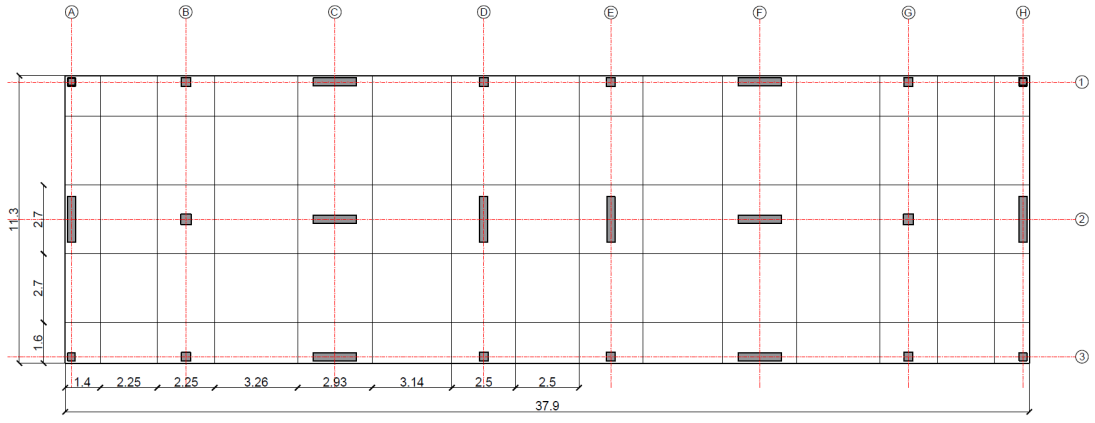

Figure 6.26: Division of panels Model III

The maximum negative bending moment is localized at the slab-column connection B2. Top reinforcement at slab-column connection B2 in Y-direction is listed below.

Table 6.76: Maximum top reinforcement. Model III

Parameter	**Value**
Strip width, $b[mm]$	2250
Slab depth, $h[mm]$	200
Concrete cover, $c[mm]$	30
Bar diameter, $\phi[mm]$	20
# of bars	19
Area of steel, A_s $[mm^2]$	5969
Acting moment $M_{Ed,y}$	240
Resisting moment $M_{Rd,y}$	250

The following table shows the bottom reinforcement used for the span C1-C2 in Y-direction.

Table 6.77: Bottom reinforcement. Model III

Parameter	**Value**
Strip width, $b[mm]$	2925
Slab depth, $h[mm]$	200
Concrete cover, $c[mm]$	30
Bar diameter, $\phi[mm]$	12
# of bars	12
Area of steel, A_s $[mm^2]$	1357
Acting moment $M_{Ed,x}$	97
Resisting moment $M_{Rd,x}$	102

It is worth noting that the bottom reinforcement is the same in all the slab, except at the slab column connection where at least two bars must pass through the column. This was done in order to avoid a very complex arrangement of steel reinforcement. A uniform mesh of bars #12 spaced at 25 cm was selected for whole slab except at the slab column connection where the spacing is 20 cm.

Punching shear resistance

Punching shear resistance was determined according to Eurocode 2 (see Section 4.2.1). Two basic verification are performed in order to evaluate the punching shear in the slab-column connection.

The first verification is performed at the column face. The results obtained are listed in the following table:

Table 6.78: Punching shear at column face. Model III

Parameter	**Corner column**	**Edge column**	**Interior column**
Column Dimensions, $[mm]$	300x300	350x350	400x400
Slab depth, $h[mm]$	200	200	200
Concrete cover, $c[mm]$	30	30	30
Effective depth, $d[mm]$	158	156	153
β	1.5	1.4	1.15
Control perimeter, $U_0[mm]$	473	817	1600
$V_{Ed}[KN]$	80.60	199.00	457.30
$v_{Ed}[MPa]$	1.62	2.19	2.15
$v_{Rd,max}[MPa]$	4.22	4.22	4.22

The second verification is performed at the basic control perimeter. Results are presented in table below.

Table 6.79: Punching shear at basic control perimeter. Model III

Parameter	**Corner column**	**Edge column**	**Interior column**
Column Dimensions, $[mm]$	300x300	350x350	400x400
Slab depth, $h[mm]$	200	200	200
Concrete cover, $c[mm]$	30	30	30
Effective depth, $d[mm]$	158	156	153
β	1.5	1.4	1.15
ρ_l	0.0060	0.0122	0.0200
Basic control perimeter, $U_1[mm]$	1295	2227	3522
$V_{Ed}[KN]$	75.30	189.70	443.20
$v_{Ed}[MPa]$	0.554	0.767	0.946
$v_{Rd}[MPa]$	0.629	0.797	0.940

From the table above. It is shown that the slab-column connections for interior

columns are not able to resist the acting punching shear at ULS for gravity loads. For this reason, the dimension of the column is increased to 0.45 m x 0.45 m. After increasing the dimensions of internal columns, the acting shear stress results $v_{Ed} = 0.895\ MPa.$, which is a value lower than the resisting shear stress v_{Rd}.

Once the cross section of interior columns is updated in the model, the performance of the slab-column connection can be determined. According to Ramos et al. (see Eq. (6.26)), the ultimate inter-story drift ratio that the slab-columns connection can developed is listed in Table 6.53.

Table 6.80: Ultimate inter-story drift Model III. Ramos et al.

Parameter	**Corner column**	**Edge column**	**Interior column**
$V_{Ed}\,[KN]$	50.1	119.5	281.1
$v_{Ed}\,[MPa]$	0.369	0.483	0.568
$v_{Rd}\,[MPa]$	0.554	0.767	0.946
GSR	0.59	0.61	0.60
$d_r[\%]$	0.86	0.80	0.81

According to the results presented above, the slab-column connections are able to withstand the displacements imposed by the shear walls during design seismic actions. The inter-story drifts reached by the structure under the design seismic excitation (Table 6.33) are smaller than the ultimate inter-story drift of the slab column-connections.

Additional checks are performed in order to evaluate the performance of the slab-column connections under lateral loads. According to ACI 318-19, the ultimate drift slab-columns connection can reach without shear reinforcement is shown in the following table.

Table 6.81: Ultimate inter-story drift Model III. ACI 318-19

Parameter	**Corner column**	**Edge column**	**Interior column**
$v_u\,[MPa]$	0.425	0.716	1.055
$v_c\,[MPa]$	1.818	1.818	1.818
$v_u/\phi v_c$	0.312	0.525	0.774
d_r [%]	1.94	0.88	0.50

In accordance with ACI 318-19, punching shear reinforcement must be provided for internal slab column connections because the inter-story drift ratios for the seismic design action are bigger than the ultimate inter-story drift ratio that the slab-column connection can develop.

Table 6.82: Ultimate inter-story drift Model III.
Draft 2^{nd} generation of Eurocode 2

Parameter	**Corner column**	**Edge column**	**Interior column**
$v_{Ed}\,[MPa]$	0.367	0.559	0.831
$v_{Rd}\,[MPa]$	1.79	1.81	1.66
GSR	0.20	0.31	0.50
$\psi_{slab,R}$ [%]	1.17	1.08	0.66

Different from the results obtained using ACI 318-19, results obtained using the draft of the second generation of Eurocode 2, suggest that no punching shear reinforcement is needed at the slab column connection because the inter-story drift ratios generated by the displacements imposed by the primary elements under the seismic design situation, are below the ultimate inter-story drift ratio that the slab-column connections can develop.

A punching shear evaluation for walls is also carried out here, according to the provision inside Model Code 2010 (see Section 4.2.3) for defining the control perimeter and according to the draft of New Generation of Eurocode 2 (see Eq. (6.28) and Eq. (6.29)) for the evaluation of punching shear resistance.

Table 6.83: Punching shear at basic control perimeter for walls. Model III

Parameter	Wall C1 connection	Wall C2 connection	Wall A2 connection	Wall D2 connection
Wall dimensions, $[mm]$	1700x320	1700x320	1800x320	1800x320
Slab depth, $h[mm]$	200	200	200	200
Concrete cover, $c[mm]$	30	30	30	30
Effective depth, $d[mm]$	158	156	158	157
ρ_l	0.0055	0.0155	0.0055	0.0108
Basic control perimeter, $U_1[mm]$	771	1033	771	1035
$V_{Ed}[KN]$	131.9	320.2	124.4	270.8
$v_{Ed}[MPa]$	1.082	2.032	1.021	1.671
$v_{Rd}[MPa]$	1.857	2.252	1.905	1.997

Maximum rotation that the slab can develop at the corner of the wall is shown in the following table:

Table 6.84: Ultimate inter-story drift for walls Model III.
Draft 2^{nd} generation of Eurocode 2

Parameter	Wall C1 connection	Wall C2 connection	Wall A2 connection	Wall D2 connection
$v_{Ed}\,[MPa]$	0.692	1.259	0.644	1.049
$v_{Rd}\,[MPa]$	1.857	2.252	1.905	1.997
GSR	0.372	0.559	0.338	0.525
$\psi_{slab,R}\,[\%]$	0.87	0.43	0.84	0.57

The slab-wall connection C2 and D2 are not able to withstand the drift developed by the ULS design seismic situation.

Therefore, an increment of the cross-section dimensions of the walls are proposed in order to reduced the maximum inter-story drift reached at ULS seismic situation. New dimensions of the walls and punching shear checks are shown in the following tables:

Table 6.85: Punching shear at basic control perimeter. Model III

Parameter	Wall C1 connection	Wall C2 connection	Wall A2 connection	Wall D2 connection
Wall dimensions, $[mm]$	1800x320	1800x320	2200x400	2200x320
Slab depth, $h[mm]$	200	200	200	200
Concrete cover, $c[mm]$	30	30	30	30
Effective depth, $d[mm]$	158	156	158	157
ρ_l	0.0055	0.0155	0.0055	0.0108
Basic control perimeter, $U_1[mm]$	771	1033	811	1035
$V_{Ed}[KN]$	132.5	321.4	127.7	275.2
$v_{Ed}[MPa]$	1.087	2.039	0.996	1.698
$v_{Rd}[MPa]$	1.990	2.251	1.858	2.023

Table 6.86: Ultimate inter-story drift Model III.
Draft 2^{nd} generation of Eurocode 2

Parameter	Wall C1 connection	Wall C2 connection	Wall A2 connection	Wall D2 connection
$v_{Ed}\,[MPa]$	0.695	1.264	0.627	1.064
$v_{Rd}\,[MPa]$	1.990	2.251	1.858	2.023
GSR	0.349	0.562	0.3374	0.526
$\psi_{slab,R}\,[\%]$	0.81	0.43	0.87	0.55

Although the ultimate slab rotations remain almost the same, the inter-story drifts reached at ULS seismic situation are reduced. A maximum inter-story drift of 0.40% in both direction is obtained. After increasing the dimension of the walls, the slab-wall connection are now able to resist the drift at ULS seismic situation. Steel reinforcement arrangement of modified walls is found in Appendix B.

6.4.3 Discussion

An increment of the inter-story drift ratio compared to the other structures is observed. A bigger increment in the lateral displacements along the Y axis is reported. The reason why the increment is bigger in Y-direction, is because the dimension of the spans in that direction were increased 20% whereas in X-direction

the span length was increased 17%.

Also, an increment in the demand of the top reinforcement of the slab near the column connections is reported. This increment is induced by the same fact that the span length between columns was increased producing higher values of acting actions in the slab element.

As it was mentioned before, the previous dimension used for the internal columns (0.40 m x 0.40 m) is not sufficient to resist the acting punching shear in the internal slab column connections. Punching shear demand is not acceptable at ULS for vertical loads.

After increasing the dimension of the internal columns, the ultimate drift ratio obtained using the formula proposed by Ramos et al., suggests that there is not necessity to add punching shear reinforcement to the slab column connections. Nevertheless, the computation done according to ACI 318-19, says that the acting punching shear is not acceptable for internal columns and punching shear reinforcement should be provided. Although the check performed with the provisions inside the draft of the second generation of Eurocode 2 suggests that all the slab-column connections are able to withstand the punching shear effects under the displacements imposed by the primary elements, the values values of the maximum drift ration that the internal connection can develop are very close to the drift imposed by the shear walls. Therefore, it is recommended to increase the performance of the slab column connection either by increasing the depth of the slab or providing punching shear reinforcement. As an alternative, an increase of the dimension of the primary elements can also help to reduce the inter-story drift of the structure.

After performing the corresponding checks for the slab-wall connection, the results shows that the ultimate punching shear resistance of the connections are really close to the acting punching shear at ULS for gravity loads. Additionally, walls C2 and D2, with their initial proposed dimensions, are not able to develop the sufficient slab rotation to resist the drift produced at ULS seismic situation. It was also observed that it is more convenient to reduced the spans of the structure that increasing the dimension of the elements or the amount of the steel to increase the performance of the slab-wall connection under lateral loading. In conclusion, lateral drift capacity of the flat-slab is the critical condition for the design of this structure.

Chapter 7

Conclusions

Three fictitious flat slabs structures have been analyzed and designed in order to evaluate the punching shear at the slab-column connections under vertical and lateral loads. The structures maintain some similarities with the specimen from the experimental tests carried out on a full-scale two-story flat-slab building subjected to gravity and lateral loads (Coronelli et al. [1]). Different structural layouts were proposed, and different top reinforcement ratios for the slabs have been considered to analyze the impact of the punching shear in the design of the proposed structures.

Comparison between numerical results from model 0 and experimental results regarding the horizontal displacement and the fundamental period of the structure have been performed in order to calibrate the structural modeling for the other structures. In addition, the performance of the slab-column connections obtained during the test are used as a reference to compare the results obtained from the modeling of the other three structures.

From the analysis and results obtained from the three structures proposed in this thesis, the main findings are listed below:

- The first important finding was obtained after calibrating model 0 with the experimental results. In order to correctly model a flat-slab structure in a FEM software, a reduction of the lateral stiffness of the elements due to cracking of concrete shall be considered when the structure is analyze under lateral loading. The effective lateral stiffness values which are recommended

to be used are listed in Table 5.6.

- Model I and Model II obtained similar results of acting punching shear in the slab-columns connections because the plan geometry of the structure were similar to the structure experimentally tested. The only different was the increase of concentration of top reinforcement of the slab near the columns for model II. This resulted in an increment of the punching shear resistance of the slab-column connections in such model.

- Model III showed that the use of very long spans can lead to serious problems of punching shear under gravity loads, especially for internal columns. Additionally, punching shear is critical for slab-wall connections at ULS seismic situation. Although these problems can be solved by increasing the amount of steel in slabs, and the cross-section size of walls, slabs and columns, it is recommended to use relative small spans between 4.5 m - 5.0 m when a flat-slab is used.

- Although in this work different values of GSR were used to analyze the impact on the ductility of a slab column-connection, it is recommended to maintain a GSR between 0.3 - 0.4, as it is suggested in literature, to guarantee a good level of ductility of the slab-column connections.

- The use of a lateral-force resistance systems is highly recommended when the structure is located in seismic zones. In this way, the lateral displacements are controlled ensuring a good performance of the structure. A maximum designed inter-story drift of 0.5% is suggested.

- The use of identical reinforcement for different structural members in each structure, in some cases it is not an optimal design. This simplification was adopted to reduce the amount of work, which has been developed manually. The reinforced proposed for structural members, definitely, does not correspond to an economical solution. This issue is principally present in the design of the slabs and columns.

- There is still a need to correctly define a process to evaluate the punching shear at slab-wall connection. No specifications are given by the current version of Eurocode 2 [3]. Nonetheless, a simplified method is proposed here, which is based on exiting information in literature.

- The nominal punching shear resistance calculated using the draft of the second generation of Eurocode 2 resulted to be bigger than the one obtained

using the current version of Eurocode 2 [3]. Less conservative values of shear strength are obtained using the draft of the second generation of Eurocode 2 because of the refinement in the formulation and the adjustment based on experimental data.

The recommendation given in this work for modeling flat-slabs structures under lateral loads were validated using as reference an experimental work. The work done here demonstrated that using a linear analysis for the design of flat-slabs structure, with the correct considerations, is still reliable and it can produce coherent and good results.

Although some codes are still being improved to evaluate in a more reliable way the punching shear and the drift capacity of slab-column connections under lateral loading, it is evident that more experimental data coming from tests on full-scale specimens is needed. Further investigations and improvements can be developed in the future using as a reference the work developed here.

Bibliography

[1] D. Coronelli, M. Lamperti Tornaghi, L. Martinelli, F. J. Molina, A. Muttoni, I. R. Pascu, P. Pegon, M. Peroni, A. P. Ramos, G. Tsionis, and T. Netti, "Testing of a full-scale flat slab building for gravity and lateral loads," *Engineering Structures*, vol. 243, 2021.

[2] CEN, "EN 1998-1 Eurocode 8: Design of structures for earthquake resistance – Part 1: General rules, seismic actions and rules for buildings," 2004.

[3] CEN, "EN 1992-1-1 Eurocode 2: Design of concrete structures - Part 1-1: General rules and rules for buildings," 2004.

[4] A. Muttoni, D. Coronelli, M. Lamperti Tornaghi, L. Martinelli, I. R. Pascu, A. Pinho Ramos, G. Tsionis, P. Bamonte, B. Isufi, and A. Setiawan, "Deformation capacity evaluation for flat slab seismic design," *Bulletin of Earthquake Engineering*, vol. 20, no. 3, pp. 1619–1654, 2022.

[5] D. Coronelli, A. Muttoni, I. R. Pascu, A. P. Ramos, and T. Netti, "A state of the art of flat-slab frame tests for gravity and lateral loading," *Engineering Structures*, vol. 21, no. 6, pp. 2764–2781, 2020.

[6] D. N. Farhey, M. A. Adin, and D. Z. Yankelevsky, "RC flat slab-column subassemblages under lateral loading," *Journal of Structural Engineering*, vol. 119, no. 6, pp. 1903–1916, 1993.

[7] A. F. Almeida, M. M. Inácio, V. J. Lúcio, and A. P. Ramos, "Punching behaviour of RC flat slabs under reversed horizontal cyclic loading," *Engineering Structures*, vol. 117, pp. 204–219, 2016.

[8] A. F. Almeida, B. Alcobia, M. Ornelas, R. Marreiros, and A. P. Ramos, "Behaviour of reinforced-concrete flat slabs with stirrups under reversed horizon-

tal cyclic loading," *Magazine of Concrete Research*, vol. 72, no. 7, pp. 339–356, 2020.

[9] B. Isufi, A. Pinho Ramos, and V. Lúcio, "Reversed horizontal cyclic loading tests of flat slab specimens with studs as shear reinforcement," *Structural Concrete*, vol. 20, no. 1, pp. 330–347, 2019.

[10] B. Isufi, A. P. Ramos, and V. Lúcio, "Post-earthquake performance of a slab-column connection with punching shear reinforcement," *Journal of Earthquake Engineering*, vol. 26, no. 3, pp. 1171–1193, 2022.

[11] A. F. Almeida, A. P. Ramos, V. Lúcio, and R. Marreiros, "Behavior of RC flat slabs with shear bolts under reversed horizontal cyclic loading," *Structural Concrete*, vol. 21, no. 2, pp. 501–516, 2020.

[12] I. S. Drakatos, A. Muttoni, and K. Beyer, "Internal slab-column connections under monotonic and cyclic imposed rotations," *Engineering Structures*, vol. 123, pp. 501–516, 2016.

[13] E. Coelho, P. Candeias, and G. Anamateros, "Assessment of the seismic behaviour of RC flat slab building structures," *13th World Conference on Earthquake Engineering*, no. 2630, 2004.

[14] M. Lamperti Tornaghi, G. Tsionis, P. Pegon, J. Molina, M. Peroni, D. Coronelli, L. Martinelli, A. P. Ramos, R. Pascu, and A. Muttoni, "Experimental study of a two-storey flat slab building under seismic and gravity loads," *17th World Conference on Earthquake Engineering*, pp. 3f–0027, 2020.

[15] A. Pan and J. P. Moehle, "Lateral Displacement Ductility of Reinforced Concrete Flat Plates," *ACI Structural Journal*, vol. 86, no. 13, pp. 250–258, 1989.

[16] J. P. Moehle and J. W. Diebold, "Experimental study of the seismic response of a two-story flat-plate structure," *Berkeley: University of California*, no. UCB/EERC-84/08, 1984.

[17] D. Coronelli, A. Muttoni, I. R. Pascu, A. P. Ramos, and T. Netti, "A state of the art of flat-slab frame tests for gravity and lateral loading," *Structural Concrete*, vol. 21, no. 6, pp. 2764–2781, 2020.

[18] S. J. Hwang and J. Moehle, "Vertical and lateral load tests of nine-panel flat-plate frame," *ACI Structural Journal*, vol. 97, pp. 193–203, 01 2000.

[19] T. H. Kang and J. W. Wallace, "Shake table tests of reinforced concrete flat plate frames and post-tensioned flat plate frames," *13th World Conference on Earthquake Engineering*, no. 1119, 2004.

[20] C. Rha, T. Kang, M. Shin, and J. b. Yoon, "Gravity and lateral load-carrying capacities of reinforced concrete flat plate systems," *ACI Structural Journal*, vol. 111, pp. 753–764, 07 2014.

[21] D. R. Fick, M. A. Sozen, and M. E. Kreger, "Response of Full-Scale Three-Story Flat-Plate Test Structure to Cycles of Increasing Lateral Load," *Structural Journal*, vol. 114, no. 6, pp. 1507–1517, 2017.

[22] ACI, *Guide to Seismic Design of Punching Shear Reinforcement in Flat Plates*. 2010.

[23] O. Brooker, "How to design reinforced concrete flat slabs using finite element analysis," *The Concrete Centre*, 2006.

[24] C. E. Broms, "Punching of flat plates-a question of concrete properties in biaxial compression and size effect," *ACI Structural Journal*, vol. 87, pp. 292–304, 1990.

[25] S. Kinnunen and H. Nylander, "Punching of Concrete Slabs Without Shear Reinforcement," *Transactions of The Royal Institute of Technology*, no. 158, p. 112, 1960.

[26] A. Muttoni and A. Windisch, "Punching shear strength of reinforced concrete slabs without transverse reinforcement," *ACI Structural Journal*, vol. 106, no. 3, p. 381, 2009.

[27] CEB/fib Task Group Utilisation of concrete tension in design, "Punching of structural concrete slabs," *fib Bulletin No.12*, p. 314, 2001.

[28] A. Muttoni and J. Schwartz, "Behaviour of beams and punching in slabs without shear reinforcement," *IABSE Colloquium*, vol. 62, pp. 703–708, 1991.

[29] A. Muttoni, M. Fernández Ruiz, and J. T. Simões, "The theoretical principles of the critical shear crack theory for punching shear failures and derivation of consistent closed-form design expressions," *Structural Concrete*, vol. 19, no. 1, pp. 174–190, 2018.

[30] ACI Committee 318, *Building Code Requirements for Structural Concrete (ACI 318-19) and Commentary on Building Code Requirements for Structural Concrete (ACI 318R-19)*. 2019.

[31] The Fédération internacionale du béton (fib), *Model Code 2010 - Final draft, Volume 2*. No. 66 in fib bulletin, Jan. 2012.

[32] Ministero Delle Infrastrutture e dei Trasporti, *Decreto 17 gennaio 2018. Aggiornamento delle «Norme tecniche per le costruzioni»*. Gazzetta Ufficiale Della Repubblica Italiana, 2018.

[33] CEN, "EN 1991-1-1 Eurocode 1: Actions on structures - Part 1-1: General actions - Densities, self-weight, imposed loads for buildings," 2002.

[34] CEN, "EN 1990:2002 + A1 Eurocode - Basis of structural design," 2002.

[35] S.-W. Han, Y.-M. Park, and S.-H. Kee, "Stiffness Reduction Factor for Flat Slab Structures under Lateral Loads," *Journal of Structural Engineering*, vol. 135, no. 6, pp. 743–750, 2009.

[36] A. Setiawan, R. L. Vollum, L. Macorini, and B. A. Izzuddin, "Punching shear design of RC flat slabs supported on wall corners," *Structural Concrete*, vol. 21, no. 3, pp. 859–874, 2020.

[37] ASCE, *American Society of Civil Engineers, Fema 356 Prestandard and Commentary for the Seismic Rehabilitation of Building*. 2000.

[38] A. Ramos, R. Marreiros, A. Almeida, B. Isufi, and M. Inácio, "Punching of flat slabs under reversed horizontal cyclic loading," *fib Bulletin, Punching shear of structural concrete slabs: Honoring Neil M. Hawkins*, vol. 81, pp. 253–272, 2017.

Appendix A

Structural design results

Model I

Shear walls

For all the walls in this structures, the same arrangement of vertical and horizontal reinforcement as it is described in Section 6.2.2.1, is used.

Columns

All the columns are reinforced using the corresponding steel designed in Section 6.2.2.2 for interior, edge of corner column, respectively.

Slab

Top reinforcement of slab-column connection A1.

Table A.1: Top reinforcement slab-column connection A1. Model I X-direction

Parameter	**Value**
Strip width, $b[mm]$	1375
Slab depth, $h[mm]$	200
Concrete cover, $c[mm]$	30
Bar diameter, $\phi[mm]$	12
# of bars	8
Area of steel, A_s $[mm^2]$	905
Acting moment $M_{Ed,x}$	36
Resisting moment $M_{Rd,x}$	57

Table A.2: Top reinforcement slab-column connection A1. Model I Y-direction

Parameter	**Value**
Strip width, $b[mm]$	1375
Slab depth, $h[mm]$	200
Concrete cover, $c[mm]$	30
Bar diameter, $\phi[mm]$	12
# of bars	8
Area of steel, A_s $[mm^2]$	905
Acting moment $M_{Ed,y}$	38
Resisting moment $M_{Rd,y}$	57

Top reinforcement of slab-column connection B1.

Table A.3: Top reinforcement slab-column connection B1. Model I X-direction

Parameter	**Value**
Strip width, $b[mm]$	1375
Slab depth, $h[mm]$	200
Concrete cover, $c[mm]$	30
Bar diameter, $\phi[mm]$	14
# of bars	9
Area of steel, A_s $[mm^2]$	1385
Acting moment $M_{Ed,x}$	60
Resisting moment $M_{Rd,x}$	77

Table A.4: Top reinforcement slab-column connection B1. Model I Y-direction

Parameter	**Value**
Strip width, $b[mm]$	2250
Slab depth, $h[mm]$	200
Concrete cover, $c[mm]$	30
Bar diameter, $\phi[mm]$	14
# of bars	14
Area of steel, A_s $[mm^2]$	2155
Acting moment $M_{Ed,y}$	58
Resisting moment $M_{Rd,y}$	105

Top reinforcement of slab-column connection C2.

Table A.5: Top reinforcement slab-column connection C2. Model I Y-direction

Parameter	**Value**
Strip width, $b[mm]$	2250
Slab depth, $h[mm]$	200
Concrete cover, $c[mm]$	30
Bar diameter, $\phi[mm]$	16
# of bars	16
Area of steel, A_s $[mm^2]$	3217
Acting moment $M_{Ed,y}$	108
Resisting moment $M_{Rd,y}$	120

Top reinforcement of wall C1 connection. Same reinforcement is placed for wall A2.

Table A.6: Top reinforcement wall C1 connection. Model I X-direction

Parameter	**Value**
Strip width, $b[mm]$	1375
Slab depth, $h[mm]$	200
Concrete cover, $c[mm]$	30
Bar diameter, $\phi[mm]$	12
# of bars	8
Area of steel, A_s $[mm^2]$	905
Acting moment $M_{Ed,x}$	40
Resisting moment $M_{Rd,x}$	57

Table A.7: Top reinforcement wall C1 connection. Model I Y-direction

Parameter	**Value**
Strip width, $b[mm]$	2250
Slab depth, $h[mm]$	200
Concrete cover, $c[mm]$	30
Bar diameter, $\phi[mm]$	12
# of bars	10
Area of steel, A_s $[mm^2]$	1130
Acting moment $M_{Ed,y}$	58
Resisting moment $M_{Rd,y}$	72

Model II

Shear walls

Reinforcement steel for wall C1

Table A.8: Vertical reinforcement wall C1. Model II

	Boundary element	**Web**
Concrete cover, c[mm]	30	30
Bar diameter, $\phi[mm]$	14	12
# of bars	12	18
Area of vertical reinforcement, A_{sv} [mm^2]	1847	2035
Vertical reinforcement ratio ρ_v	0.012	0.008

Table A.9: Horizontal reinforcement Wall C1. Model II

	Boundary element	**Web**
Concrete cover, c[mm]	30	30
Bar diameter, $\phi[mm]$	8	10
# of arms	2	2
Spacing, $s_w[mm]$	50	100
Area of horizontal reinforcement, A_{sv} [mm^2]	101	157
Horizontal reinforcement ratio ρ_h	0.006	0.005

Reinforcement steel for wall E3.

Table A.10: Vertical reinforcement wall E3. Model II

	Boundary element	**Web**
Concrete cover, c[mm]	30	30
Bar diameter, $\phi[mm]$	14	14
# of bars	14	20
Area of vertical reinforcement, A_{sv} [mm^2]	2155	3079
Vertical reinforcement ratio ρ_v	0.011	0.007

Table A.11: Horizontal reinforcement Wall E3. Model II

	Boundary element	**Web**
Concrete cover, c[mm]	30	30
Bar diameter, $\phi[mm]$	10	8
# of arms	2	2
Spacing, $s_w[mm]$	50	50
Area of horizontal reinforcement, A_{sv} [mm^2]	157	101
Horizontal reinforcement ratio ρ_h	0.01	0.006

Strength verification at base of walls.

Table A.12: Strength verification of walls. Model II

Wall [m]	$\mathbf{M_{Ed}}$ **[KN-m]**	$\mathbf{M_{Rd}}$ **[KN-m]**	$\mathbf{M_{Rd} > M_{Ed}}$	$\mathbf{V_{Ed}}$ **[KN]**	$\mathbf{V_{Rd,max}}$ **[KN]**	$\mathbf{V_{Rd,s}}$ **[KN]**	$\mathbf{V_{Rd,S}}$ **[KN]**
Wall C1	2270	2660	Ok	917	1298	1162	1002
Wall E3	2810	3240	Ok	1131	1406	1477	1419

Columns

All the columns are reinforced using the corresponding steel designed in Section 6.3.2.2 for interior, edge of corner column, respectively.

Slab

Top reinforcement of slab-column connection A1.

Table A.13: Top reinforcement slab-column connection A1. Model II X-direction

Parameter	Value
Strip width, $b[mm]$	1375
Slab depth, $h[mm]$	200
Concrete cover, $c[mm]$	30
Bar diameter, $\phi[mm]$	12
# of bars	8
Area of steel, A_s $[mm^2]$	905
Acting moment $M_{Ed,x}$	37
Resisting moment $M_{Rd,x}$	57

Table A.14: Top reinforcement slab-column connection A1. Model II Y-direction

Parameter	Value
Strip width, $b[mm]$	1375
Slab depth, $h[mm]$	200
Concrete cover, $c[mm]$	30
Bar diameter, $\phi[mm]$	12
# of bars	10
Area of steel, A_s $[mm^2]$	1130
Acting moment $M_{Ed,y}$	48
Resisting moment $M_{Rd,y}$	67

Top reinforcement of slab-column connection B1.

Table A.15: Top reinforcement slab-column connection B1. Model II X-direction

Parameter	Value
Strip width, $b[mm]$	1375
Slab depth, $h[mm]$	200
Concrete cover, $c[mm]$	30
Bar diameter, $\phi[mm]$	16
# of bars	10
Area of steel, A_s $[mm^2]$	2010
Acting moment $M_{Ed,x}$	70
Resisting moment $M_{Rd,x}$	140

Table A.16: Top reinforcement slab-column connection B1. Model II Y-direction

Parameter	**Value**
Strip width, $b[mm]$	2250
Slab depth, $h[mm]$	200
Concrete cover, $c[mm]$	30
Bar diameter, $\phi[mm]$	16
# of bars	17
Area of steel, A_s $[mm^2]$	3418
Acting moment $M_{Ed,y}$	91
Resisting moment $M_{Rd,y}$	145

Table A.17: Top reinforcement slab-column connection B2. Model II X-direction

Parameter	**Value**
Strip width, $b[mm]$	2250
Slab depth, $h[mm]$	200
Concrete cover, $c[mm]$	30
Bar diameter, $\phi[mm]$	20
# of bars	17
Area of steel, A_s $[mm^2]$	5340
Acting moment $M_{Ed,y}$	121
Resisting moment $M_{Rd,y}$	230

Top reinforcement of wall A3 connection.

Table A.18: Top reinforcement wall A3 connection. X-direction

Parameter	**Value**
Strip width, $b[mm]$	2600
Slab depth, $h[mm]$	200
Concrete cover, $c[mm]$	30
Bar diameter, $\phi[mm]$	12
# of bars	10
Area of steel, A_s $[mm^2]$	1131
Acting moment $M_{Ed,x}$	48
Resisting moment $M_{Rd,x}$	73

Table A.19: Top reinforcement wall A3 connection. Y-direction

Parameter	**Value**
Strip width, $b[mm]$	1375
Slab depth, $h[mm]$	200
Concrete cover, $c[mm]$	30
Bar diameter, $\phi[mm]$	12
# of bars	9
Area of steel, A_s $[mm^2]$	1017
Acting moment $M_{Ed,y}$	51
Resisting moment $M_{Rd,y}$	62

Top reinforcement of wall C1 connection.

Table A.20: Top reinforcement wall C1 connection. X-direction

Parameter	**Value**
Strip width, $b[mm]$	1375
Slab depth, $h[mm]$	200
Concrete cover, $c[mm]$	30
Bar diameter, $\phi[mm]$	12
# of bars	8
Area of steel, A_s $[mm^2]$	904
Acting moment $M_{Ed,x}$	37
Resisting moment $M_{Rd,x}$	57

Table A.21: Top reinforcement wall C1 connection. Y-direction

Parameter	**Value**
Strip width, $b[mm]$	2400
Slab depth, $h[mm]$	200
Concrete cover, $c[mm]$	30
Bar diameter, $\phi[mm]$	12
# of bars	10
Area of steel, A_s $[mm^2]$	1031
Acting moment $M_{Ed,y}$	49
Resisting moment $M_{Rd,y}$	67

Top reinforcement of wall E3 connection.

Table A.22: Top reinforcement wall E3 connection. X-direction

Parameter	**Value**
Strip width, $b[mm]$	2600
Slab depth, $h[mm]$	200
Concrete cover, $c[mm]$	30
Bar diameter, $\phi[mm]$	16
# of bars	25
Area of steel, A_s $[mm^2]$	5026
Acting moment $M_{Ed,x}$	225
Resisting moment $M_{Rd,x}$	235

Table A.23: Top reinforcement wall E3 connection. Y-direction

Parameter	**Value**
Strip width, $b[mm]$	2250
Slab depth, $h[mm]$	200
Concrete cover, $c[mm]$	30
Bar diameter, $\phi[mm]$	20
# of bars	23
Area of steel, A_s $[mm^2]$	7226
Acting moment $M_{Ed,y}$	204
Resisting moment $M_{Rd,y}$	280

Model III

Shear walls

Reinforcement steel for wall C1

Table A.24: Vertical reinforcement wall C1. Model III

	Boundary element	**Web**
Concrete cover, c[mm]	30	30
Bar diameter, $\phi[mm]$	12	12
# of bars	12	6
Area of vertical reinforcement, A_{sv} [mm^2]	1357	679
Vertical reinforcement ratio ρ_v	0.008	0.003

Table A.25: Horizontal reinforcement Wall C1. Model III

	Boundary element	**Web**
Concrete cover, c[mm]	30	30
Bar diameter, $\phi[mm]$	8	8
# of arms	2	2
Spacing, $s_w[mm]$	50	100
Area of horizontal reinforcement, A_{sv} [mm^2]	101	101
Horizontal reinforcement ratio ρ_h	0.006	0.003

Reinforcement steel for wall C2

Table A.26: Vertical reinforcement wall C2. Model III

	Boundary element	**Web**
Concrete cover, c[mm]	30	30
Bar diameter, ϕ[mm]	12	12
# of bars	12	6
Area of vertical reinforcement, A_{sv} [mm^2]	1357	679
Vertical reinforcement ratio ρ_v	0.008	0.003

Table A.27: Horizontal reinforcement Wall C2. Model III

	Boundary element	**Web**
Concrete cover, c[mm]	30	30
Bar diameter, ϕ[mm]	8	8
# of arms	2	2
Spacing, s_w[mm]	50	100
Area of horizontal reinforcement, A_{sv} [mm^2]	101	101
Horizontal reinforcement ratio ρ_h	0.006	0.003

Reinforcement steel for wall D2

Table A.28: Vertical reinforcement wall D2. Model III

	Boundary element	**Web**
Concrete cover, c[mm]	30	30
Bar diameter, ϕ[mm]	14	14
# of bars	12	8
Area of vertical reinforcement, A_{sv} [mm^2]	1847	1231
Vertical reinforcement ratio ρ_v	0.012	0.005

Table A.29: Horizontal reinforcement Wall D2. Model III

	Boundary element	**Web**
Concrete cover, c[mm]	30	30
Bar diameter, $\phi[mm]$	8	10
# of arms	2	2
Spacing, $s_w[mm]$	50	100
Area of horizontal reinforcement, A_{sv} [mm^2]	101	157
Horizontal reinforcement ratio ρ_h	0.006	0.005

Columns

All the columns are reinforced using the corresponding steel designed in Section 6.4.2.2 for interior, edge of corner column, respectively.

Slab

Top reinforcement of slab-column connection A1.

Table A.30: Top reinforcement slab-column connection A1. Model III X-direction

Parameter	**Value**
Strip width, $b[mm]$	1600
Slab depth, $h[mm]$	200
Concrete cover, $c[mm]$	30
Bar diameter, $\phi[mm]$	12
# of bars	9
Area of steel, A_s [mm^2]	1017
Acting moment $M_{Ed,x}$	42
Resisting moment $M_{Rd,x}$	57

Table A.31: Top reinforcement slab-column connection A1. Model III Y-direction

Parameter	**Value**
Strip width, $b[mm]$	1375
Slab depth, $h[mm]$	200
Concrete cover, $c[mm]$	30
Bar diameter, $\phi[mm]$	14
# of bars	8
Area of steel, A_s $[mm^2]$	1231
Acting moment $M_{Ed,y}$	52
Resisting moment $M_{Rd,y}$	70

Top reinforcement of slab-column connection B1.

Table A.32: Top reinforcement slab-column connection B1. Model III X-direction

Parameter	**Value**
Strip width, $b[mm]$	1600
Slab depth, $h[mm]$	200
Concrete cover, $c[mm]$	30
Bar diameter, $\phi[mm]$	14
# of bars	13
Area of steel, A_s $[mm^2]$	2001
Acting moment $M_{Ed,x}$	82
Resisting moment $M_{Rd,x}$	105

Table A.33: Top reinforcement slab-column connection B1. Model III Y-direction

Parameter	**Value**
Strip width, $b[mm]$	2250
Slab depth, $h[mm]$	200
Concrete cover, $c[mm]$	30
Bar diameter, $\phi[mm]$	16
# of bars	17
Area of steel, A_s $[mm^2]$	3418
Acting moment $M_{Ed,y}$	108
Resisting moment $M_{Rd,y}$	171

Top reinforcement of slab-column connection B2.

Table A.34: Top reinforcement slab-column connection B2. Model III X-direction

Parameter	**Value**
Strip width, $b[mm]$	2700
Slab depth, $h[mm]$	200
Concrete cover, $c[mm]$	30
Bar diameter, $\phi[mm]$	16
# of bars	19
Area of steel, A_s $[mm^2]$	3820
Acting moment $M_{Ed,x}$	170
Resisting moment $M_{Rd,x}$	190

Top reinforcement of wall A2 connection.

Table A.35: Top reinforcement wall A2 connection. X-direction

Parameter	**Value**
Strip width, $b[mm]$	2700
Slab depth, $h[mm]$	200
Concrete cover, $c[mm]$	30
Bar diameter, $\phi[mm]$	12
# of bars	14
Area of steel, A_s $[mm^2]$	1583
Acting moment $M_{Ed,x}$	89
Resisting moment $M_{Rd,x}$	99

Table A.36: Top reinforcement wall A2 connection. Y-direction

Parameter	**Value**
Strip width, $b[mm]$	1375
Slab depth, $h[mm]$	200
Concrete cover, $c[mm]$	30
Bar diameter, $\phi[mm]$	14
# of bars	8
Area of steel, A_s $[mm^2]$	1231
Acting moment $M_{Ed,y}$	51
Resisting moment $M_{Rd,y}$	71

Top reinforcement of wall C1 connection.

Table A.37: Top reinforcement wall C1 connection. X-direction

Parameter	**Value**
Strip width, $b[mm]$	1600
Slab depth, $h[mm]$	200
Concrete cover, $c[mm]$	30
Bar diameter, $\phi[mm]$	12
# of bars	9
Area of steel, A_s $[mm^2]$	1017
Acting moment $M_{Ed,x}$	47
Resisting moment $M_{Rd,x}$	60

Table A.38: Top reinforcement wall C1 connection. Y-direction

Parameter	**Value**
Strip width, $b[mm]$	2925
Slab depth, $h[mm]$	200
Concrete cover, $c[mm]$	30
Bar diameter, $\phi[mm]$	12
# of bars	19
Area of steel, A_s $[mm^2]$	2148
Acting moment $M_{Ed,y}$	67
Resisting moment $M_{Rd,y}$	130

Top reinforcement of wall C2 connection.

Table A.39: Top reinforcement wall C2 connection. X-direction

Parameter	**Value**
Strip width, $b[mm]$	2700
Slab depth, $h[mm]$	200
Concrete cover, $c[mm]$	30
Bar diameter, $\phi[mm]$	14
# of bars	21
Area of steel, A_s $[mm^2]$	3233
Acting moment $M_{Ed,x}$	147
Resisting moment $M_{Rd,x}$	171

Table A.40: Top reinforcement wall C2 connection. Y-direction

Parameter	**Value**
Strip width, $b[mm]$	2925
Slab depth, $h[mm]$	200
Concrete cover, $c[mm]$	30
Bar diameter, $\phi[mm]$	20
# of bars	24
Area of steel, A_s $[mm^2]$	7540
Acting moment $M_{Ed,y}$	320
Resisting moment $M_{Rd,y}$	335

Top reinforcement of wall D2 connection.

Table A.41: Top reinforcement wall D2 connection. X-direction

Parameter	**Value**
Strip width, $b[mm]$	2700
Slab depth, $h[mm]$	200
Concrete cover, $c[mm]$	30
Bar diameter, $\phi[mm]$	14
# of bars	23
Area of steel, A_s $[mm^2]$	3541
Acting moment $M_{Ed,x}$	156
Resisting moment $M_{Rd,x}$	180

Table A.42: Top reinforcement wall D2 connection. Y-direction

Parameter	**Value**
Strip width, $b[mm]$	2500
Slab depth, $h[mm]$	200
Concrete cover, $c[mm]$	30
Bar diameter, $\phi[mm]$	14
# of bars	20
Area of steel, A_s $[mm^2]$	3078
Acting moment $M_{Ed,y}$	125
Resisting moment $M_{Rd,y}$	160

Appendix B

Steel reinforcement. Drawings

Model I

Slab top reinforcement

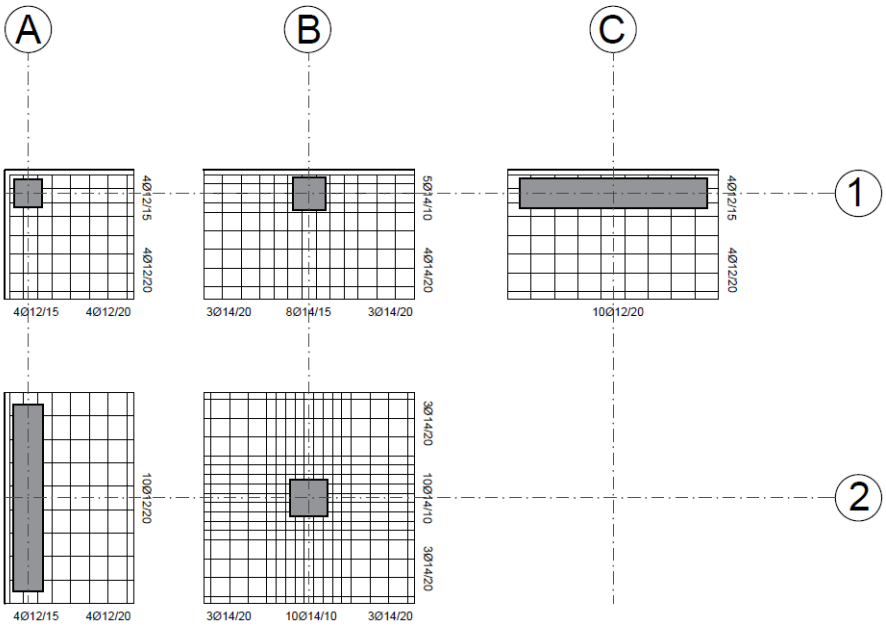

Figure B.1: Slab top reinforcement. Model I

Model II

Slab top reinforcement

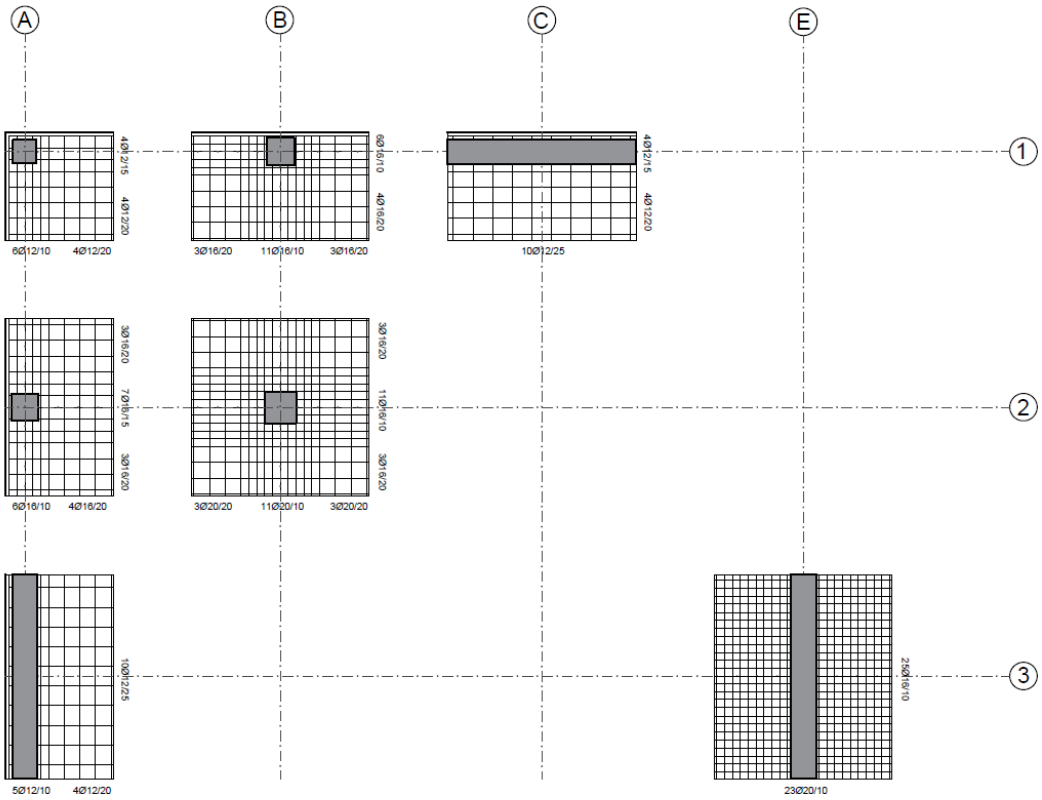

Figure B.2: Slab top reinforcement. Model II

Reinforcement steel of walls

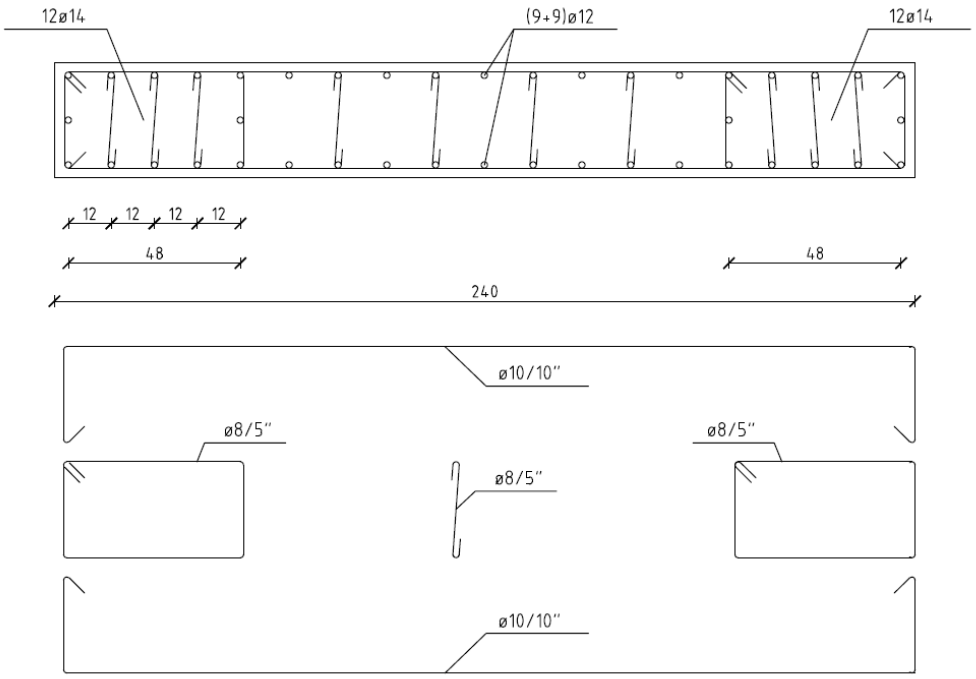

Figure B.3: Vertical reinforcement wall C1. Model II

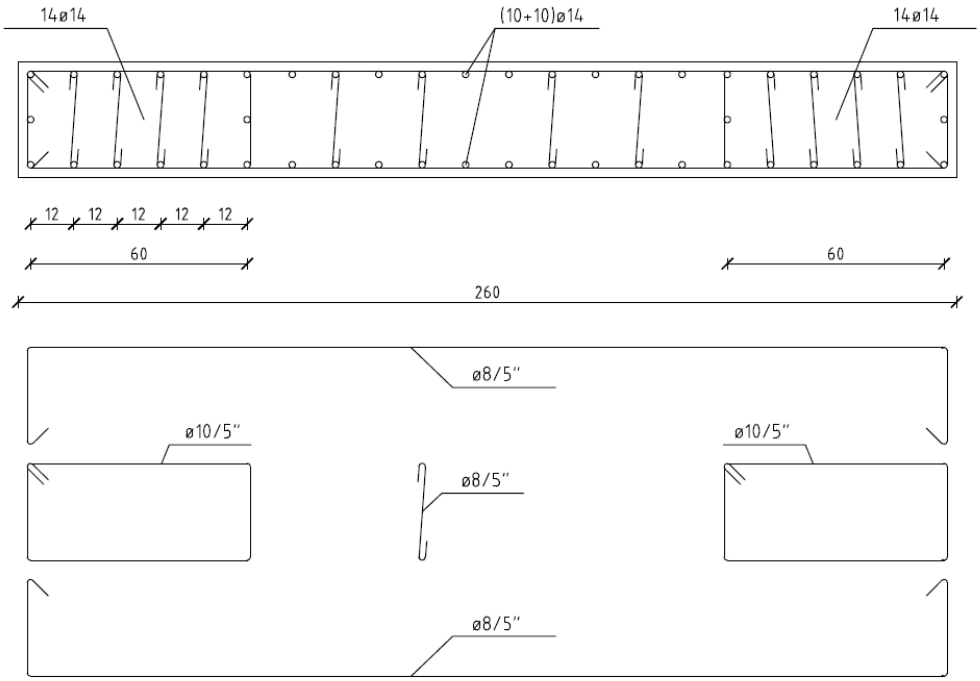

Figure B.4: Vertical reinforcement wall E3. Model II

Model III

Slab top reinforcement

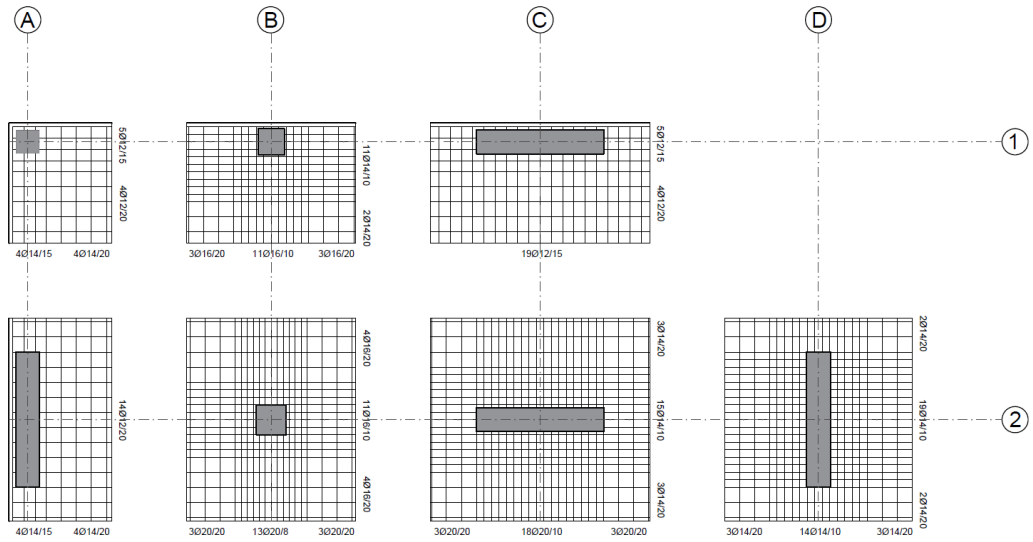

Figure B.5: Slab top reinforcement. Model III

Reinforcement steel of walls

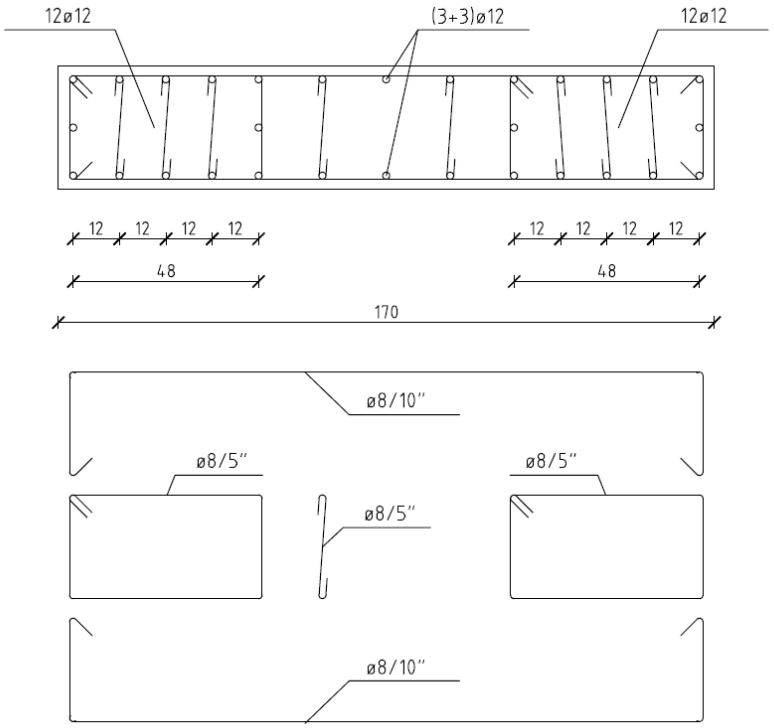

Figure B.6: Vertical reinforcement of wall C1 and C3. Model III

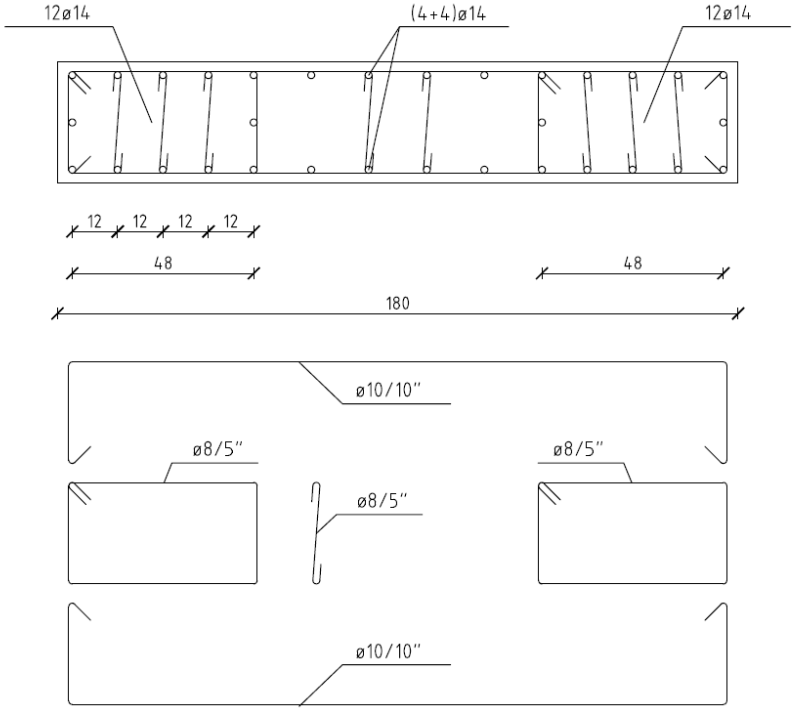

Figure B.7: Vertical reinforcement wall D2. Model III